SAND81-0100
Unlimited Release
UC-66
Printed April 1982



# FY80 ANNUAL PROGRESS REPORT-- MAGMA ENERGY RESEARCH PROJECT

John L. Colp, Editor
Geothermal Research Division, 4743
Sandia National Laboratories
Albuquerque, NM 87185

## ABSTRACT

The objective of the Magma Energy Research Project is to determine the scientific feasibility of extracting energy from magma bodies. Project activities are divided into five individual tasks representing all aspects of the concept.

Task I -- Resource Location and Definition. A joint Sandia/USGS geophysical sensing experiment was performed at Kilauea Iki lava lake. The seismic experiments suggested the presence of three reflectors; continued analysis of the data is required to discern definitive depths. Electromagnetic profiling experiments did not seem to show significant differences in the total volume of the inferred molten zone when compared to the 1976 data. A heat transfer model of a hydrothermal, hot dry-out zone, and melt zone of a lava lake was developed and verified by in situ measurements.

Petrologic analysis of Kilauea Iki cores from the 1979 drill holes was continued. Some results were: (1) the melt lens contained a maximum of 35% silicate liquid, 7 m of it had greater than 25% liquid; (2) the liquid trends continuously from basaltic to rhyolitic, this was inferred to be a product of in-situ crystallization.

Task II -- Source Tapping. Triaxial mechanical testing of water saturated granodiorite, basalt, and andesite to 1000°C and 3 kb was completed. A water weakening effect was noticed only in andesite only at temperatures over 850°C. Brittle failure occurred in dry and saturated systems suggesting that boreholes will be stable at 5010 km depth.

Task III -- Magma Characterization. The characterization of volcanic-magmatic gases for basaltic and alkaline lavas was completed, and a data base of C-O-H-S-Cl gas compositions typical of mafic lavas is now available

for material compatability studies. Petrographic computer codes were developed and used to reduce microprobe analyses to classify glasses and to calculate mineral composition of igneous rock core.

Task IV -- Magma/Material Compatability. Preliminary results from evaluations of 15 pure metals and 16 alloys in low pressure, simulated magma environments suggest that: (1) the chromium content of both ferritic and austenitic stainless steels is the most important factor in providing corrosion resistance; (2) Type 310 is by far the most corrosion-resistant alloy of any of the commercial stainless steels.

Task V -- Energy Extraction. Performed heat extraction calculations for a closed heat exchanger in various hypothetical magmas. These included the effects of high Prandtl number, crust formation, curvature effects, laminar/turbulent transition, and non-Newtonian rheology. Laboratory tests on convection heat transfer measurements in basalt were initiated and gave convective heat transfer rates of 30 $kW/m^2$ in 1290°C basalt.

CONTENTS

## LIST OF ILLUSTRATIONS

LIST OF ILLUSTRATIONS (Cont)

LIST OF ILLUSTRATIONS (Cont)



LIST OF TABLES

LIST OF TABLES (Cont)

MAGMA ENERGY RESEARCH PROJECT --
FY1980 ACCOMPLISHMENTS SUMMARY

A. Magma body location and definition

1. A joint USGS/Sandia geophysical survey of Kilauea Iki (a ponded molten rock body representing a complete geothermal system) was completed and analyses have identified subsequent geophysics research required for location of deeply buried bodies.

2. Lava Lake Geothermal Model -- Developed a heat transfer model of the hydrothermal, hot dry rock, melt system, of a lava lake and verified by in situ measurements.

3. Conducted 1980 Sandia/USGS lava lake sensing experiment. Obtained additional geophysical data for use in Sandia funded study "Geophysical Characterization of the Geothermal/Magma Environment." Also obtained thermal data for off-edge study of molten lens.

4. Kilauea Iki lava lake drill core studies.

   a. The 1978-79 drilling penetrated through a magma lens near the center of the lava lake. Core analysis indicated that the lens contained a maximum of 35% silicate liquid, and up to 7 m of the lens contained greater than 25% liquid.

   b. The silicate liquid of the magma lens shows a continuous trend in composition from basaltic to rhyolitic. Mass balance calculations support the inference that this trend is mainly a product of in situ crystallization in a temperature gradient and not due to crystal fractionation.

   c. Much of the change in liquid composition occurs in an upper magma transition zone. There also is significant re-equilibration of plagioclase and olivine in this transition zone.

d. There are several vertical zoning features that are critical to the geophysical modeling:

1) The modes for 79-1 indicate an olivine enrichment zone below approximately 54 m. Mass balance calculations support this interpretation.

2) The amount, composition, and distribution of liquid phase change as a function of depth and temperature.

3) The transitions between mineralogic/geochemical zones are continuous, for the most part, and not sharp discontinuities.

It is clear from the present studies that the zoning in the lower half of the lava lake must be defined to fully evaluate existing geophysical and mass balance models.

B. Source Tapping.

1. Experimentally measured confined and unconfined strength of basalt, andesite, and granodiorite to 1000°C and developed wellbore stability criteria. Preliminary studies showed correlation of criteria with stability of geothermal wells.

2. Triaxial mechanical testing of water saturated granodiorite, basalt and andesite to 1000°C and 3 kb has been completed at Texas A&M. A water weakening effect was noticed only in andesite; this occurred at temperatures over 850°C.

3. Brittle failure occurred in dry and saturated systems suggesting that boreholes will be stable at 5-10 km.

C. Magma Characterization.

1. The characterization of volcanic-magmatic gases for basaltic and alkaline lavas has been completed, and a data base of C-O-H-S-Cl

gas compositions typical of mafic lavas is now available for material compatibility investigations. Several papers based on these studies have been published or are in press.

2. Petrographic computer codes have been developed and are being used to reduce microprobe analyses to classify glasses and to calculate mineral composition of igneous rock cores.

   Characterization of cores from Kilauea Iki lava lake has quantified compositions as a function of depth and is providing insight into the mechanisms of solidification of magma bodies.

3. The Magma Simulation Facility (4 kbar/1600°C/800 cc vol.) has continued operation this year. Improvements continue to be made in viscosity measurement and sample preparation techniques. "Apparent viscosities" have been determined for N.M. and Hawaiian basalts, Mt. Hood andesite, and a variety of calibration glasses. Upgrading of the facility continues and the reliability of the High Pressure/ High Temperature system has been excellent.

4. The apparent viscosity of Mt. Hood andesite and Hawaiian olivine tholeiite has been measured at 1 atm., in an argon atmosphere, with a direct observation, real time falling sphere viscometer. For Mt. Hood andesite, $\text{Log}_{10}\,\eta_a = 3.3$ poise at 13090°C, and $\text{Log}_{10}\,\eta_a = 3.9$ poise at 1245°C.

   The viscosity measurements were made with sample boules prepared by an approach involving premelting and casting at high temperatures, with subsequent characterization steps to eliminate bubbles.

D. Magma/Material Compatibility

Fifteen pure metals and 16 alloys have been evaluated in low-pressure, simulated-magma environments. Preliminary results suggest that iron, cobalt and molybdenum, each containing chromium, will show little degradation. The chromium content of both ferritic and austenitic

stainless steels is the most important factor in providing corrosion resistance. Type 310 is by far the most corrosion-resistant alloy of any of the commercial stainless steels.

E. Energy Extraction.

1. Performed heat extraction calculations for a closed heat exchanger in various hypothetical magmas. These calculations included the effects of high Prandtl number, crust formation, curvature effects, laminar/turbulent transition and non-Newtonian rheology. Laboratory tests on convection heat transfer measurements in basalt were initiated.

2. Laboratory experiments in basalt to 1290°C gave convective heat transfer rates of 30 $kW/m^2$ confirming the heat transfer models.

3. Exchanged data and analytical techniques with scientists in Iceland. Preliminary indications show that heat extraction rate of 40 $kW/m^2$ are possible in margin zone heat extraction systems.

F. Other

In support of the USGS effort during the Mt. St. Helens eruption, measurements were made of gas compositions, thermal gradients and ash compositions. Other instrumentation was also provided for assessment of hazards.

FY80 ANNUAL PROGRESS REPORT--MAGMA ENERGY RESEARCH PROJECT

## I. Introduction

The objective of the Magma Energy Research Project is to determine the scientific feasibility of extracting energy from magma bodies. Activities to accomplish the objectives are divided into five tasks:

Task 1 - Resource Location and Identification

Task 2 - Source Tapping

Task 3 - Magma Characterization

Task 4 - Materials Compatibility

Task 5 - Energy Extraction

Status of the project has been reviewed in previous reports (Colp et al., 1976; Colp and Traeger, 1979; Colp, 1979a). This report summarizes the program activities of FY1980 according to the individual tasks.

Major project activities during FY1980 were:

Field experimentation with the United States Geological Survey (USGS) in geoscience studies in the lava lake laboratory at Kilauea Iki crater on Kilauea volcano.

Laboratory analysis and characterization of core samples recovered from Kilauea Iki lava lake during the FY1979 drilling program.

Calculational evaluations of heat extraction rates for a closed heat exchanger in several magma types.

Laboratory measurements of convective heat transfer in molten basalt.

Activities and results are summarized for each of the tasks. Names of individuals responsible for each of the areas are noted; these individuals should be contacted for further information. Detailed data and analyses included in published topical reports will be referenced rather than duplicated in this report.

## II. Task 1 - Resource Location and Definition

A major requirement in the development of viable processes to use magma sources for energy applications is the capability to define the existence of a magma body, its depth, its areal extent, and its general form (i.e., whether it is in a finite homogenous pool or in a honeycomb of solid crevices filled with molten material).

A few studies have been conducted to locate and identify a buried magma source, with most of the existing remote sensing methods--seismic, microseismic, resistivity, gravity, magnetic, magnetotelluric, infrared, thermal--having been used (Eaton et al., 1975). The USGS has examined areas under Yellowstone National Park; Long Valley, CA; Kilauea Volcano, HI; Geysers/Clear Lake, CA; and at other locations in the Western US. While these studies have provided some evidence of magma sources, there are sufficient uncertainties associated with each of the remote sensing methods that conclusive proof of magma location and other characteristics has not yet been obtained.

Recognizing this state of uncertainty, the Magma Workshop (Colp et al., 1975) recommended that various geophysical techniques be tested and confirmed on a known buried molten rock body so that the effectiveness of the different methods could be determined.

Lava Lake Laboratory Program (J. L. Colp)

Kilauea Iki Lava Lake provides a unique microcosm of a total geothermal system. It has been and continues to be used as a field laboratory by the Magma Energy Research Project. Based on the recommendations of the Magma Workshop (Colp et al., 1975), geophysical measurements were performed at Kilauea Iki in 1976 to evaluate techniques over a known molten rock body (Colp and Traeger, 1979). Although the measurements did define the upper frozen crust regions and the edge of the liquid lens, the nature or thickness of the liquid lens could not be quantified. Analysis of the data by Hermance et al. (1979), resulted in the development of a physical model of a vertical section of the lake (Figure 1).

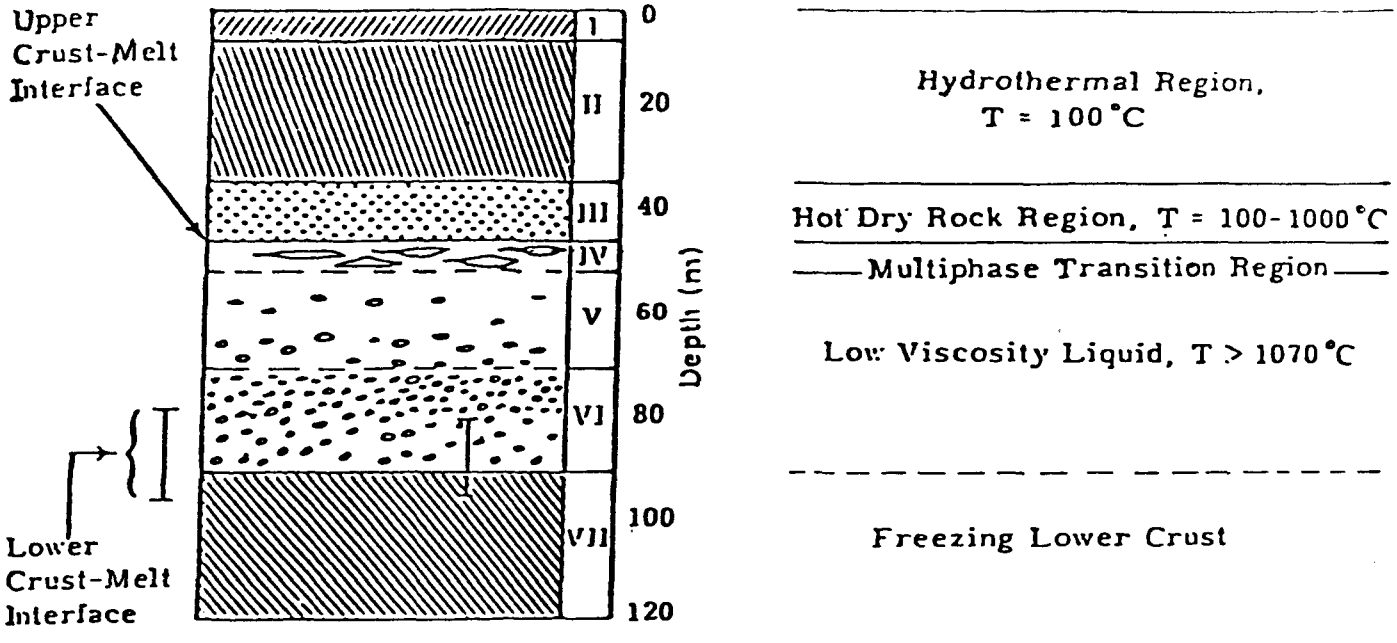


Figure 1. Vertical Model of Kilauea Iki Lava Lake

In mid-1978, a set of experiments was defined for the 1979 Lava Lake Drilling Program, whose objective was to penetrate into the molten lens and obtain data to help interpret the 1976 geophysical measurements. Two topical reports (Neel et al., 1979; Colp, 1979) describe the experiments and preliminary results in more detail. The FY 1979 Project Annual Report (Colp 1979a) describes further results.

FY 1980 Sandia/USGS Lava Lake Geophysical Sensing Program

The primary purpose of this program of geophysical sensing studies was to obtain additional current information on the performance of geophysical sensing systems--seismic and electromagnetic--at Kilauea Iki lava lake. This information was required for Professor J. F. Hermance to include in his Sandia-funded study on the Geophysical Characterization of the Geothermal/Magma Environment. The results of this study will be used as input on the planning of the Sandia/USGS Kilauea Iki Lava Lake Experiment scheduled as part of the Magma Energy Research Project in FY 1981.

A secondary purpose of this program was to provide an opportunity for H. M. Iyer and his colleagues at USGS Menlo Park to evaluate their seismic techniques currently being used on real magma body investigations over a known molten rock location. From this year's experiment, they will be able to evaluate the performance of their existing equipment and methods and improve them for participation in the FY 1981 series.

Seismic Experiments - 1980 (J. F. Hermance)

The interpretation of a seismic refraction experiment in the Kilauea Iki crater by Aki et al. (1978) revealed the existence of a P-wave low-velocity zone in the area of the magma lens. However, the thickness, depth, and velocity in the zone were not uniquely determined by this refraction work. A constraint on the maximum thickness ($T < 10$ m) of a Newtonian fluid layer was derived by Aki et al. (1978) from the observed vertical transmission coefficient for SH waves through the magma lens. The measurement of near-vertical reflection times and reflection coefficients from the top and bottom of

the magma lens should allow one to place stronger constraints on the thickness and P-velocity of the lens. The purpose of the 1980 USGS seismic experiment was to determine if the coherent reflections could be obtained from the top and bottom of the magma lens.

USGS personnel planned to perform two seismic experiments for the spring of 1980 to measure the properties of the Kilauea Iki magma lens. However, only an active seismic experiment to detect near vertical reflections from the top and bottom of the magma lens as well as reflections from interfaces between steam-filled and water-filled cracks was carried out. Heavy rainfall and high steam concentrations near the crater floor caused an unacceptable moisture buildup in the recorder electronics and prevented field personnel from carrying out the second experiment, which was a passive experiment to measure thickness variations of the magma lens from analyzing travel-time residuals of local earthquake.

A preliminary interpretation of the 1980 data suggests the presence of three reflectors (R1, R2 and R3) within the lava lake. Although the correlation of these reflectors with physical discontinuities measured or inferred by other experiments is speculative, an attempt was nevertheless made by the USGS personnel. Their results are now summarized. According to Stauber (1980), R1 appears within a depth range of 31 to 37 metres and may correspond to the depth of the transition from water-/steam-filled cracks above to steam-filled cracks below, found at 33 metres (Hermance, Forsyth and Colp, 1979). The top of the magma lens occurred near 45 metres in 1976 (Hermance, Forsyth and Colp, 1979) and it was probably a few metres deeper in 1980 when the reflection experiment was performed. The R2 reflection, which occurs between 44 and 88 metres depth, may occur at this interface. If the R2 reflector is the top of the zone of molten sills, the interval velocity between R1 and R2 must be less than the velocities above R1. If the interval velocity were 500 or 100 m/sec, the depth to the R2 reflector would be 48 or 62 metres, respectively. The interval between R1 and R2 could correspond to the steam zone above the magma lens. Lower velocities in this zone are expected due to the higher compressibility of the steam-filled rock compared to water-saturated rock above. The permissible depth range of the R2 reflector

does not preclude the possibility that it originates in or at the base of the magma lens. The R3 reflector could occur from the base of the magma lens to well into the old crater floor. Further constraints on the depths of possible interfaces for the R2 and R3 reflections will be possible when the reflection coefficients are calculated.

Conclusions of the 1980 Seismic Experiment--Several conclusions were drawn from the seismic experiment and were reported by Stauber (1980). Coherent near vertical reflections appear to originate from interfaces in the Kilauea Iki lava lake. The scattering caused by joint fractures and the near surface bubbles does not seem to completely obscure these reflections. The surface waves and shear waves generated by the impulsive vertical point forces used as sources, however, do partly obscure the early reflections. It is hoped that these low velocity phases can be removed by filtering in the frequency-wavenumber domain. Stauber (1980) feels that the reflections seen in the preliminary analysis may originate from a discontinuity in seismic properties associated with the transition from water-filled to steam-filled cracks at some distance above the magma lens, as well as from the top of the magma lens itself.

## Electromagnetic Experiments - 1980 (J. F. Hermance)

During the month of March, 1980, the U.S. Geological Survey performed a number of electromagnetic (EM) sounding and profiling experiments on Kilauea Iki lava lake. The objective of the program was to determine whether any significant changes in the electrical properties and the configuration of the molten magma core had taken place since the previous electrical soundings were made in April of 1976 (Smith and Frischknecht, 1980).

Electromagnetic Profiling (Slingram Method)--The slingram method is basically an electromagnetic induction profiling technique using two small, portable, vertical axis, magnetic dipole coils. One is used as transmitter and the other as receiver with a fixed separation between them. During the 1980 USGS experiments, slingram profiles were made at loop

spacings of 400 and 600 feet along the east-west baseline, line 17 west, and along northwest-southeast and northeast-southwest radials through 17 west on the baseline. The results were used to make a new estimate of the edge of the conductive or melt zone (Figure 2).

Separate estimates of the edge were made from the profiles taken at 222 Hz and 3555 Hz and the results were averaged to give the boundary indicated in the figure. Tick marks indicate the estimates for each spacing. The trace of the edge is dashed in the vicinity of the north-south line because measurements could not be carried far enough south to adequately define this boundary. For comparison, the edge determined from turam measurements in 1976 by Flanigan and Zablocki (1977) is also included in the figure.

The outline of the edge from the slingram measurements appears to be more elliptical than from the turam measurements. On the other hand there does not seem to be a significant difference between the 1976 experiment and the 1980 experiment in the total volume of what is inferred to be a molten core. It is possible that the north-south edges have shrunk inward some 200-300 feet from 1976 to 1980. Another possibility is that there is a systematic bias in interpreting one, or both, of the experiments.

Electromagnetic Soundings--The EM sounding measurements were made using the horizontal loop-loop method described by Smith et al (1977). A total of ten soundings were made, although all of these did not produce reliable data due to various electronic problems caused by the inclement weather. These data were taken with generally different equipment than was used to make the 1976 soundings described by Smith et al (1977).

Soundings S-1-80 and S-2-80 were located in exactly the same position on the lava lake as the two soundings made in 1976. Though the sounding data are somewhat suspect due to instrumental problems, it is useful to make a comparison of their interpretation. Table 1 summarizes the interpretation of the soundings based upon a three layer earth model. Previous interpretations of both Schlumberger sounding experiments (Zablocki, 1976)

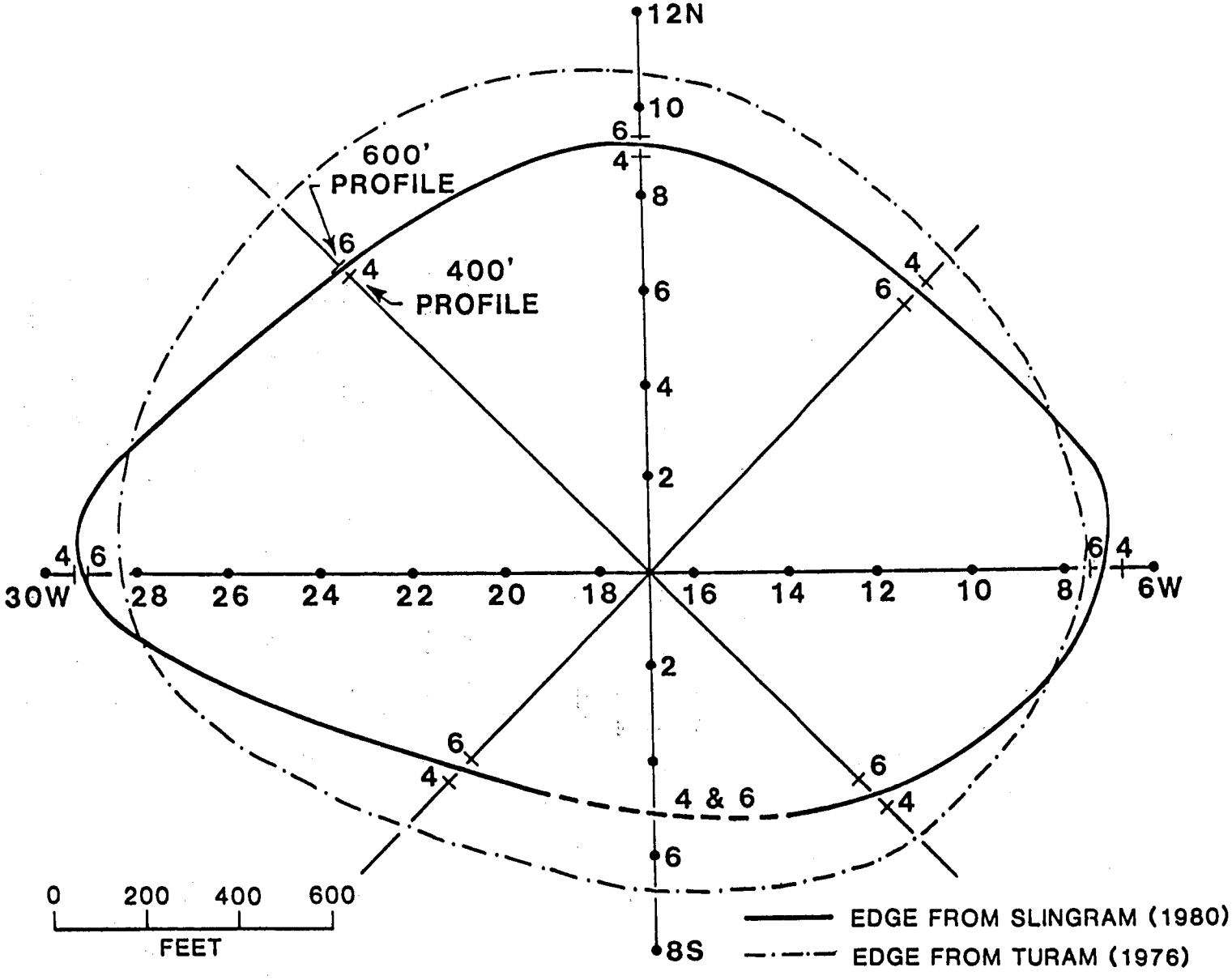


Figure 2. Edge of Conductor, Kilauea Iki

Table 1.

Three Layer Earth Model Comparison for 1976 and 1980 Soundings

| Sounding | $\rho_2$ | +/-% | $t_1$,m. | +/-% | $t_2$,m. | +/-% | $\rho_2 t_2$, Siemens |
|---|---|---|---|---|---|---|---|
| S-1-76 (300') | 4.6 Ω-m | 6% | 34.5 m. | 3% | 49.5 m. | 3% | 10.8 |
| S-1-80(1) (300') | 10.6 | 19% | 31.7 | 10% | — | -- | -- |
| S-2-76 (600') | 5.5 | 10% | 43.3 | 1% | 47.0 | 1% | 7.87 |
| S-2-80 (600') | 7.5 | 30% | 46.1 | 6% | 46.0 | 50% | 6.13 |

and electromagnetic sounding experiments (Smith et al., 1977; 1978) suggest that the upper chilled portion of the lava lake has a very high resistivity and is essentially non-conducting as far as induction experiments are concerned. Hence the three-layer models of Smith and Frischknecht (1980) were constrained to have a melt layer having a resistivity, $\rho_2$, and thickness, $t_2$, sandwiched between two electrically insulating layers. Noise in the data of S-1-80 was not low enough to resolve a three layer earth. Thus for this model, the melt is considered to be a half-space. The 1976 values of parameters are taken from Smith et al (1978). Values given in the +/- column are the one parameter standard deviations given in percent of the parameter. Although the three layer model interpretations do not conclusively indicate that a change in melt parameters has taken place (Smith and Frischknecht, 1980), it is possible that the melt conductivity-thickness product has decreased by as much as a factor of 2 since 1976. This is supported by referring to the data and interpretations illustrated in Figure 3. Two sets of two-loop sounding data are presented for a fixed separation of 105.6 m. One data set was acquired in 1976, the

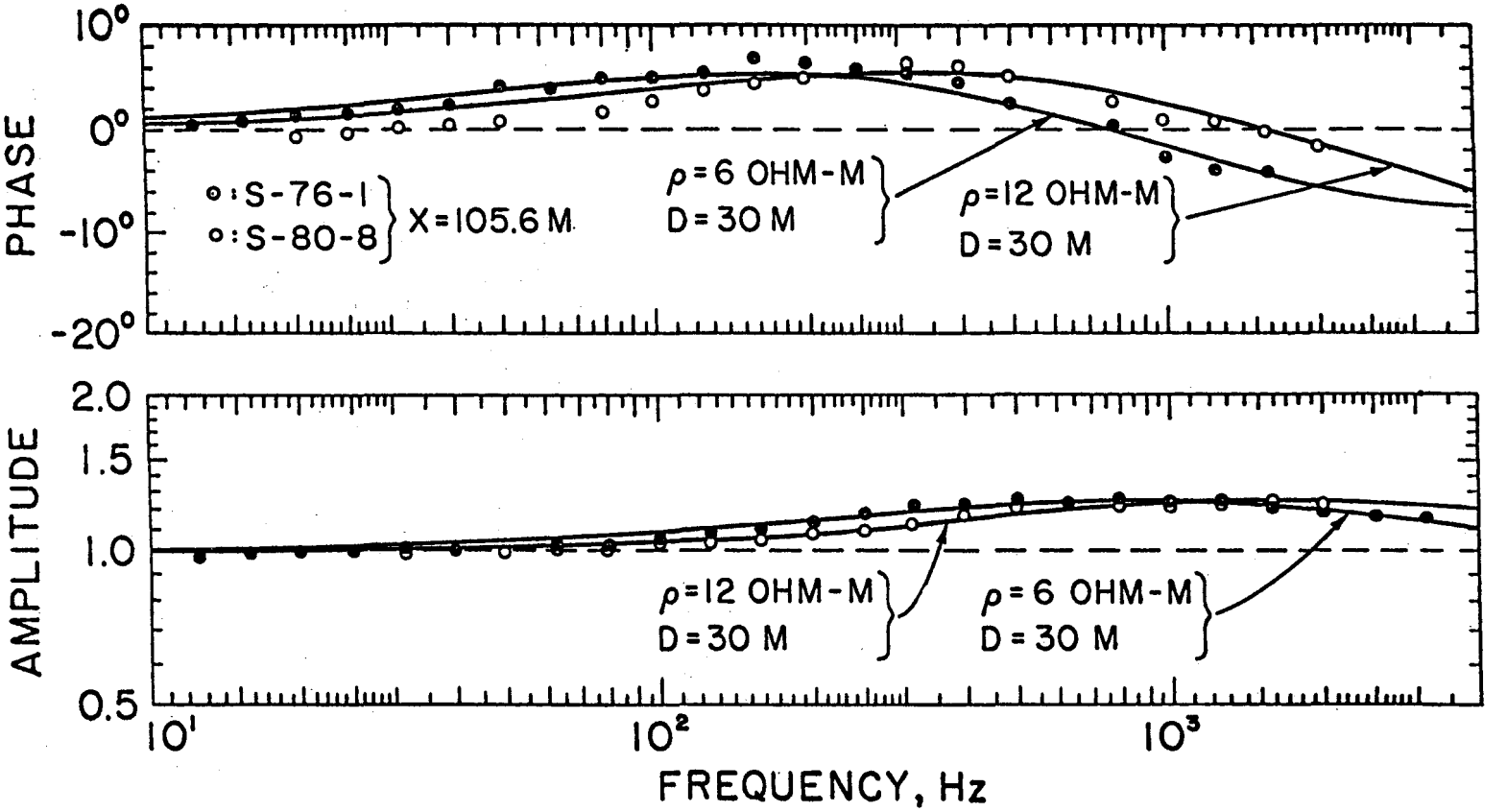


FIGURE 3

The results of fitting simple two-layer models to the 1976 and 1980 dipole soundings at a loop-loop spacing of 105.6m. The first layer was infinitely resistive in both cases. The second layer was at a depth D and had a resistivity ρ. Actual values for these parameters are shown next to the approximate curves. Amplitude and phase are the observed values relative to an equivalent source and receiver in free-space.

other in 1980. The experiments occupied the same sites both years.

A very simple model is used to interpret the data; simply an infinitely resistive layer extending to a depth, D, underlain by a half-space having a finite resistivity, $\rho$. The amplitude data for S-76-1 is reasonably well-fitted over most of the frequency range by 6 ohm-m material at a depth of 30 m. The amplitude data for S-80-8 appears to be satisfied by 12 ohm-m material also at a depth of 30 m. The fit to the phase data is not so good in either case. However, the results are strongly suggestive of a systematic increase in resistivity by a factor of 2 from 1976-1980. Clearly, a better match between the model response and the actual data is provided by the refined models proposed by the USGS workers (Smith et al., 1977; 1978; Smith and Frischknecht, 1980). The point is that a first-order requirement for satisfying the data is a systematic increase by up to a factor of 2 from 1976-1980 in the resistivity of the high temperature core of the lava lake.

A summary of laboratory work on the electrical conductivity ( $\sigma = 1/\rho$) of basalt as a function of temperature is presented in Figure 4. It seems quite apparent from these data that temperatures as low as 1000°C are still quite capable of producing resistivities in the range 6-12 ohm-m needed to satisfy the field results in Figure 3.

## Thermal Studies (R. G. Hills)

During March and April of 1980, temperature profiles in nine existing boreholes were recorded. These profiles, when used in conjunction with previous profiles, lead to an improved understanding of the cooling dynamics of magma bodies.

The boreholes which were used for the 1980 temperature measurements are shown in Figure 5. The only holes in which the temperatures significantly exceeded 100°C were 79-3 and 79-5. A maximum temperature of 173°C at the bottom of 79-3 (39.1 m) was observed. Other holes in the immediate vicinity of 79-3 of comparable depth (75-1, 76-1, 79-2) did not reveal temperatures

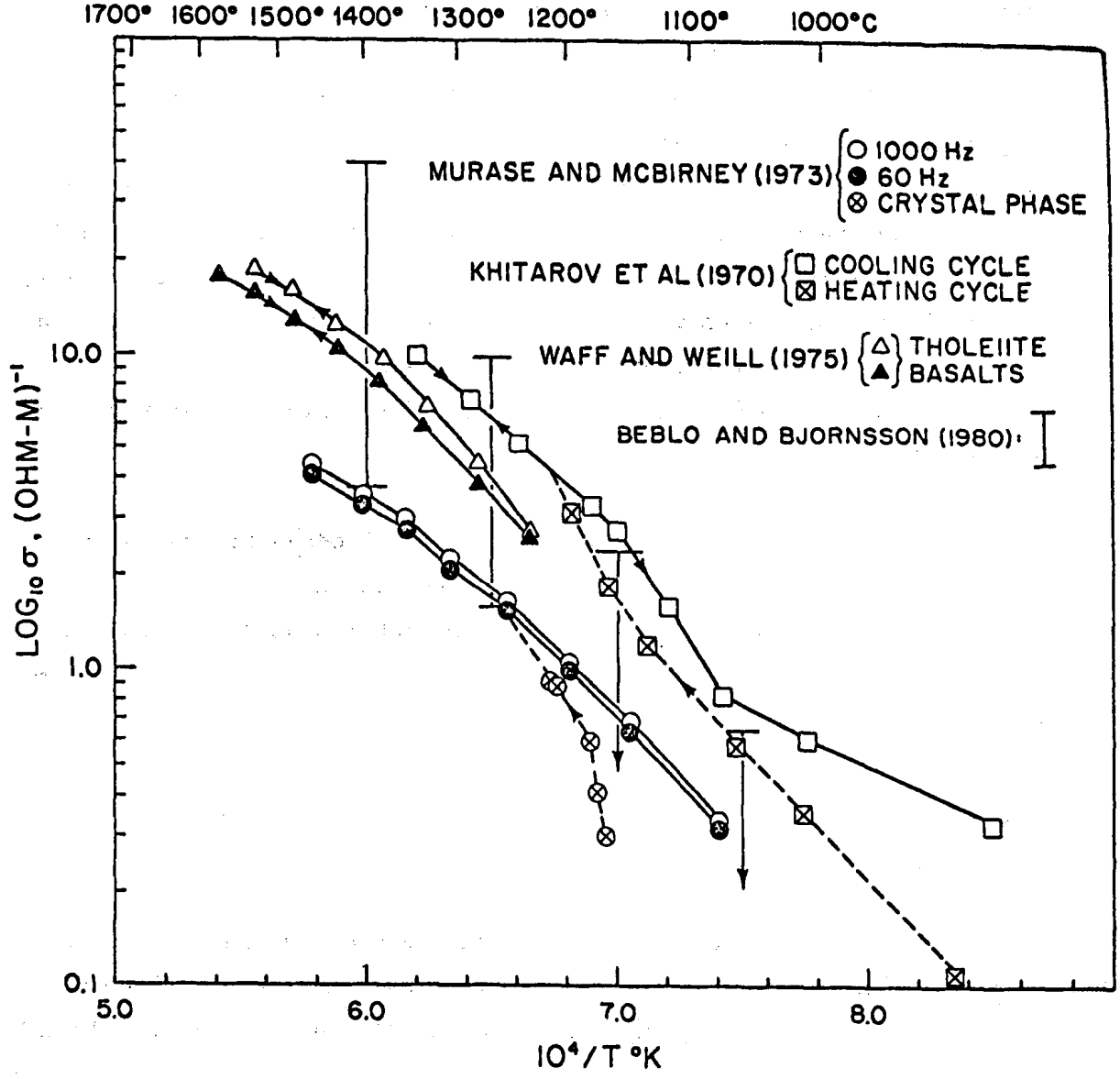


Figure 4. A summary of laboratory measurements on the electrical conductivity of basalt.

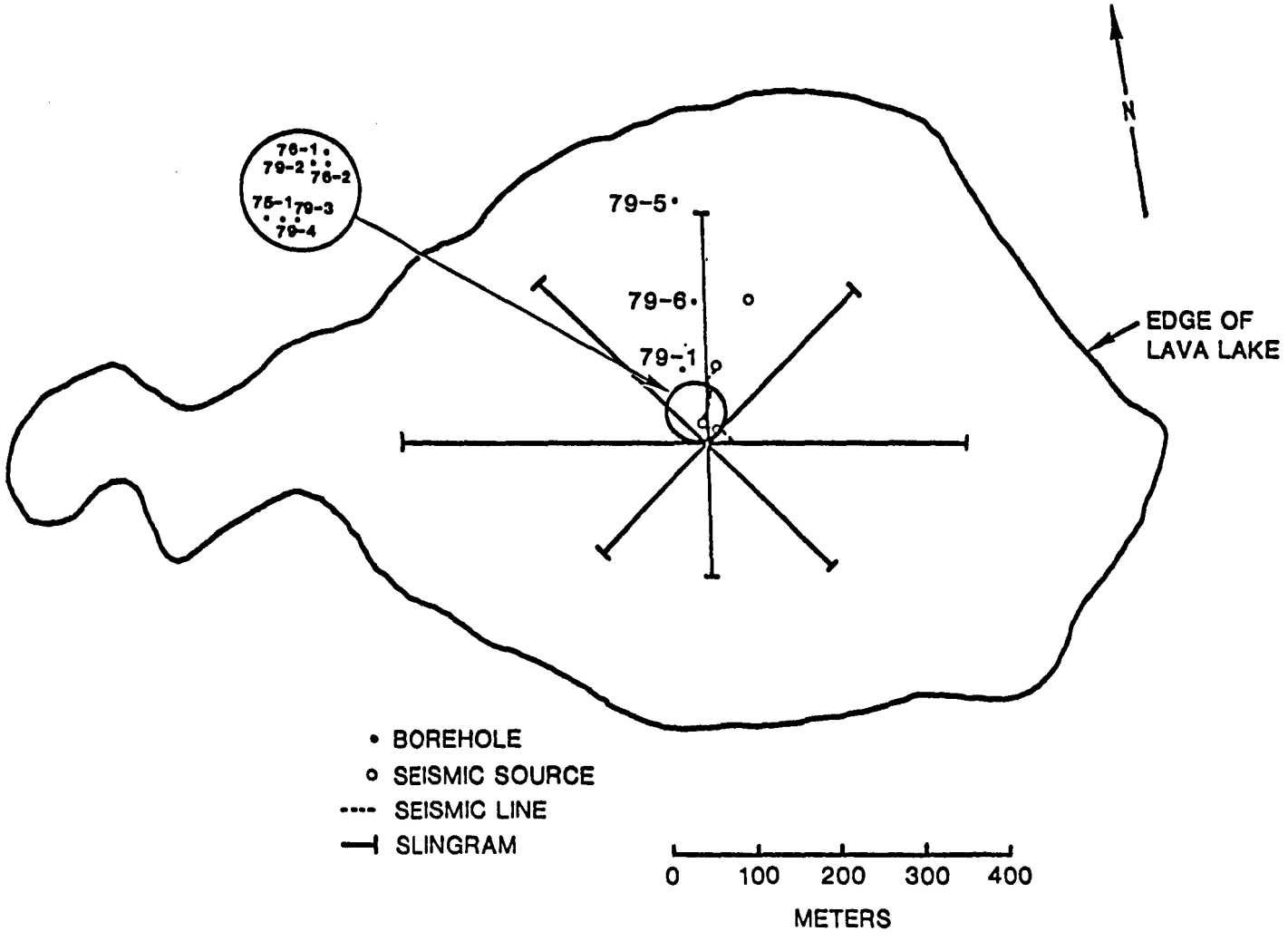


Figure 5. FY-80 Kilauea Iki Lava Lake Experiments

significantly higher than 100°C. Prior to the measurement, 79-3 was blocked at 1 m. Whether the anomalous behavior of 79-3 is due to hole blockage or due to hydrothermal circulation through a fracture system leading into the hole is difficult to determine with the present data.

The deepest borehole is 79-5, which is on the margins of the molten body. A plot of the temperature distributions at various times since the drilling of the hole is shown in Figure 6. The figure illustrates the continuing rise in temperature throughout the hole. The behavior in the 70 to 100 metre depth range of 79-5 suggests some type of transient heat source must be present at depth. A possible mechanism for this source is the hydrothermal convection of superheated steam passing through fractures in the formation. As the formation cools, new fractures are formed due to thermal stresses. In order for the convection to act as a heat source, the fracture pattern must extend laterally from the high temperature zone in the center of the lake to a point below 79-5.

A second unexpected trend in the temperature profile of 79-5 is illustrated in Figure 7. In the figure, temperature as a function of depth for the upper 50 metres of 79-5 is plotted. The temperatures labeled "INITIAL CONDITION" are the temperatures measured by Graeber on 4/26/79 (see Figure 6). The measurements observed 11 months later were taken by Colp and Hills on 3/10/80. The expected change in temperature over the same 11 month period due to one-dimensional conduction (thermal diffusivity = $5 \times 10^{-7}$ $m^2s$) is also shown. The discrepancy between observation and one-dimensional conduction theory is as much as 100°C. A second discrepancy in the behavior of the upper 50 metres of 79-5 is the fact that super 100°C temperatures are observed within 5 metres of the surface, whereas over the hotter center region of the lake the super 100°C region is not observable within 30 m of the surface in 79-3 or observable at all in the other holes ($\sim$ 40 m depth).

A probable reason for the unexpected behavior in the upper 50 metres of 79-5 is the effect that the upflowing steam has on the long term temperature measurements. Steam flowing uphole from the high temperature region below will heat the borehole walls. The result of steam flowing up

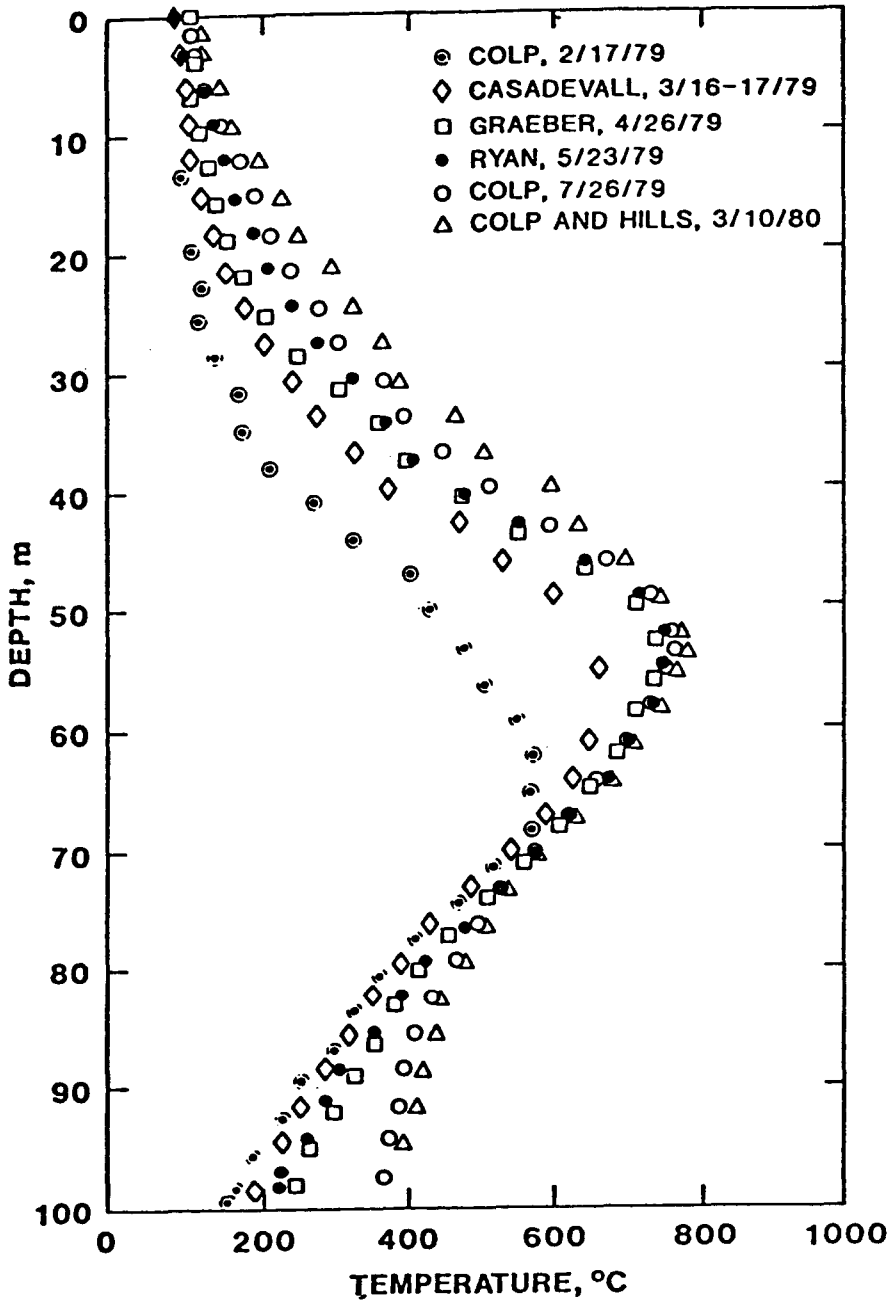


Figure 6. Temperature Profiles in KI 79-5

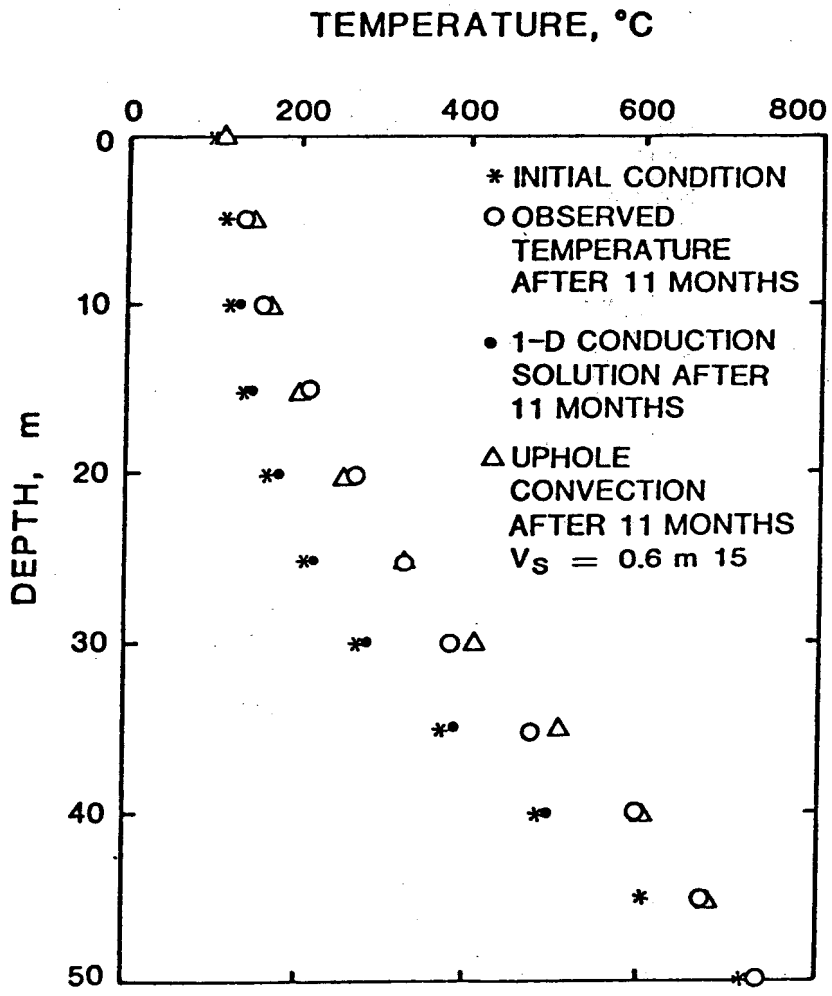


Figure 7. Effect of Steamflow in a Borehole

79-5 at 0.6 m/s was modeled by finite difference. In the model, steam was injected into the hole at 50 metres depth at 720°C. The steam temperatures at various depths in the hole (the thermocouples actually detect the temperature of steam flowing up the hole and not formation temperature) that result from the changes in the borehole wall temperature after 11 months of heating are shown in Figure 7. Reasonable agreement exists between observation and theory. A steam velocity of 0.6 m/s out of the hole is also reasonable in light of visual observations at Kilauea Iki. Thus the temperature measurements after 11 months of steam contamination probably do not reflect true formation temperature and, according to the model, could be off by 100°C.

Previous tests (see Colp, 1979) indicate that the steam contamination effect is not significant over the center of the lake. This result is probably due to the impermeable molten lens acting as a barrier to convection from depth. The steam in the super 100°C zone above the magma is essentially stagnant (Hardee, 1980). After the magma body solidifies, however, steam will rise from depth through newly formed thermal fractures. Because of the steam contamination effect, all future temperature holes should be adequately cased.

## FY81 Kilauea Iki Lava Lake Experiments (J. C. Dunn)

Twelve experimental studies have been proposed to wrap up Sandia's field laboratory work at Kilauea Iki lava lake. These proposed experiments, to be conducted during FY81, are designed to complete the geophysical study of a cooling magma body, to measure in-situ magma properties, to gain insight into the later stages of the cooling dynamics of magma bodies, and to study the scientific feasibility of extracting energy from magma bodies on a scale greater than can be achieved in conventional laboratory experiments.

The planned experiments have been divided into three general headings and are listed as follows.

1. Geophysics

- Chemical and petrological analyses of recovered drillhole core.
- Two-dimensional temperature profile.
- Downhole steam flow measurement.
- In-situ electrical conductivity measurements.
- In-situ seismic measurements.

2. Energy Extraction

- Energy extraction in molten basalt using an open system.
- Energy extraction in a permeable medium above molten basalt.
- Heat transfer rate measurements in molten basalt.
- Heat transfer rates using a downhole calorimeter.

3. Drilling Technology

- Drill and core to pre-1959 surface near center of the lake.
- Water-jet augmented core bit drilling in molten lava.
- Evaluation of conventional core bit design in upper crust.

The proposed geophysical experiments are designed to complement but not duplicate the previous geophysical experiments in such a way as to form a comprehensive study of the life history of a buried magma body from not only a petrological, chemical, and thermal point of view, but also from a geophysical sensing point of view. The knowledge gained from the study is necessary in order to locate and define and estimate the age (which has important consequences as to the energy content) of a magma body in the earth's crust. Two experiments are designed to measure in-situ magma electrical and seismic properties. Information on these properties, which is not presently available, is necessary in order to accurately locate and define magma bodies. Two experiments are proposed to study the later stages (also applies to the mid-stages) of the cooling dynamics of a buried magma body. In contrast to earlier work, these experiments will study not only the region over the center of the body, but also the regions on the

margin and beneath the body. Such a study is necessary in order to understand how a magma body cools and how the thermal signature of the body, which can be seen from the earth's surface and from boreholes, relates to the energy content, exact location, and configuration of the body. A chemical and petrological experiment is planned and involves analysis of the core samples that are obtained during the drilling required for the other experiments. In order to obtain a complete mass balance model of the crystallization and differentiation of Kilauea Iki lava lake, coring through the center of the lake must be done. The resulting data, when used in combination with previous core analyses, will be used to test thermodynamic equilibrium models of crystallization and provide a capability for predicting magmatic evolution and energy content that will be applicable to basaltic chambers other than Kilauea Iki.

Both open and closed systems are proposed to measure energy extraction rates in molten basalt. Neither of these measurements have ever been made in-situ. For the open system experiment, the magma will be water cooled in an attempt to thermally induce fractures in order to create a large surface area for heat transfer.

This should result in energy extraction rates that are much greater than rates obtained with closed heat exchanger systems. The basic idea of thermally inducing fractures in a magma has never been tried. The success of such a scheme could be of major importance when assessing the feasibility of the project's task 5, energy extraction. One experiment is designed to measure in-situ thermal properties and heat transfer rates to a closed system. Measurements will be obtained by heating, rather than cooling, the magma, thereby allowing data collection at temperatures higher than the in-situ state. These measurements will complement data obtained in the laboratory at Sandia where geometry restrictions are limiting. In addition to the measurements in magma, one experiment is planned to measure energy extraction rates in the high temperature margin above a magma or plastic body. This measurement is important to assess the potential for energy extraction above a magma body without direct entry into the magma chamber.

The development of drilling technology is not part of the Magma Energy Research Project. However, drilling in the lava lake is necessary to conduct the proposed geophysical and energy extraction experiments. During the drilling, the Magma Energy Research Project would be remiss if it did not evaluate drilling performance, especially in high temperature regions of the lake.

In light of the recent data of Hardee (1980) and Gerlach and Luth (this report) by 1982 there may not be sufficient melt present in Kilauea Iki lava lake to justify the downhole calorimeter experiment. However, the other experiments do not require a molten lens; they are just as relevant whether melt is present or not, as long as a high temperature, plastic region does exist. The in-situ property experiments should still be run to establish how very hot rock ($>800°C$) differs in geophysical appearance from magma. The cooling dynamic experiments (temperature, steam flow) are still appropriate, since a hot impermeable body surrounded by a wet permeable medium, which is characteristic of many magma bodies, will still exist at Kilauea Iki. The energy extraction experiments are all meaningful experiments with or without the presence of melt in the Kilauea Iki lava lake. The open system only requires a large region of plastic material that can be thermally fractured (temperatures greater than about 725°C). The margin experiment is conducted in the crust at relatively low temperatures (below about 700°C), and the heat transfer rate experiment uses a downhole heater to create melt around the heater. The calorimeter experiment can still be used to measure heat transfer rates in the drillhole, but this particular experiment would be more meaningful with the presence of melt. Therefore, the calorimeter experiment would probably be canceled if melt does not exist.

The experiments described in this test plan directly relate to the investigation of the scientific feasibility of energy extraction from magma bodies. However, the knowledge gained from these experiments can have important applications in other areas of research. For example, the geophysics of magma body location and definition are also applicable to the magma bodies located under geothermal fields. The evaluation of the final location of the Continental Scientific Drilling Program (CSDP)

borehole can benefit from the geophysical techniques associated with magma body location and definition. The study of the hydrothermal circulation around magma bodies will help to understand not only the thermal signatures observed over magma bodies at the earth's surfaces, but also those observed from boreholes (CSDP). The study of hydrothermal circulation around magma bodies in a permeable medium will also be applicable to the study of mineral deposition. Energy extraction using open systems in hot, plastic rock may have application below present geothermal fields. Investigating energy extraction rates in the margins near a magma body can provide important information for intermediate systems in the temperature range between magma and hot dry rock. Finally, data obtained from the heater experiment may show that this method can be used effectively to measure in-situ thermal conductivity at high temperature.

Characterization of Kilauea Iki Lava Lake Core Samples (W. C. Luth and T. M. Gerlach, 5541)

Introduction--The Kilauea Iki drill core studies have three direct applications to the Magma Energy Research Project:

(1) To constrain and check geophysical models of the lava lake by providing data on vertical and lateral variations in its petrological properties.

(2) To provide information for assessing the practicality and design of future energy extraction experiments in the lake.

(3) To examine the geochemical responses of magma and hot rock to thermal perturbations caused by drilling fluids and energy extraction, and to compare these with the effects of natural cooling processes.

In addition to filling the above project needs, the core characterization studies provide information of considerable scientific significance. Kilauea Iki lava lake qualifies as a field model for a basic igneous intrusion of modest size ($38 \times 10^6$ $m^3$), formed under exceptionally well-documented

conditions (P,T,X,t) from magmas with minor volatile concentrations, and sampled at various stages of its cooling history. The lava lake also provides a rare opportunity to obtain, analyze, and interpret high temperature specimens, including melt phase, before the imposition of modifications by subsolidus recrystallization. These factors make Kilauea Iki lava lake an attractive field cruicible for examining differentiation processes and the degree of phase equilibria in a real crystallizing magma.

Accurate and precise data on the proportions and compositions of mineral and glass phases in the drill core samples are required by both project needs and scientific questions. From such data, it is possible to ascertain the overall petrologic "state" of the lake, including the amount of remaining liquid. Data on variations in composition within and between grains of the same mineral provide information on the importance of equilibrium crystallization and can yield clues to processes active during and subsequent to magmatic crystallization. Preliminary examinations of the Kilauea Iki thin sections indicated, however, that large amounts of modal and chemical data would be necessary to obtain statistically significant sample characterizations, because of the magnitude of textural variations and both intra- and inter-grain composition variations in olivines and plagioclases.

Data Acquisition--The automated CAMECA CAMBAX electron microprobe operation facility, developed by W. F. Chambers (Div. 5822), was employed to acquire large numbers of individual analyses from each thin section at minimum manpower costs. This system is fully automated with respect to beam current, spectrometer motion, and crystal changing, X, Y, and Z stage motion, element distribution mapping and photography, and data reduction by Bence-Albee or AZF methods.

Twelve-element (SI, Al, Mg, Fe, Ca, Na, K, P, Ti, Cr, Mn, and Ni) quantitative analyses have been obtained on Kilauea Iki glass and mineral phases. Typical instrumental conditions for the analyses are:

1. 15 kV, 12 nA beam 2-5 m, square raster beam

2. Mg, Na, Al, Si, P, TAP — 10 sec maximum count

   K, Ca, Ti — PET — spectrometers running asynchronously

   Cr, Mn, Fe, Ni $XIl_3$ — LIF

3. Bence Albee data reduction scheme using crystal standards

The automated procedure employed here requires programmed definition of points forming ends of vectors on the thin section and specification of the number of points and the step interval between them. Vectors are selected to eliminate backlash in X and Y. Then, in an unattended mode of operation, the analytic data are collected, reduced, listed, and stored on flexible disc. Typically, some three to four hundred analyses (each requiring about 2.9 minutes) are collected along three vectors subparallel to the long axis of the thin section.

Periodic analyses of a standard basaltic glass sample (from Makaopuhi lava lake (1969), provided by R. Helz of the U.S.G.S.) during analytical runs provided "corrections" for glass analyses. Time dependent instrumental drift was not observed for any sample and deviations in analytical values from the reference values were less than the uncertainty attributed to counting statistics. The glass analyses, nevertheless, have been "corrected" to the Makaopuhi glass standard to provide a consistent basis for comparison with the results of other researchers.

Independent replications were obtained for 4 thin sections, and petrographic optical modes of 1000 points were counted for 10 sections. Several hundred spot microprobe analyses, under direct operator control, were also obtained; these agreed with those collected in the automated fashion.

In addition to the microprobe data, H. Westrich (5541) obtained 4 XRF wholerock analyses during FY80 on equipment at Arizona State University. A procedure is currently under development for acquiring additional wholerock analyses with the XRF facility at Sandia Labs.

Data Reduction--During FY80 approximately 13,000 automated twelve-element analyses were collected (Table 2). It was therefore necessary to develop a computer-based data reduction procedure (PETRA) for rapid and consistent processing of the data.

The analytical data are stored on a mass storage device that can be randomly accessed from calls in PETRA during execution on a CDC 7600 system. The data are processed in blocks corresponding to all analyses collected during three-vector traverses across a thin section. The following information is obtained for each thin section:

(1) Each analysis is examined relative to chemical parameters that are used to determine if it is a mineral, glass, or "other" (mixed phases, cracks, pores, etc.). PETRA is currently capable of identifying 10 common igneous rock-forming mineral groups (olivines, clinopyroxenes, low-Ca pyroxenes, plagioclases, alkali feldspars, etc.).

(2) The volume proportions of each phase are calculated from the results of (1). A significant number (15%) of analyses are mixtures of phases or epoxy filled cracks and voids. PETRA is capable of identifying these analyses and dropping them from the mode calculations. The 95% and 99% confidence levels are calculated for the volume proportions.

(3) The variations in composition of each phase are expressed and displayed in several forms:

(a) Analyses are listed in order of increasing amounts of an oxide of interest (e.g., CaO for Plagioclase, MgO for olivines and pyroxenes, $SiO_2$ for glasses).

(b) The analyses are displayed on oxide composition diagrams (Fig. 8), frequency diagrams (Fig. 9), and cumulative frequency diagrams (Fig. 10). These diagrams are useful for expressing

Table 2

Kilauea Iki Sample Analysis Status

| Hole | Depth (m) | Reference | Probe Data | Probe Data Reduced | XRF Whole Rock |
|---|---|---|---|---|---|
| 79-2-06.10 | | 20 | | | |
| | -12.19 | 40 | X | Y | |
| | -18.29 | 60 | | | |
| | -24.38 | 80 | | | |
| | -30.48 | 100 | X | N | |
| | -36.58 | 120 | | | |
| | -40.75 | 140 | X | Y | |
| | -42.95 | 1 | X | N | |
| | -43.16 | 2 | | | |
| | -43.65 | 3 | X | N | |
| | -43.89 | 4 | | | |
| | -44.14 | 5 | X | N | |
| | -44.32 | 6 | | | |
| | -44.53 | 7 | | | |
| | -44.74 | 8 | | | |
| | -44.87 | 9 | | | |
| | -45.29 | 10 | X | Y | |
| | -46.33 | 160 | | | |
| | -48.19 | 165 | X | Y | |
| | -49.38 | 170 | X | Y | |
| | -50.51 | 175 | X | Y | |
| 79-1-50.62 | | 1 | X | Y | |
| | -51.89 | 2 | X | Y | |
| | -53.01 | 3 | X | Y | |
| | -53.95 | 4 | X | Y | |
| | -55.25 | 5 | X | Y | |
| | -56.49 | 6 | X | Y | |
| | -57.61 | 7 | X | Y | |
| | -58.83 | 8 | X | Y | |
| | -59.74 | 9 | X | Y | |
| | -60.35 | 10 | X | Y | |
| | -60.96 | 11 | X | Y | |

X refers to automated probe analyses.

S refers to spot probe analyses.

| Hole | Depth (m) | Reference | Probe Data | Probe Data Reduced | XRF Whole Rock |
|---|---|---|---|---|---|
| 79-6-47.42 | | 155-7 | | | |
| | -49.63 | 162.10 | | | |
| | .50.11 | 164.5 | X | N | |
| | -50.83 | 166-9 | | | |
| | -51.77 | 169-10 | | | |
| | -52.76 | 173-1 | X | Y | |
| | -53.21 | 174.7 | | | |
| | -53.52 | 175-7 | | | |
| | -54.18 | 177-9 | X | N | X |
| | -54.64 | 179-3 | X | Y | X |
| | -55.25 | 181-3 | X | N | X |
| | -56.24 | 184-6 | | | |
| | -56.72 | 186-1 | X | N | |
| | -57.12 | 187-5 | X | N | X |
| | -57.43 | 188-5 | | | |
| | -57.66 | 189-2 | X | Y | X |
| | -57.91 | 190-0 | X | N | |
| 79-5-08.33 | | 1 | S | | |
| | -15.14 | 2 | S | | |
| | -22.76 | 3 | S | | |
| | -30.48 | 4 | S | | |
| | -38.25 | 5 | | | |
| | -46.02 | 6 | S | | |
| | -48.46 | 7 | | | |
| | -51.82 | 8 | S | | |
| | -54.86 | 9 | | | |
| | -57.99 | 10 | S | | |
| | -60.85 | 11 | | | |
| | -64.36 | 12 | S | | |
| | -66.95 | 13 | | | |
| | -70.10 | 14 | | | |
| | -73.15 | 15 | | | |
| | -76.20 | 16 | | | |
| | -80.92 | 17 | | | |
| | -85.04 | 18 | | | |
| | -89.81 | 19 | | | |
| | -94.64 | | | | |

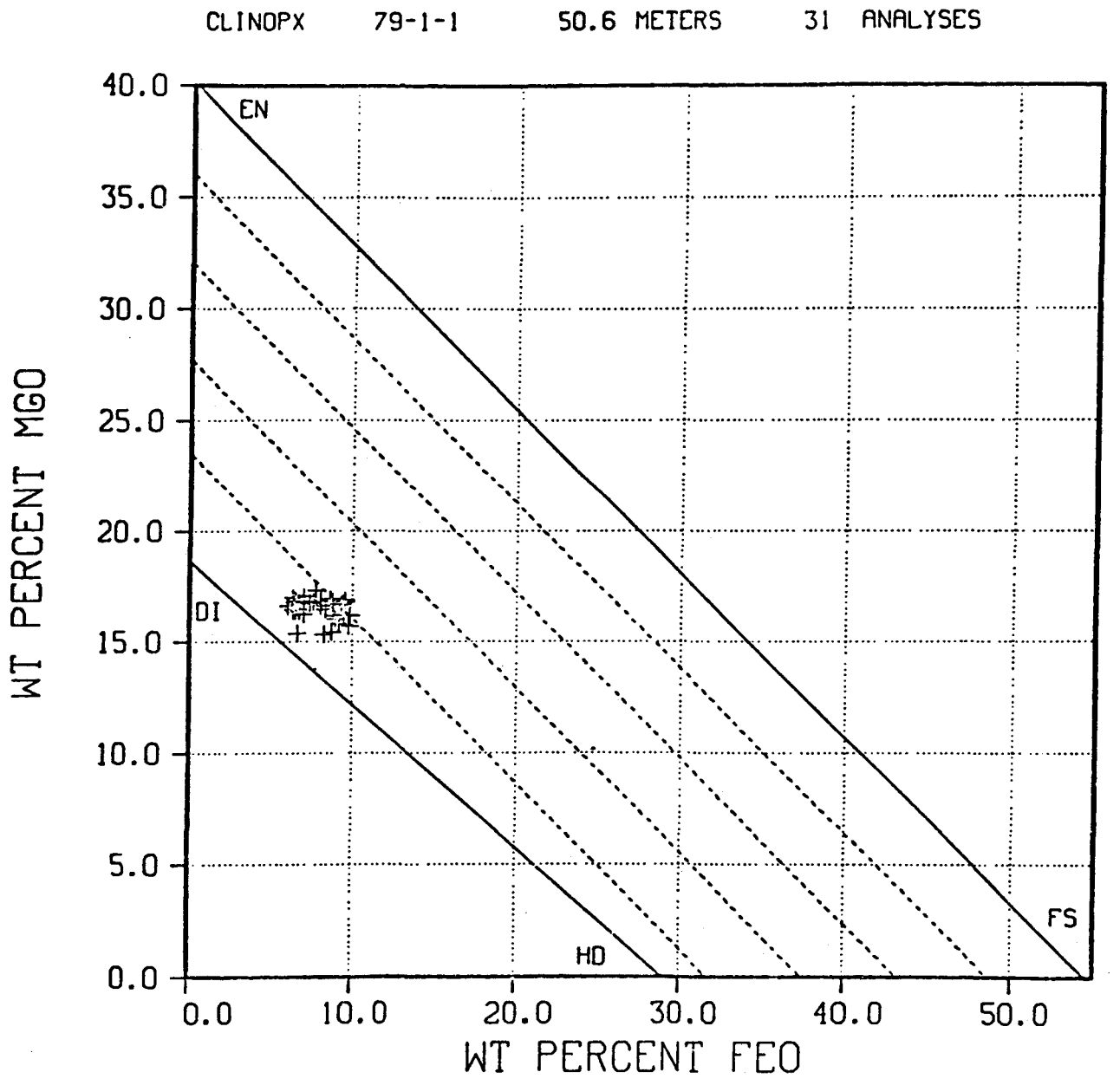


Figure 8. Oxide composition plot for 31 clinopyroxene analyses of sample 79-1-1 (50.6 m). The clinopyroxene compositions (+) are expressed in terms of weight percent MgO and FeO. The weight percent MgO and FeO are also shown for the reference compositions EN($MgSiO_3$), FS($FeSiO_3$), Di($CaMgSi_2O_6$), and HD($CaFeSi_2O_6$). The dashed lines show weight percent MgO and FeO for ideal clinopyroxenes with weight percent CaO increasing in increments of 5% from the EN-FS join.

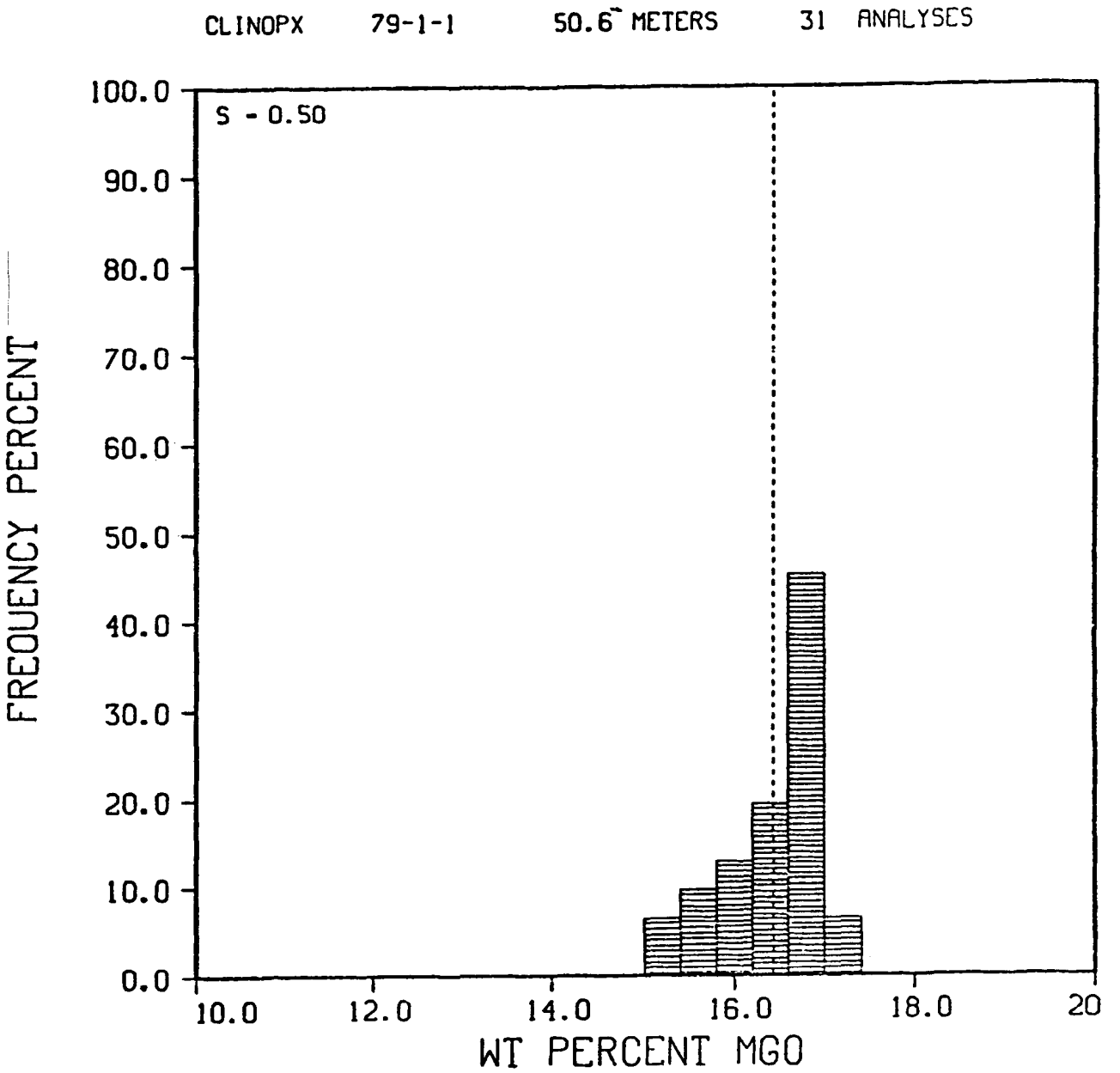


Figure 9. Weight percent MgO frequency plot for 31 clinopyroxenes from sample 79-1-1 (50.6 m). The dashed line indicates the mean MgO wt.% for the 31 clinopyroxenes; standard deviation (s) is .50.

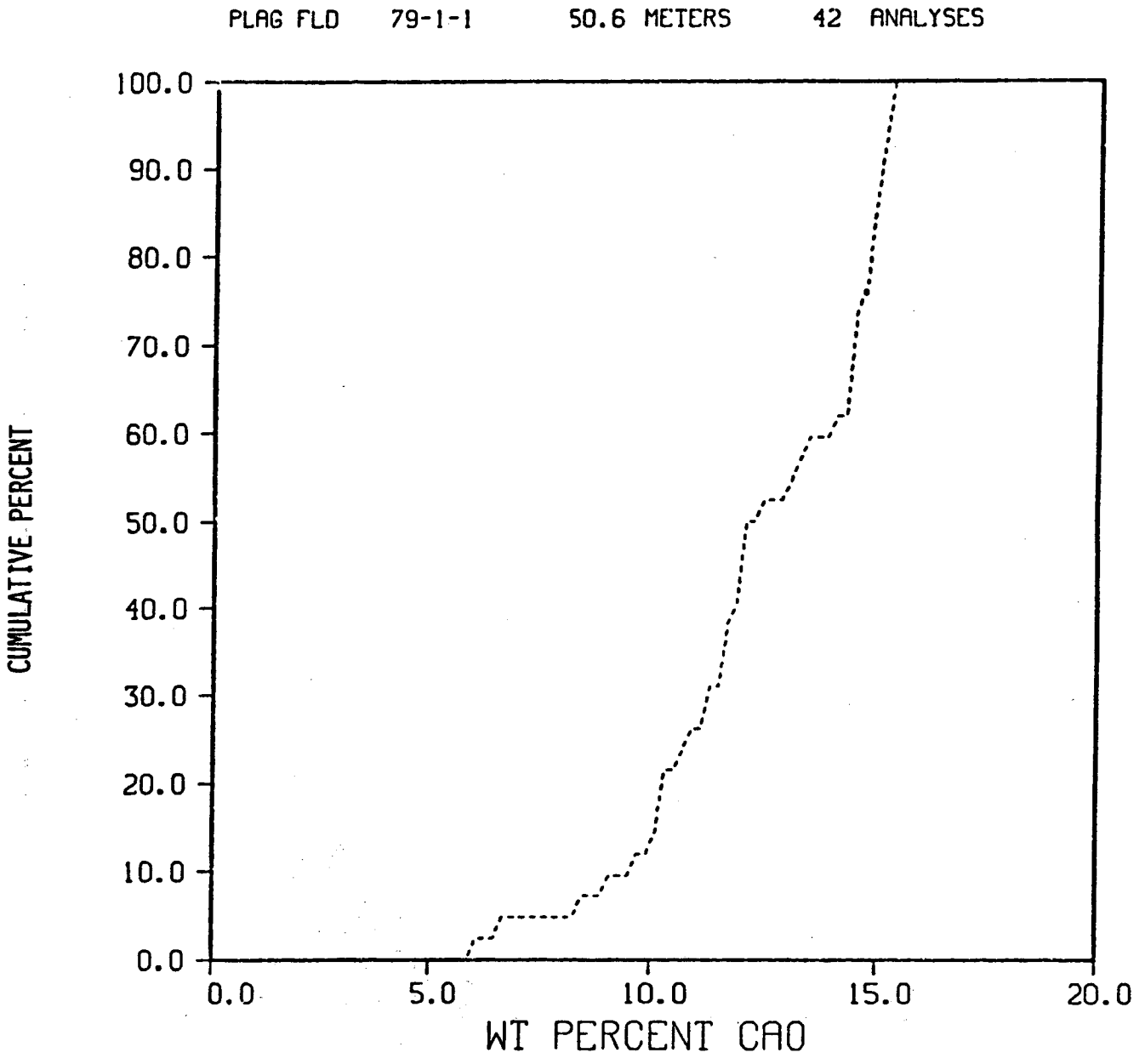


Figure 10. Weight percent CaO cumulative frequency plot for 42 plagioclase analyses from sample 79-1-1 (50.6 m).

sample variance characteristics, finding anomalous analyses, and identifying clusters of analyses.

(c) The difference between the sample and population means is calculated at the 95% and 99% confidence levels for the major oxides of each phase. These differences are compared with precision limits based on instrument counting statistics to determine if more analytical data are warranted. If the differences are less than counting statistics uncertainties, there is no object in collecting more data.

(4) The analyses of mixtures of two or more phases are listed as a special group, and can be resolved into their constituent phases by mass balance calculations. This information is useful for characterizing the chemistry of interface regions of the rock.

(5) The weight percent modes and an estimated wholerock composition are computed from the mean compositions of the phases, the volume percent modes, and the estimated phase densities.

(6) All the above results are output on hard copy and microfiche.

Compositions, Proportions, and Distributions of Major Phases--Approximately two-thirds of the data obtained in FY80 has been reduced (Table 2) and forms the basis for the results presented in the remainder of this report. Most of the reduced data summarized here are from drill hole 79-1, but similar if not identical petrologic characteristics are evident so far in the reduced data from drill holes 79-2 and 79-6. The data reduced thus far led to the conclusion that drill holes 79-1, 79-2, and 79-6 intersected a magma lens. Drill hole 79-1 penetrated through the magma lens, but did not extend into the rock (lower crust?) below it. The possibility of other magma lenses below the one defined by present drilling seems remote, but cannot be dismissed at this time.

The 20 samples of reduced data from the 3 drill holes define 4 zones within the lava lake. The depths of the zones in the 3 holes suggest a centrally located magma body in the upper half of the lake. At 79-1, 87 m north of the lake's center, the zones are defined as follows:

(1) Upper crust (UC), 0-50.5 m.
(2) Upper Masgmatic Transition Zone (UMTZ), 50.5-54. m.
(3) Magma Zone (MS), 54.-61 m.
(4) Lower Magmatic Transition Zone (LMTZ), 61-63 (?) m.

Glass compositions (Table 3) define smooth continuous paths on oxide variation and AFM diagrams (Figs. 11 and 12), ranging from quartz basalt compositions in the LMTZ and MS to rhyolitic compositions in the UMTZ and UC. Glass compositions (Fig. 13) change only slightly in composition in the MZ and LMTZ, although glass modal abundances (vol.%) decrease from 35% in the MZ to 15% in the LMTZ (Fig. 14). Glass modal abundances decrease in the UMTZ and UC (5%), accompanying the major composition change (Fig. 13).

Olivine compositions (Fig. 15) are essentially constant ($Fo(wt)_{72}$) in the MZ and LMTZ, with a range from $Fo_{70-75}$ and no significant compositional differences between phenocrysts and microphenocrysts. Mean compositions become less Fo-rich and show greater dispersion about the mean in the UMTZ and UC (Fig. 15). Olivine modal abundance (Fig. 16) vary over a wide range (20%-47%), reflecting in situ crystallization, crystal settling, and subsolidus recrystallization.

Plagioclase modal abundances are constant (15%) in the MZ and LMTZ, increasing to 30%-35% in the UMTZ and UC (Fig. 17). Mean plagioclase compositions decrease from $An_{74}$ to $An_{70}$ (wt.) with decreasing depth in the LMTZ and MZ (Fig. 18). Mean compositions become more sodic ($An_{55}$) and compositional dispersion increases in the UMTZ and UC (Fig. 18).

Clinopyroxene modal abundances are constant (20%) in the MZ and LMTZ; they increase to 30% in the UMTZ (Fig. 19). Clinopyroxene compositions

Table 3.
Kilauea Iki (1959) Lava Lake Glass Compositions
Automated Analyses

| Hole | 79-2 | 79-2 | 79-2 | 79-2 | 79-2 | 79-2 | 79-1 | 79-1 | 79-1 | 79-1 | 79-1 | 79-1 | 79-1 |
|---|---|---|---|---|---|---|---|---|---|---|---|---|---|
| Depth | 12.19 | 40.75 | 45.29 | 48.19 | 49.38 | 50.51 | 50.62 | 50.62 | 51.89 | 51.89 | 53.01 | 53.95 | 53.95 |
| $SiO_2$ | 74.37 | 75.65 | 74.28 | 65.21 | 57.54 | 52.26 | 67.10 | 66.16 | 59.26 | 58.86 | 56.36 | 52.32 | 52.29 |
| $Al_2O_3$ | 13.82 | 13.03 | 13.11 | 15.62 | 14.19 | 12.45 | 15.59 | 15.40 | 14.43 | 14.26 | 13.82 | 13.17 | 13.15 |
| FeO | 1.28 | 1.57 | 1.90 | 5.05 | 9.30 | 13.13 | 4.13 | 4.49 | 8.18 | 8.59 | 9.76 | 11.32 | 11.37 |
| MgO | .05 | .10 | .15 | 1.42 | 3.13 | 4.23 | 1.03 | 1.19 | 2.82 | 2.89 | 3.91 | 4.80 | 4.72 |
| CaO | .29 | .48 | .51 | 2.67 | 5.86 | 7.96 | 32.13 | 2.36 | 5.32 | 5.26 | 6.75 | 8.20 | 8.22 |
| $Na_2O$ | 2.66 | 3.46 | 3.55 | 4.32 | 3.38 | 3.22 | 4.00 | 4.21 | 3.53 | 3.72 | 3.21 | 2.78 | 2.88 |
| $K_2O$ | 5.88 | 4.97 | 5.24 | 3.57 | 2.29 | 1.23 | 4.02 | 4.01 | 2.43 | 2.47 | 1.63 | 1.12 | 1.14 |
| $TiO_2$ | 1.42 | .57 | 1.10 | 1.55 | 3.01 | 4.53 | 1.54 | 1.61 | 2.68 | 2.57 | 3.62 | 5.51 | 5.43 |
| $Cr_2O_3$ | .02 | .01 | .02 | .02 | .01 | .02 | .02 | .02 | .02 | .03 | .02 | .02 | .03 |
| $P_2O_5$ | .15 | .11 | .09 | .47 | 1.06 | .73 | .33 | .48 | 1.21 | 1.19 | .78 | .55 | .56 |
| MnO | .05 | .02 | .04 | .05 | .18 | .21 | .06 | .05 | .11 | .13 | .12 | .20 | .18 |
| NiO | 0 | .01 | 0 | .05 | .04 | .03 | .04 | .02 | .02 | .03 | .02 | 0 | .03 |
| Anal. | 98.86* | 99.99 | 99.16 | 100.28 | 97.54 | | 99.89 | 97.20 | 98.76 | 96.80 | 96.52 | 96.59 | 97.05 |
| n | 2** | 11 | 7 | 11 | 33 | 181 | 12 | 22 | 16 | 35 | 39 | 13 | 87 |

| Hole | 79-1 | 79-1 | 79-1 | 79-1 | 79-1 | 79-1 | 79-1 | 79-1 | 79-1 | 79-1 | 79-6 | 79-6 | 79-6 |
|---|---|---|---|---|---|---|---|---|---|---|---|---|---|
| Depth | 55.25 | 56.49 | 57.61 | 58.83 | 59.74 | 59.74 | 59.74 | 59.74 | 60.35 | 60.96 | 52.76 | 54.64 | 57.66 |
| $SiO_2$ | 51.67 | 51.63 | 51.17 | 51.58 | 50.82 | 50.86 | 51.22 | 51.03 | 51.41 | 51.02 | 60.14 | 52.19 | 51.63 |
| $Al_2O_3$ | 13.47 | 13.16 | 13.72 | 13.64 | 13.90 | 13.85 | 14.30 | 13.85 | 14.02 | 14.01 | 14.55 | 13.23 | 13.47 |
| FeO | 11.24 | 12.07 | 11.47 | 11.19 | 11.20 | 11.38 | 10.82 | 11.55 | 11.14 | 11.08 | 7.22 | 11.09 | 11.40 |
| MgO | 5.33 | 4.99 | 5.70 | 5.87 | 6.02 | 5.83 | 6.05 | 5.98 | 6.07 | 6.10 | 2.74 | 5.04 | 5.36 |
| CaO | 8.98 | 8.80 | 9.74 | 9.85 | 10.23 | 10.09 | 9.78 | 9.75 | 9.78 | 10.10 | 4.94 | 8.44 | 9.05 |
| $Na_2O$ | 3.01 | 2.94 | 2.85 | 2.68 | 2.90 | 2.80 | 2.78 | 2.72 | 2.71 | 2.70 | 4.01 | 2.95 | 2.99 |
| $K_2O$ | .96 | .88 | .83 | .78 | .75 | .78 | .78 | .79 | .74 | .75 | 2.64 | 1.09 | .98 |
| $TiO_2$ | 4.70 | 4.82 | 3.93 | 3.83 | 3.56 | 3.79 | 3.59 | 3.73 | 3.48 | 3.65 | 2.42 | 5.23 | 4.48 |
| $Cr_2O_3$ | .03 | .02 | .03 | .04 | .03 | .04 | .03 | .03 | .05 | .04 | .02 | .04 | .03 |
| $P_2O_5$ | .46 | .48 | .37 | .34 | .37 | .37 | .48 | .36 | .36 | .35 | 1.23 | .50 | .42 |
| MnO | .16 | .18 | .16 | .15 | .19 | .17 | .15 | .18 | .19 | .16 | .08 | .16 | .15 |
| NiO | ND | .03 | .03 | .04 | .03 | .04 | .02 | .03 | .03 | .02 | .03 | .04 | .05 |
| Anal. | 96.85* | 98.37 | 97.86 | 98.44 | 98.31 | 98.37 | 99.66 | 96.91 | 97.65 | 98.30 | 98.33 | 98.01 | 98.49 |
| n | 80** | 96 | 64 | 9 | 83 | 137 | 44 | 90 | 48 | 41 | 17 | 74 | 58 |

*Anal. refers to mean of oxide totals for raw data; oxide values normalized to 100%.
**n refers to number of individual analyses.

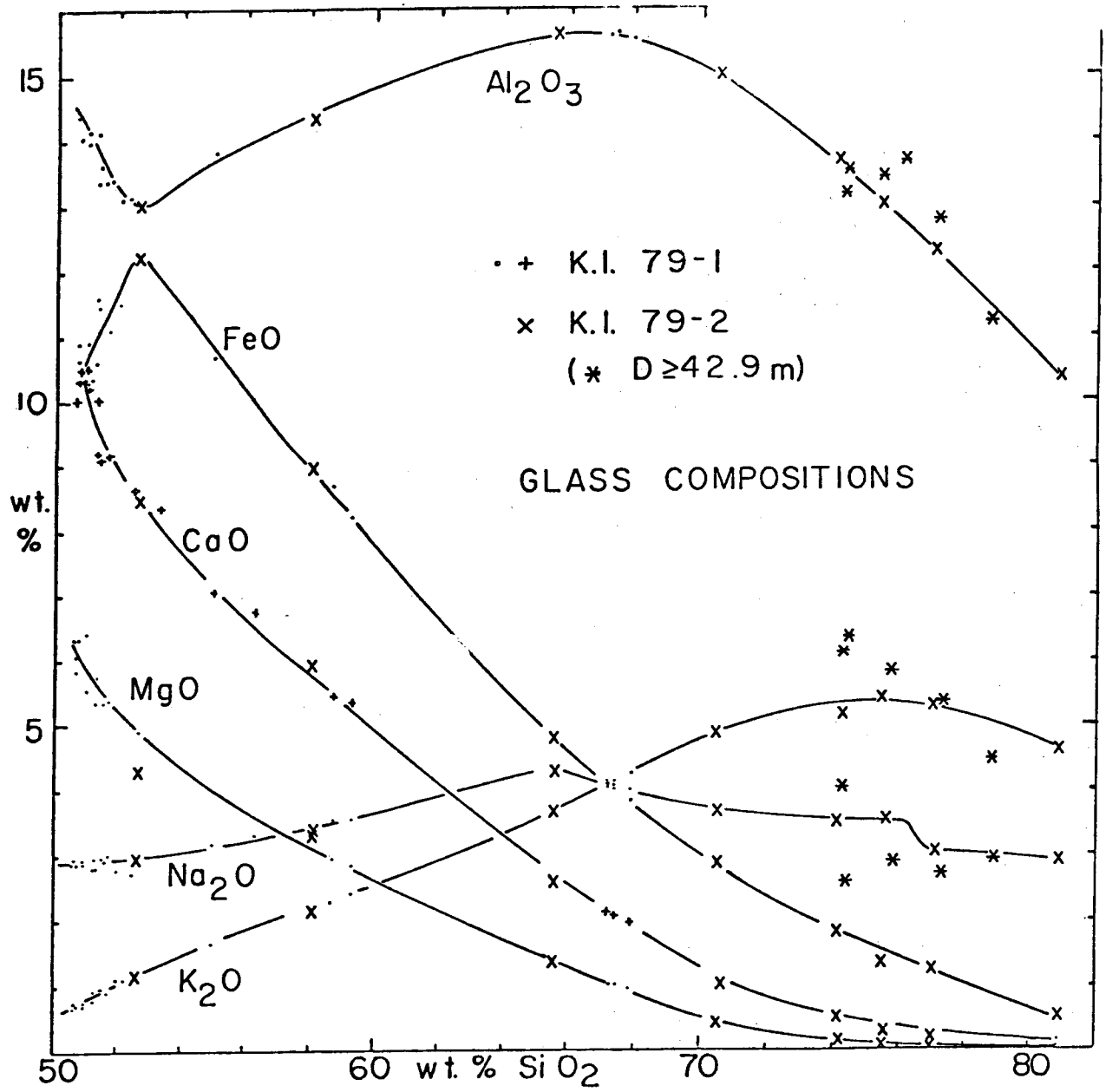


**Figure 11.** Oxide variation diagram for Kilauea Iki glasses from drill holes 79-1 (+) and 79-2 (X and *).

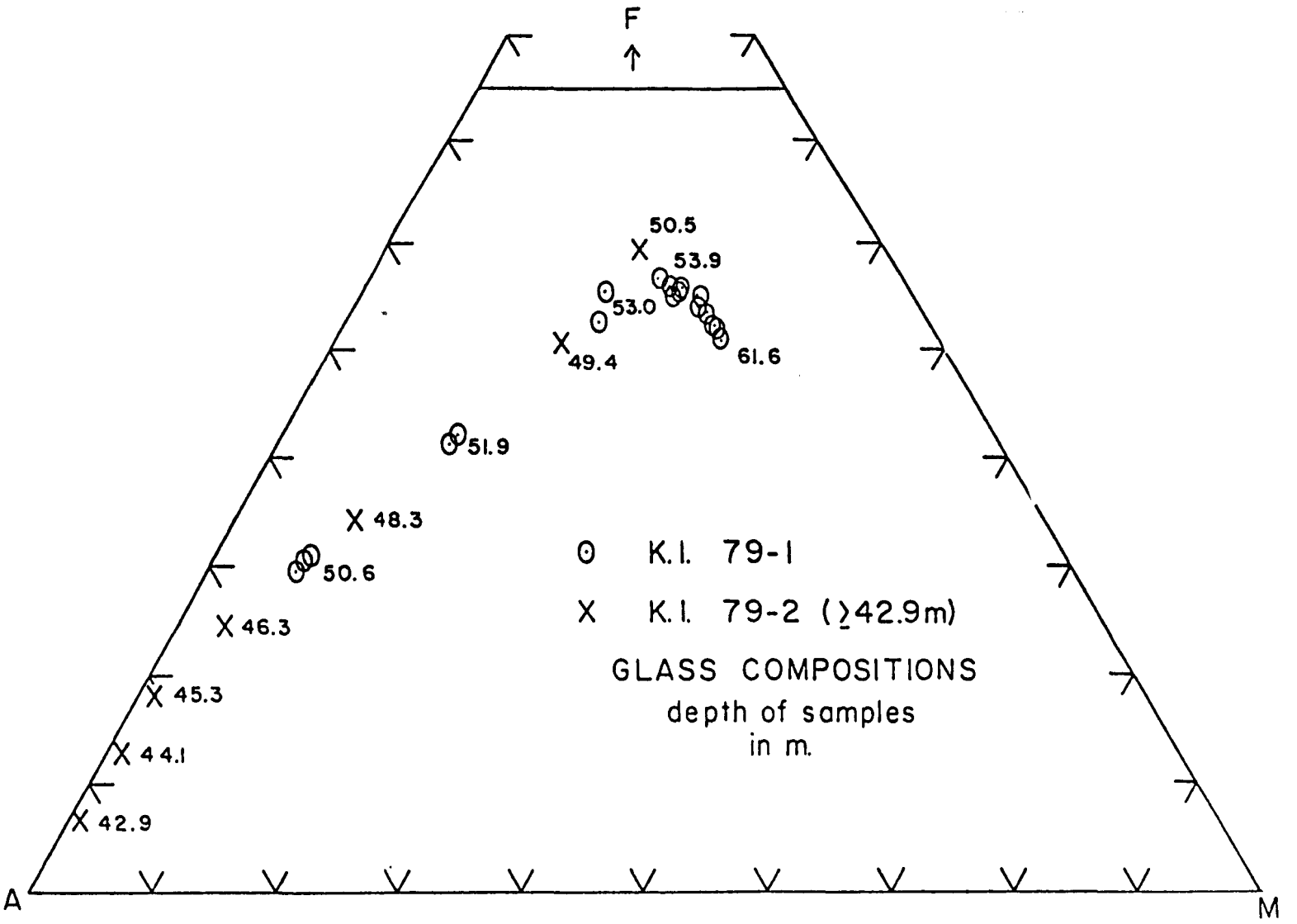


Figure 12. AMF diagram for Kilauea Iki glasses from drill holes 79-1 (0) and 79-2 (X). Sample depths indicated in meters.

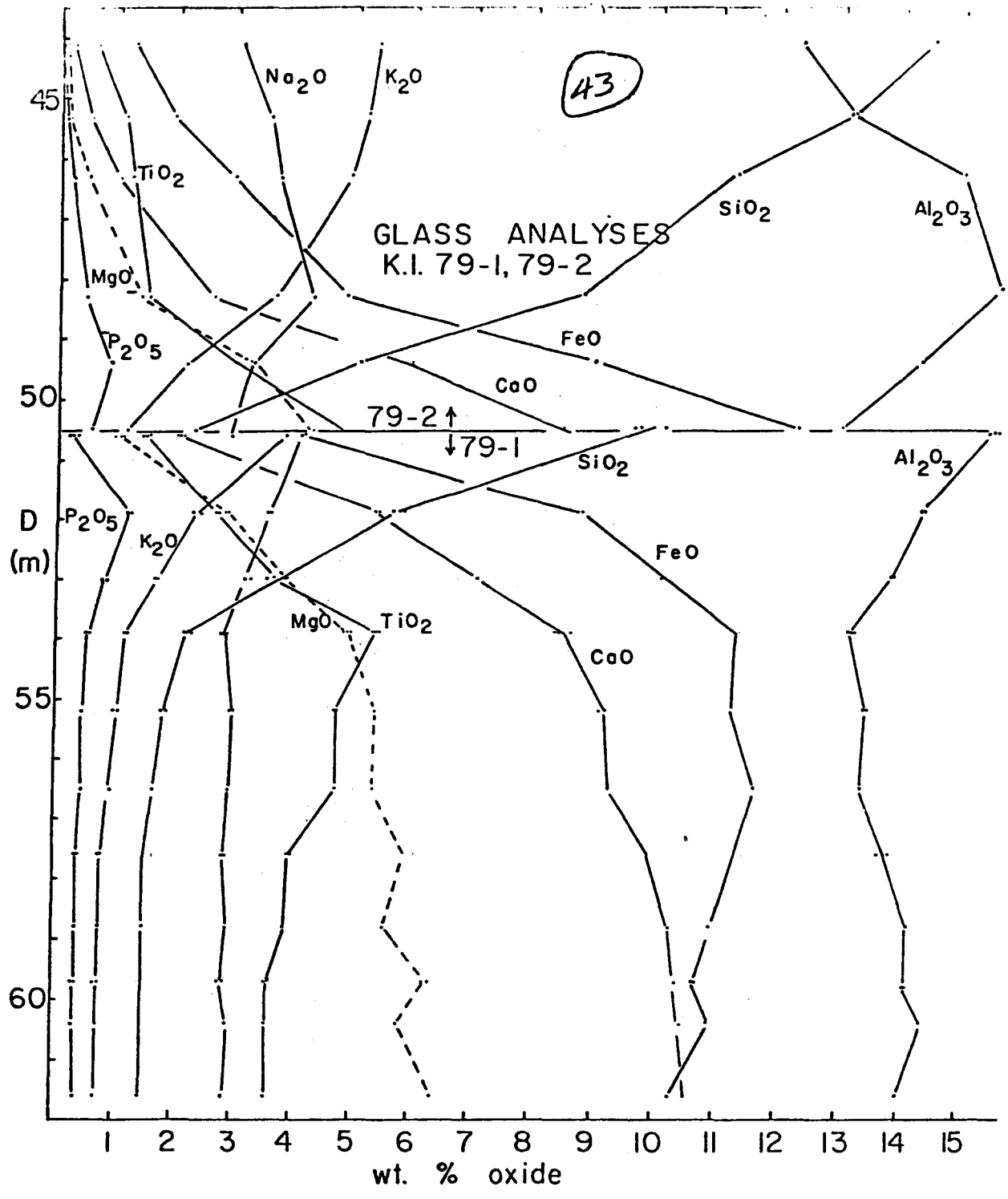


Figure 13. Oxide weight percent vs. depth (m) in drill holes 79-1 and 79.2.

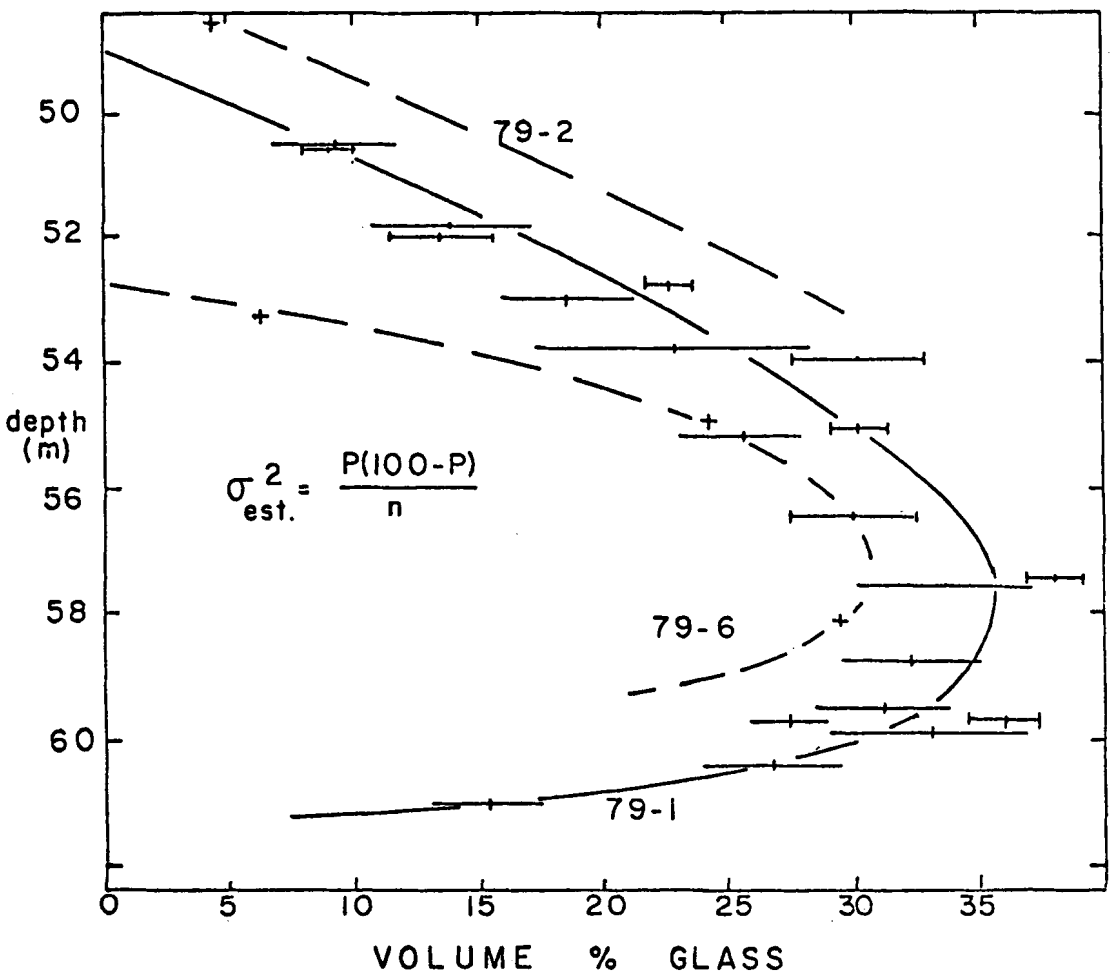


**Figure 14.** Volume percent glass vs depth (m). Smoothed and nearly solid curve is for drill hole 79-1. Dashed curves are based on available reduced data for drill holes 79-2 and 79-6. One standard deviation uncertaintaies are shown for 79-1 data. Uncertainty intervals for optical modes are bounded by vertical ticks; probe mode uncertainties are not. Replicates for 79-1 are slightly displaced vertically for clarity.

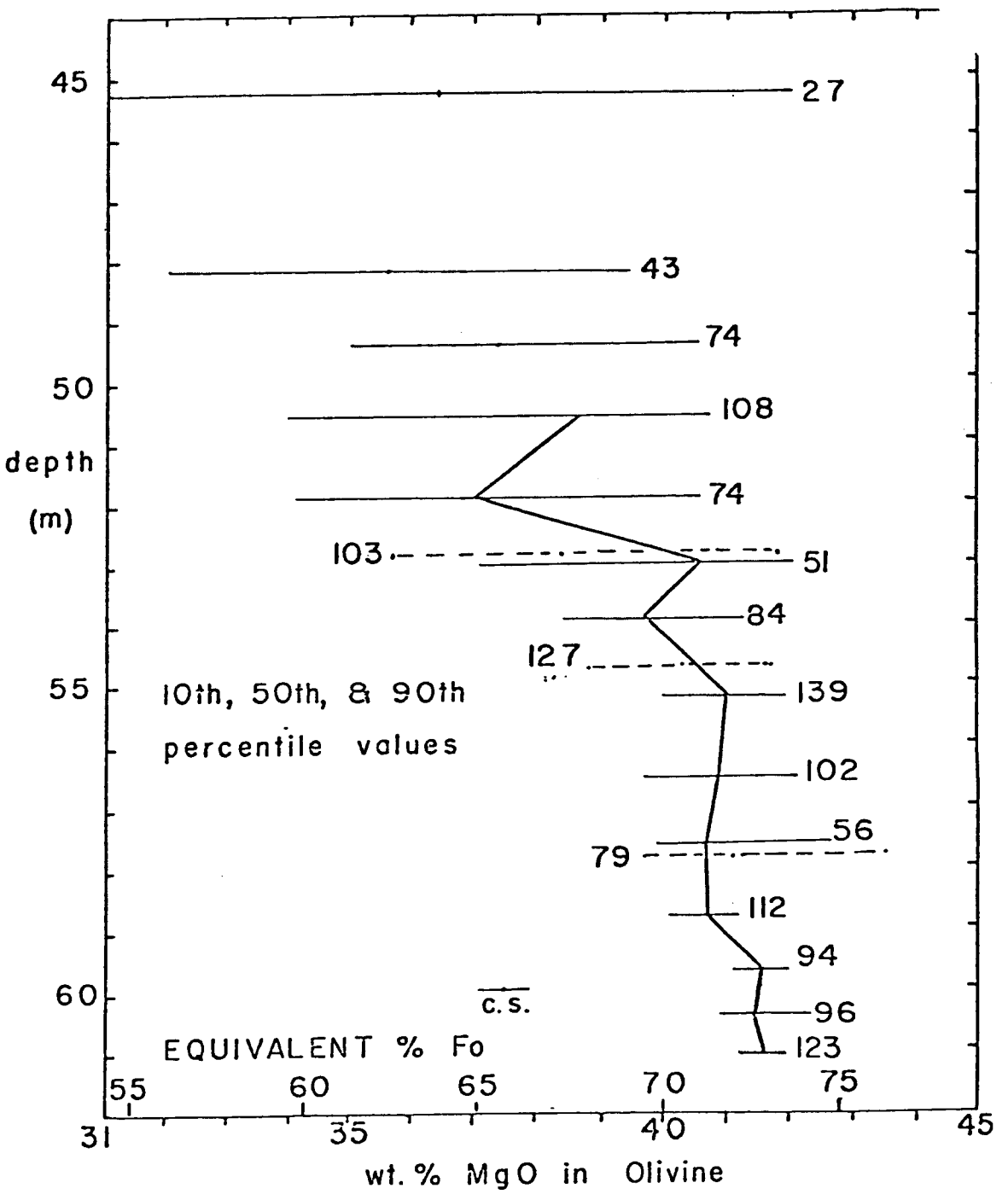


Figure 15. Olivine composition dispersion vs. depth (m) based on probe data for drill holes 79-1, 79-2, and 79-6. Compositions are scaled in eight percent MgO and Fo (wt.). Solid line connects 50th percentile values. Numbers indicate total olivine analyses for each sample. Dashed lines are for 79-6. C.S. refers to counting statistic precision for microprobe data expressed as wt. % MgO.

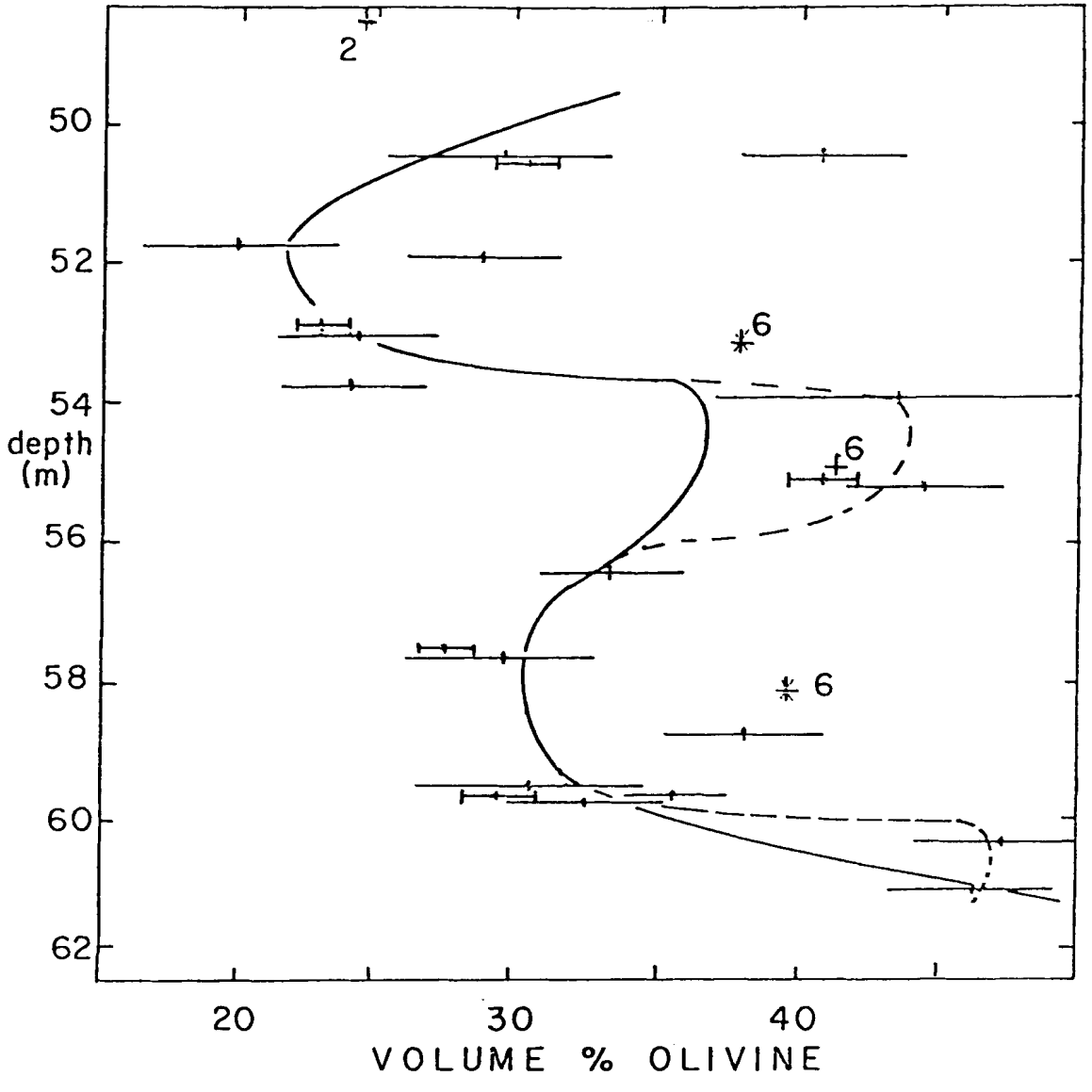


Figure 16. Volume percent olivine vs. depth (m). Smoothed dashed curve is based on data for drill hole 79-1. One standard deviation uncertainties are shown with replicates slightly displaced vertically for clarity. Uncertainty intervals for optical modes are bounded by vertical ticks; probe mode uncertainties are not. Data from 79-2 and 79-6 indicated by X's.

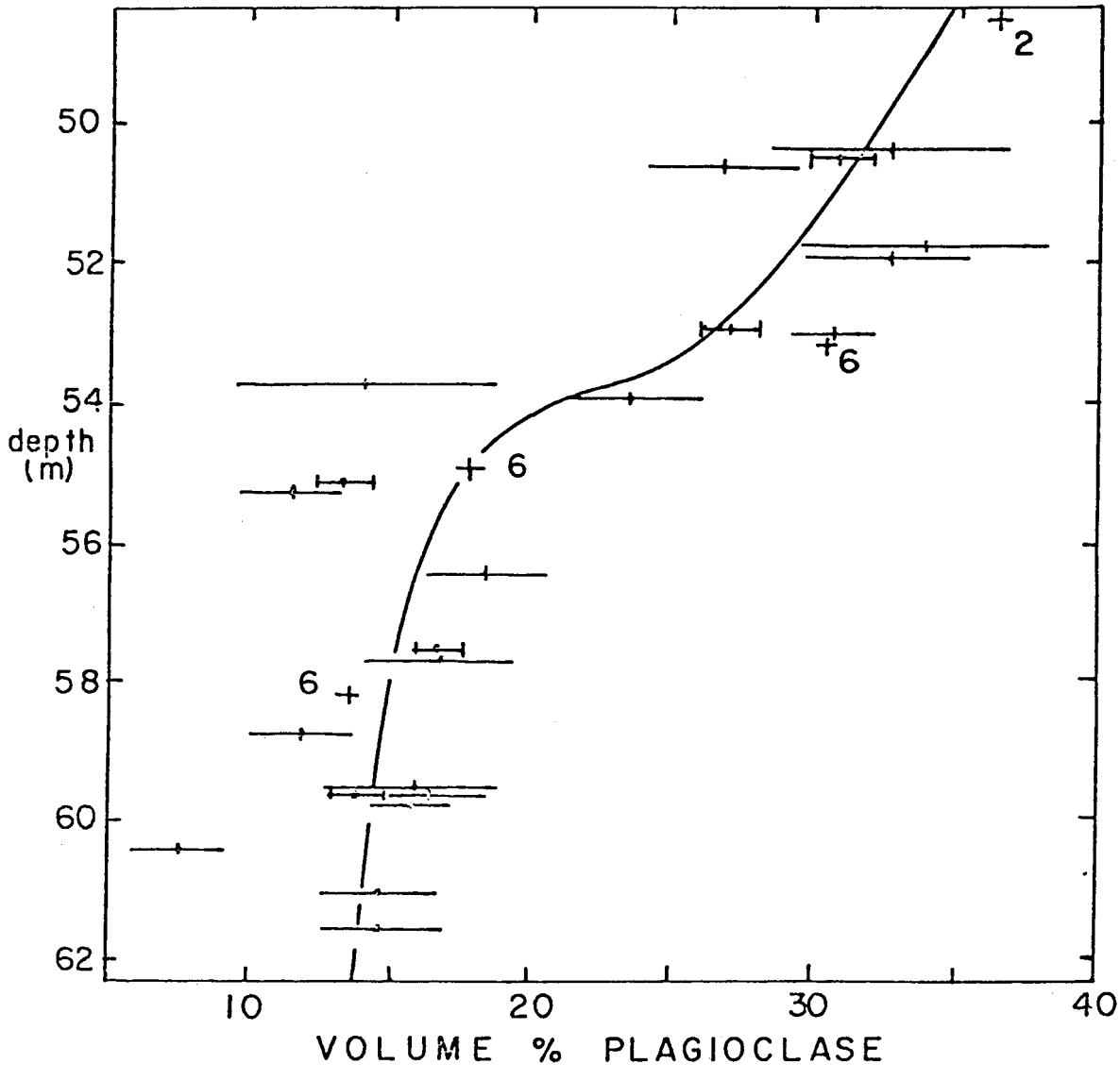


Figure 17. Volume percent plagioclase vs. depth (m). Smoothed dashed line based on data for drill hole 79-1. One standard deviation uncertainties are shown with replicates slightly displaced for clarity. Uncertainty intervals for optical modes are bounded by vertical ticks; probe mode uncertainties are not. X refers to data from 79-2 and 79-6.

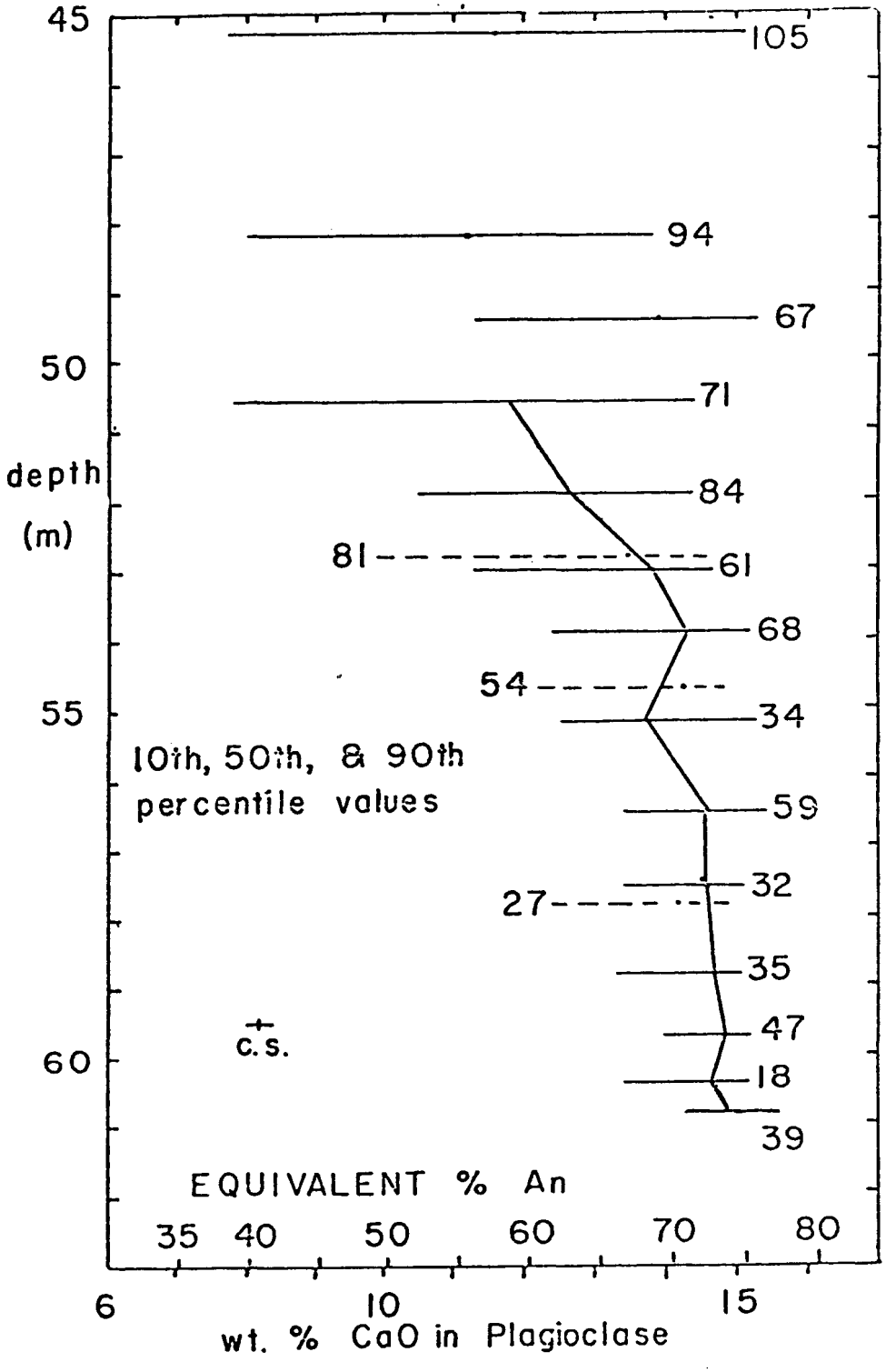


Figure 18. Plagioclase composition dispersion vs. depth (m) based on probe data for drill holes 79-1, 79-2, and 79-6. Compositions are scaled in weight percent CaO and An (wt.). Solid line connects 50th percentile values. Numbers indicate total plagioclase analyses for each sample. Dashed lines are for 79-6. C.S. refers to counting statistic precision for microprobe data expressed as wt.% CaO.

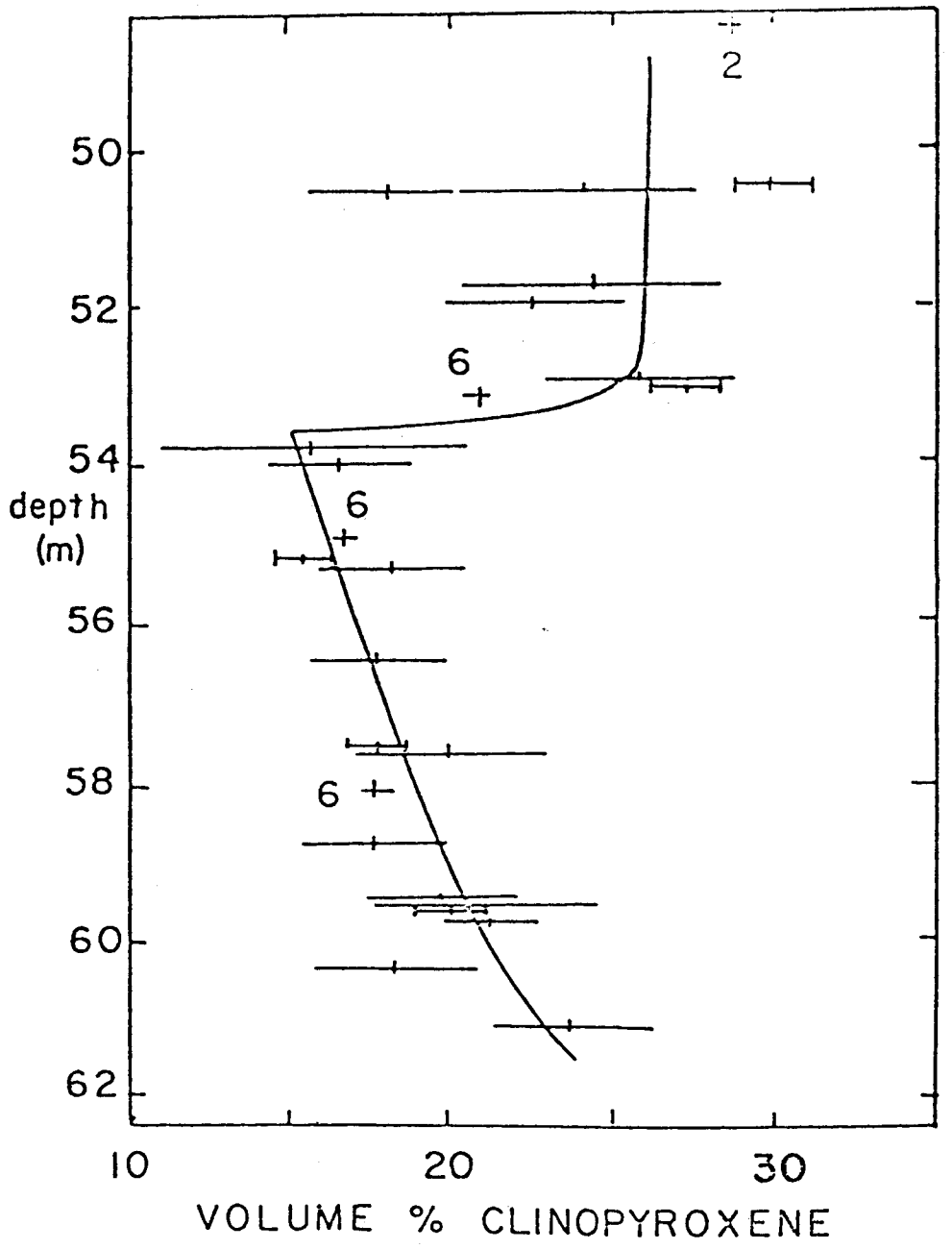


**Figure 19.** Volume percent clinopyroxene vs. depth (m). Smoothed dashed curve is for drill hole 79-1. One standard deviation uncertainties are shown with replicates slightly displaced vertically for clarity. Uncertainty intervals for optical modes are bounded by vertical ticks; probe mode uncertainties are not. X refers to data from 79-2 and 79-6.

are nearly constant ($Wo_{40}EM_{45}Fs_{15}$, wt) in the LMTZ, MZ, UMTZ, and lower part of the upper crust.

Figure 20 summarizes the smoothed modal abundances of the major phases of the 4 zones in drill hole 79-1.

Wholerock Compositions--The estimated wholerock compositions of the lava lake samples (Table 4) are based on the mean compositions of phases in each thin section, estimated phase densities, and the volume proportions of phases as determined from the automated probe data. It can be shown that these estimates are relatively insensitive to any reasonable choice of densities, but they are more sensitive to phase abundance and composition--the two parameters obtained from the probe data. Table 4 also contains the wholerock compositions for three samples of the originally erupted lavas (S15, S7, S5 from Murata and Richter, 1966) for comparison.

Table 5 shows a comparison of four estimated wholerock compositions, with corresponding XRF wholerock compositions obtained in FY80. The agreement is generally good except for MgO and $K_2O$. The discrepancy in MgO is due to the presence of abundant olivine phenocrysts, which can easily cause distortions of small sampling volumes. The XRF analyses consistently give high $K_2O$, by approximately a factor of two, relative to the probe-based estimates. The XRF $K_2O$ data are currently believed to be in error, and an improved set of XRF data for these and several other lava lake samples is a high priority for future work.

Mass Balance Calculations--Several least squares mass balance calculations have been performed on the microprobe data collected in FY80. The purposes of these calculations are to provide quantitative measures of the amounts of differentiation since the formation of the lake and to check the consistency of the newly acquired data with published data for the initial erupted lavas (Muratra and Richter, 1966). The original lavas that formed the lake showed considerable chemical variation almost entirely due to differences in olivine content, suggesting the eruption of lava from a magma chamber compositionally zoned by olivine settling. The mass balance calculations presented here emphasize differentiation that occurred in the

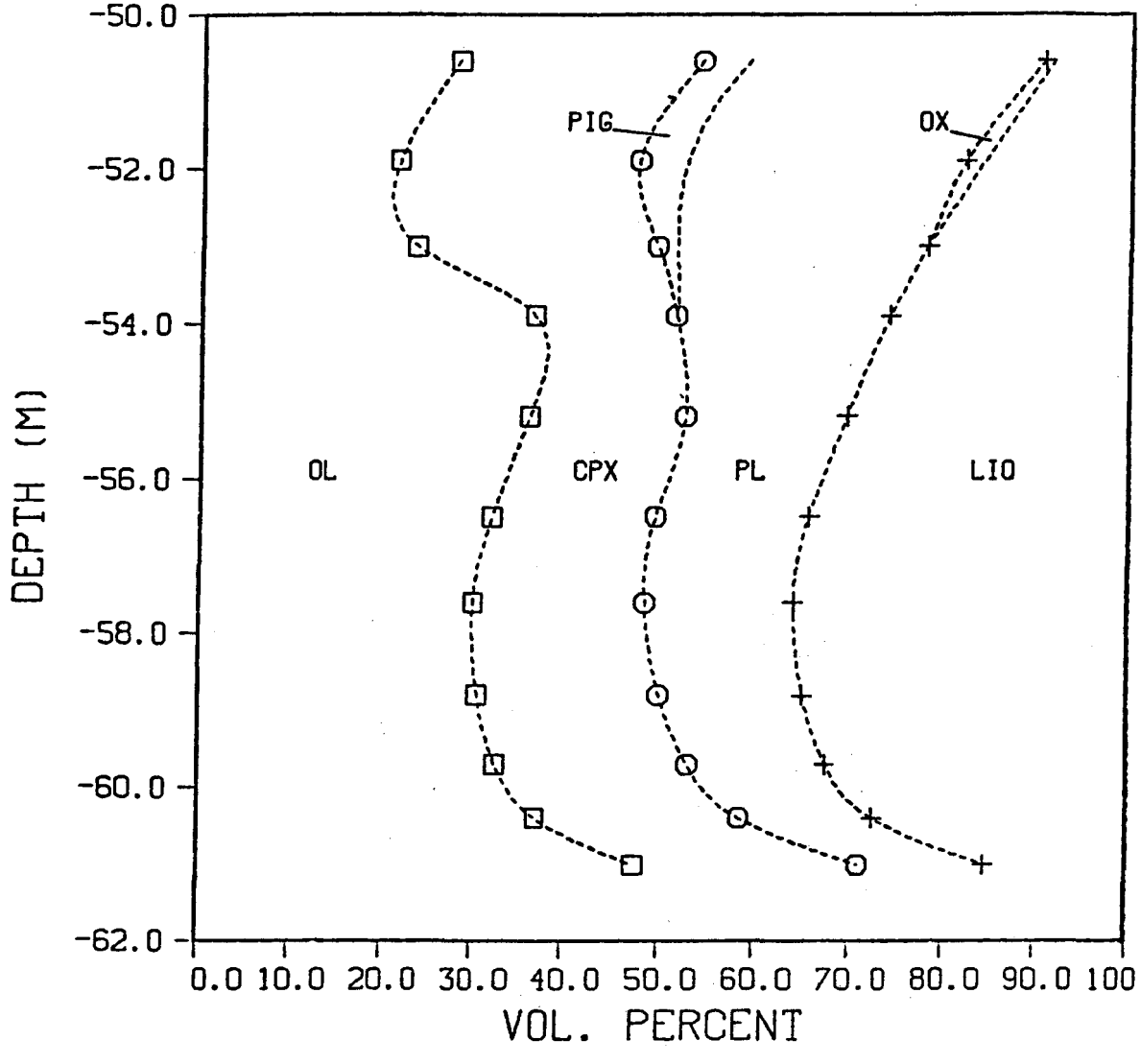


Figure 20. Smoothed modes in cumulative volume percent vs. depth (m) for all data from drill hole 79-1. Field width at a given depth corresponds to volume percent of phase. Sample depths indicated by symbol positions. OL = olivine, CPX = clinopyroxene, PIG = pigeonite, PL = plagioclase, OX = oxide, LIQ = liquid.

Table 4. Estimated Whole Rock Compositions

| | $SiO_2$ | $Al_2O_3$ | FeO | MgO | CaO | $Na_2O$ | $K_2O$ | $TiO_2$ | $Cr_2O_3$ | $P_2O_5$ | MnO | NiO |
|---|---|---|---|---|---|---|---|---|---|---|---|---|
| 79-1-1 | 48.22 | 9.85 | 11.30 | 18.05 | 8.93 | 1.59 | .38 | 1.14 | .17 | .08 | .18 | .10 |
| 79-1-2 | 48.23 | 10.59 | 11.48 | 15.54 | 9.42 | 1.61 | .42 | 2.05 | .17 | .22 | .18 | .09 |
| 79-1-3 | 49.30 | 10.77 | 9.65 | 16.73 | 9.98 | 1.54 | .38 | 1.04 | .17 | .21 | .15 | .08 |
| 79-1-4 | 45.99 | 9.66 | 12.64 | 19.82 | 7.89 | 1.41 | .32 | 1.53 | .24 | .18 | .18 | .12 |
| 79-1-5 | 46.07 | 8.77 | 12.50 | 20.68 | 8.12 | 1.41 | .31 | 1.52 | .26 | .18 | .17 | -- |
| 79-1-6 | 46.63 | 9.01 | 12.36 | 19.15 | 8.54 | 1.43 | .33 | 1.75 | .31 | .20 | .18 | .12 |
| 79-1-7 | 47.22 | 9.42 | 11.65 | 18.77 | 9.05 | 1.44 | .31 | 1.49 | .16 | .18 | .18 | .12 |
| 79-1-8 | 47.47 | 9.14 | 11.61 | 19.00 | 9.09 | 1.32 | .29 | 1.43 | .19 | .16 | .17 | .12 |
| 79-1-9 | 46.60 | 8.85 | 11.67 | 20.25 | 9.09 | 1.26 | .27 | 1.36 | .20 | .14 | .18 | .12 |
| 79-1-10 | 47.05 | 8.02 | 11.34 | 21.95 | 8.57 | 1.12 | .22 | 1.10 | .22 | .14 | .16 | .13 |
| 79-1-11 | 44.91 | 6.24 | 12.53 | 25.93 | 8.07 | .79 | .13 | .78 | .22 | .06 | .18 | .16 |
| 79-2-40 | 46.66 | 11.42 | 11.27 | 14.63 | 10.34 | 1.84 | .26 | 2.98 | .13 | .22 | .17 | .08 |
| 79-2-140 | 53.85 | 16.29 | 6.61 | 7.23 | 11.22 | 3.11 | .50 | .68 | .09 | .26 | .12 | .04 |
| 79-2-10 | 51.03 | 14.95 | 8.03 | 11.14 | 10.33 | 2.51 | .47 | 1.00 | .11 | .23 | .13 | .06 |
| 79-2-165 | 50.29 | 11.97 | 9.67 | 14.61 | 10.04 | 1.75 | .24 | .76 | .18 | .26 | .16 | .07 |
| 79-2-170 | 46.58 | 10.00 | 12.65 | 18.37 | 8.83 | 1.40 | .33 | 1.25 | .13 | .17 | .19 | .11 |
| 79-6-173.1 | 45.80 | 9.29 | 12.19 | 20.99 | 7.92 | 1.26 | .21 | 1.74 | .14 | .16 | .17 | .13 |
| 79-6-179.3 | 46.22 | 8.14 | 12.38 | 22.33 | 7.41 | 1.21 | .27 | 1.34 | .16 | .20 | .19 | .15 |
| 79-6-189.6 | 46-53 | 7.74 | 12.17 | 22.30 | 7.64 | 1.25 | .28 | 1.40 | .15 | .19 | .19 | .16 |
| *S15 | 46.94 | 9.85 | 11.79 | 18.92 | 8.33 | 1.57 | .36 | 1.86 | -- | .19 | .17 | -- |
| *S5 | 46.90 | 9.56 | 11.77 | 19.61 | 8.30 | 1.53 | .35 | 1.81 | -- | -- | .17 | -- |
| *S7 | 48.46 | 11.62 | 11.59 | 13.74 | 9.73 | 1.95 | .45 | 2.28 | -- | -- | .18 | -- |

*Samples of original lake-forming lavas (Murata and Richter, 1966)

Table 5. Kilauea Iki Whole-Rock Analyses (Wt. %): XRF vs. Probe Estimates

| | $SiO_2$ | $Al_2O_3$ | FeO | MgO | CaO | $Na_2O$ | $K_2O$ | $TiO_2$ | $Cr_2O_3$ | $P_2O_5$ | MnO | NiO |
|---|---|---|---|---|---|---|---|---|---|---|---|---|
| 79-6-189.6 | | | | | | | | | | | | |
| XRF | 46.17 | 8.19 | 12.59 | 21.49 | 7.79 | 1.22 | .44 | 1.58 | .13 | .11 | .17 | .11 |
| $Probe_{est}$ | 46.53 | 7.74 | 12.17 | 22.30 | 7.64 | 1.25 | .28 | 1.40 | .15 | .19 | .19 | .16 |
| 79-6-179.3 | | | | | | | | | | | | |
| XRF | 47.60 | 9.42 | 11.83 | 18.29 | 8.88 | 1.24 | .52 | 1.70 | .14 | .12 | .16 | .08 |
| $Probe_{est}$ | 46.22 | 8.14 | 12.38 | 22.33 | 7.41 | 1.21 | .27 | 1.34 | .16 | .20 | .19 | .15 |
| 79-2-170 | | | | | | | | | | | | |
| XRF | 48.75 | 10.43 | 11.91 | 15.26 | 9.44 | 1.47 | .53 | 1.99 | .11 | .15 | .16 | .06 |
| $Probe_{est}$ | 46.58 | 10.00 | 12.65 | 18.37 | 8.83 | 1.40 | .33 | 1.25 | .13 | .17 | .19 | .11 |
| 79-2-165 | | | | | | | | | | | | |
| XRF | 48.15 | 10.65 | 11.94 | 14.82 | 9.71 | 1.57 | .50 | 2.17 | .10 | .15 | .16 | .06 |
| $Probe_{est}$ | 50.29 | 11.97 | 9.67 | 14.61 | 10.04 | 1.75 | .24 | .76 | .18 | .26 | .16 | .07 |

MODES (Vol. %)

| | IL | OL | PL | CPX | PIG | GL |
|---|---|---|---|---|---|---|
| 79-6-189.6 | -- | 39.70 | 13.57 | 17.59 | -- | 29.15 |
| 79-6-179.3 | -- | 41.50 | 17.65 | 16.67 | -- | 24.18 |
| 79-2-170 | .85 | 31.63 | 28.64 | 21.79 | 2.99 | 14.10 |
| 79-2-165 | .43 | 18.30 | 40.00 | 30.21 | 6.38 | 4.68 |

lava lake environment subsequent to olivine settling in the preeruption chamber. The calculations are intended to illustrate the effects of lake differentiation on wholerock compositions and liquid phase compositions.

The input data for the mass balance calculations consisted of wholerock (Table 4), glass (Table 3), and mineral analyses from the current investigation and of previously published wholerock and glass analyses for the lake-forming lavas (Murata and Richter, 1966). Pure end-member mineral components were not used in the calculations. Instead, observed mineral compositions were employed, thereby further constraining solutions and testing the consistency of the new data with the data published previously. The mineral compositions used in the calculations corresponded to (1) a forsteritic olivine ($Fo_{80}$ (wt)), (2) a fayalitic olivine ($Fo_{44}$), (3) an anorthitic plagioclase ($An_{80}$), (4) an albitic plagioclase ($An_{12}$), (5) a diopsidic clinopyroxene ($Wo_{43}En_{47}Fs_{10}$), and a typical ilmenite.

The input data were not weighted, and the solutions were not forced to contain certain phases specified at the outset. Only the mathematically "best" solutions were permitted, and these were further selected on the basis of their relation to physically realistic petrologic processes. It may be underscored, however, that while mass balance calculations may demonstrate the consistency of a postulated process with analytical data, they do not do so uniquely. The residuals for the results presented here were small ($\Sigma r^2 \leq .1$), and overfitting of data was avoided by careful consideration of analytical uncertainties. The results presented here are preliminary because improvements are expected as more reduced data become available.

Two types of mass balance calculations have been performed, one dealing with differences in wholerock compositions and the other with differences in glass (liquid) compositions. The object of the wholerock mass balance calculations was to quantify evidence for the operation of open system differentiation processes occurring since the formation of the lake--for example, by examining the feasibility of generating current lava lake wholerock compositions from earlier lake-forming lava compositions via addition or removal of limiting mineral compositions observed in the lake.

The mass balance calculations for the glasses provide insight into the relationships between liquid compositions as a function of the extent of crystallization. Because the lake-forming lavas were highly variable in composition, the initial magma for the wholerock mass balance calculations was S7 (Table 6), which corresponds almost exactly to the integrated mean lava composition for the originally erupted lavas (Murata and Richter, 1966). The composition of the glass phase in S7 (S7G, Table 6) was used as a starting composition exemplary of the early "melt" of the lava lake.

Wholerock compositions of the UMTZ require the addition of 15% (wt.% relative to S7) forsteritic olivine and 3%-10% diopsidic clinopyroxene to S7 (Figure 21), but they are less enriched than S5 (Table 4, Figure 22), the most picritic lava of the 1959 eruption. The MZ is more enriched than S5, requiring addition of 20%-35% forsteritic olivine, 5%-10% diopsidic clinopyroxene, and 3%-10% anorthitic plagioclase down to 59 m. From 59 m to the LMTZ, wholerock compositions are consistent with enrichments of 10% olivine, 60% clinopyroxene, and 25% plagioclase. These results clearly suggest the operation of accumulation mechanisms (crustal foundering, crystal settling, density currents, etc.) and indicate that wholerock compositions at depth are not simply related by olivine control lines, unlike the lake-forming lavas. They also suggest that wholerock compositions for the UC should be sympathetically depleted in MgO and FeO and enriched in $Al_2O_3$ and alkalies; this expectation is substantiated by the available reduced data from the UC (see 79-2-40, 79-2-140, 79-2-10, 79-2-165 in Table 4).

Mass balance calculations for the generation of glass (liquid) compositions in the UMTZ from an initial liquid, based on an analysis of glass in S7 (S7G, Table 6) require removal of 1%-5% oxide (ilmenite), 13%-15% olivine (mixtures of observed forsteritic and fayalitic compositions), 25%-35% clinopyroxene, 25% plagioclase, and 10%-15% alkali feldspar (Figure 23). The liquids of the MZ require removal of 10% olivine, 15%-25% clinopyroxene, and 15%-20% plagioclase from the S7 glass. Hence, even the most primitive liquids present in the lava lake at the time of drilling have evolved to a significant degree by crystallization differentiation from the early lake-forming liquids.

Table 6.

Wholerock and Glass Compositions for the Lake-Forming Lavas (from Murata and Richter, 1966).

| | S7 (Wholerock) | S7G(Glass) |
|---|---|---|
| $SiO_2$ | 48.44 | 49.75 |
| $Al_2O_3$ | 11.42 | 13.15 |
| FeO | 11.58 | 11.42 |
| MgO | 14.01 | 9.21 |
| CaO | 9.78 | 11.02 |
| $Na_2O$ | 1.90 | 2.13 |
| $K_2O$ | .44 | .53 |
| $TiO_2$ | 2.25 | 2.61 |
| MnO | .18 | .17 |

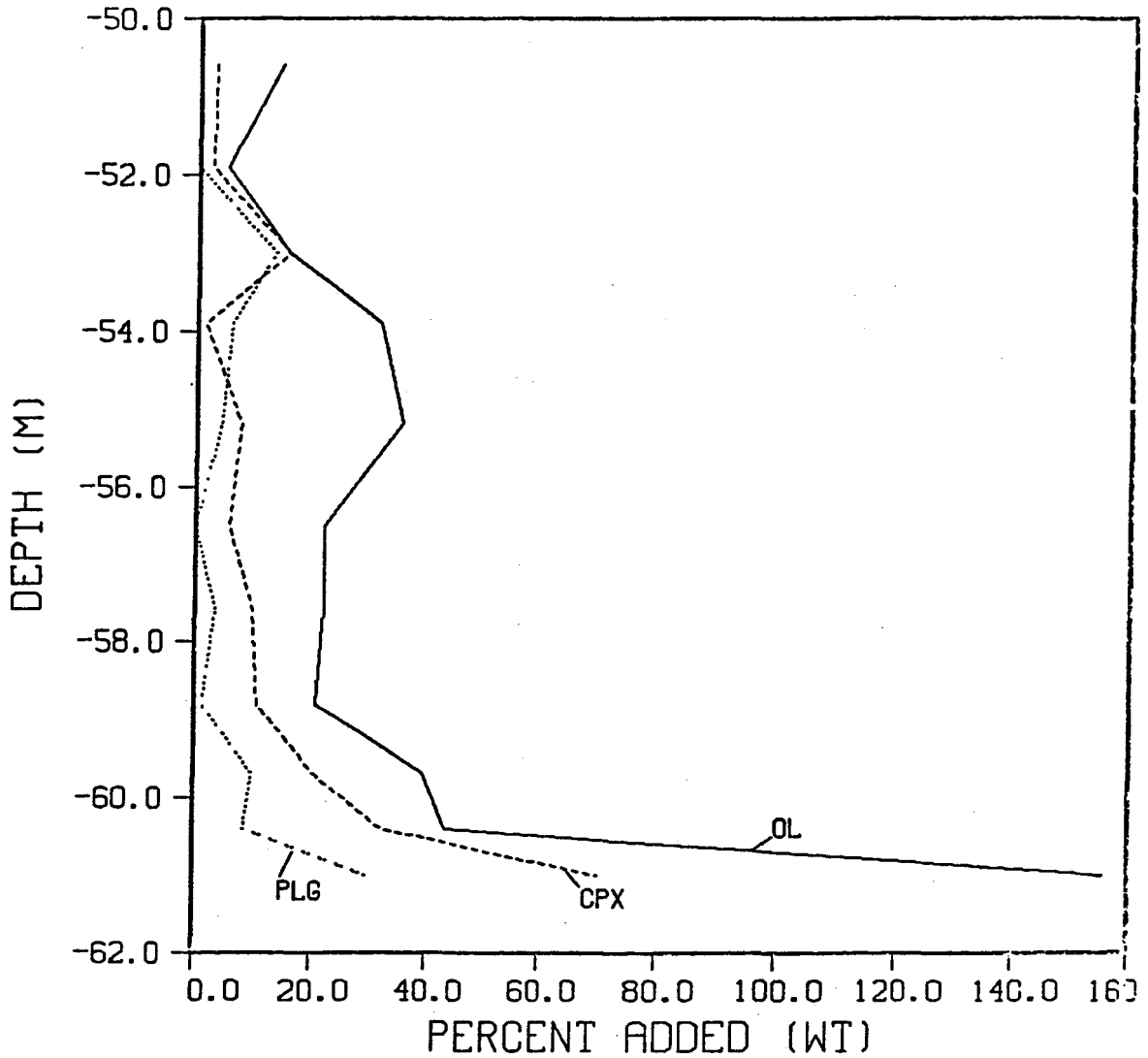


Figure 21. Amounts of olivine (OL, solid line), clinopyroxene (CPX, dashed line), and plagioclase (PLG, dotted) that must be added to S7 to produce wholerock compositions (Table 3) at various depths (m) in drill hole 79-1. The amounts of each phase added are expressed as weight percentages relative to the initial lava S7. The weight proportions required to account for the wholerock composition at 60 m depth, for example, are 1.00 S7, .41 OL, .26 CPX, and .09 PLG.

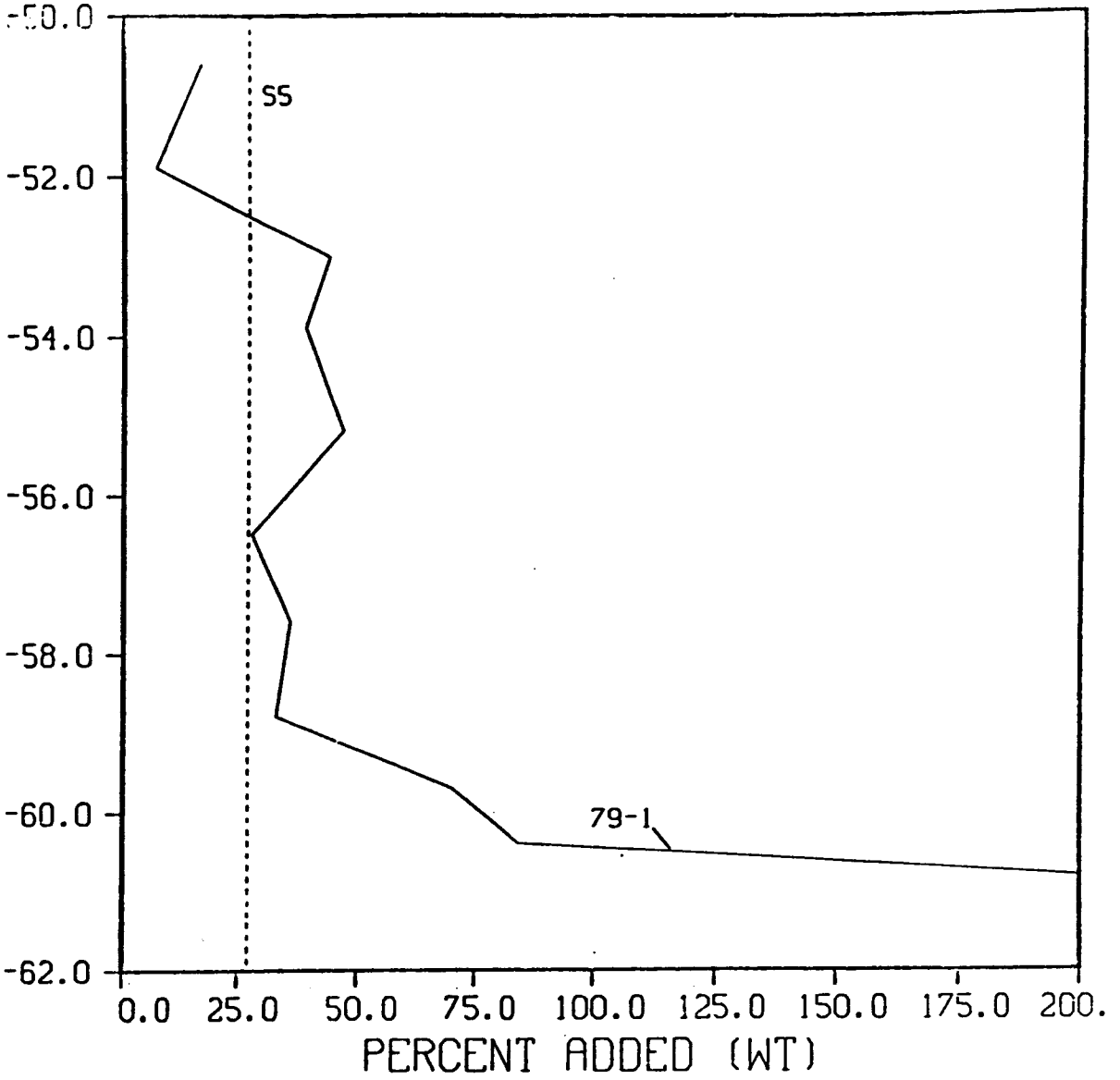


**Figure 22.** Total amounts of olivine, clinopyroxene, and plagioclase that must be added to S7 to produce wholerock compositions at various depths (m) in drill hole 79-1. Dashed line shows the total amounts of these phases (mostly OL(Fo)) that must be added to S7 to produce S5, the most MgO-rich analysis obtained for the initial lake-forming lavas. The total amounts of phases added are expressed as weight percentages of the initial lava S7.

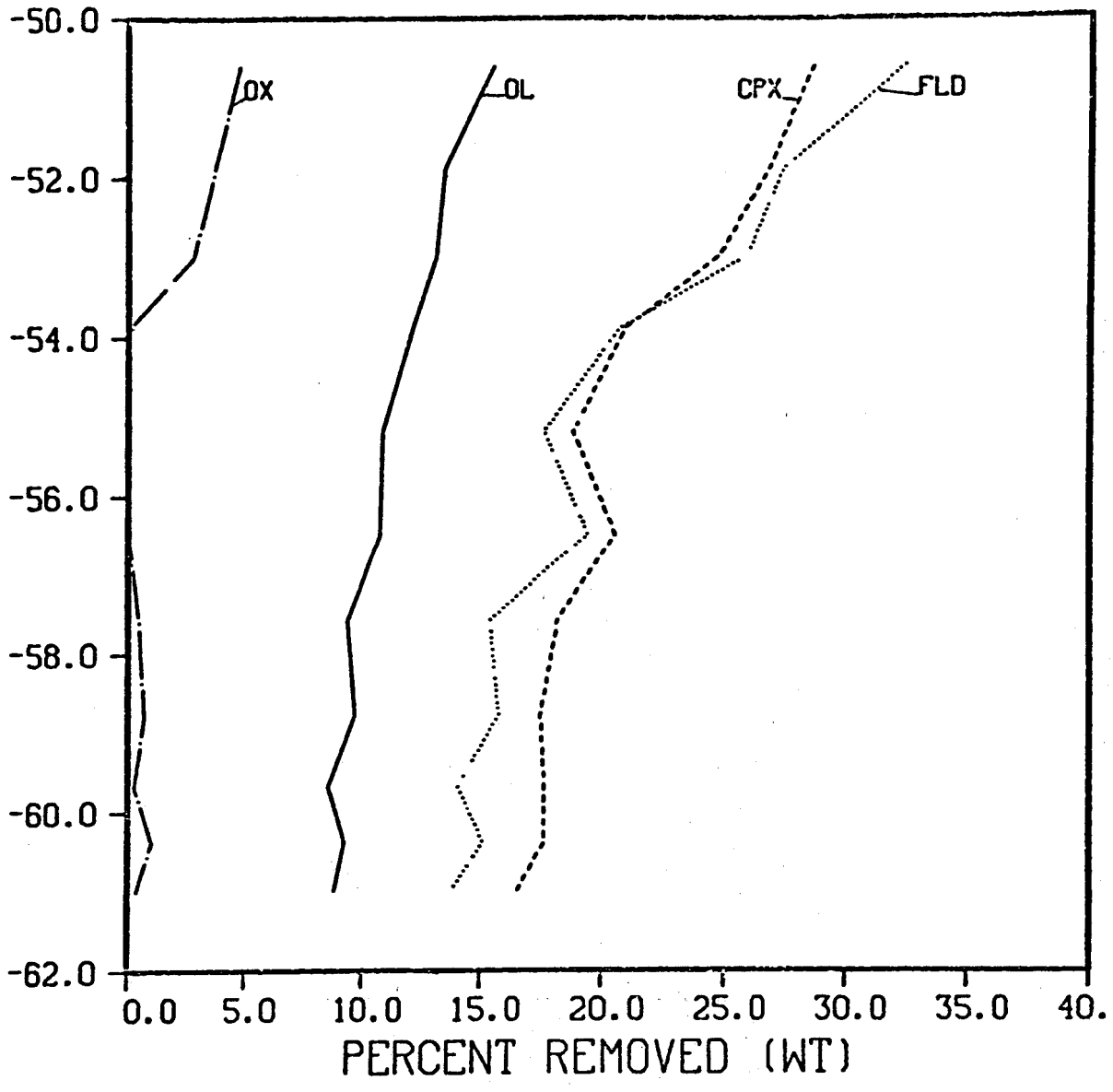


Figure 23. Amounts of olivine (OL, solid), clinopyroxene (CPX, dashed), feldspar (FLD), dotted), and ilmenite (OX, dash-dot) that must be removed from S7G to produce glass compositions (Table 3) at various depths (m) in drill hole 79-1. The amounts removed are expressed as weight percentages of starting glass composition S7G.

## III. Task 2 -- Source Tapping (J. L. Colp)

The development of technology to enter deeply buried (w 10 km) magma chambers has not been considered as part of the Magma Energy Research Project. Such a development is not compatible with the intent or the budget of the Project. However, the magnitude of such a technological development was considered and discussed in the Magma/Hydrothermal Drilling and Instrumentation Workshop (Varnado and Colp, 1978), as part of a proposed Continental Scientific Drilling Program (National Academy of Science, 1979).

The Magma Energy Research Project has addressed the physical characteristics of a hole drilled through the roof rocks overlying a magma source. The main concerns are whether those rocks fail in a brittle fashion under in-situ temperature and pressure so that they can be drilled by conventional methods, and if the borehole will stay open after drilling to allow the insertion of energy extraction equipment. A continuing laboratory research contract with the Center for Tectonophysics, Texas A&M University, to investigate these concerns has been under way since 1974. Friedman et al (1979), presented a summary of past work on this contract.

Support for the work at the Center for Tectonophysics was moved from the Sandia Magma Energy Research Project to Department of Energy/Basic Energy Sciences effective April 1, 1980. The research under way will continue unchanged. A final report (Friedman et al, 1980) describing the work done under Sandia funding has been published. The following section on borehole stability has been excerpted from that report. The complete report is available for reference to the details of the experiments and results.

### Borehole Stability (M. Friedman)

Borehole stability is one of many severe engineering problems to be anticipated should attempts ever be made to recover directly the geothermal energy stored in magma chambers, as temperatures of the order of 1000°C are expectable. How strong are the rocks to be drilled in this hostile

environment? Previous laboratory work is not very helpful because virtually all testing above 500°C has been done at either atmospheric pressure (Murrell and Chakravarty, 1973) or very high confining pressures of 400 MPa or more (Handin, 1966; Carter, 1976; Carter and Kirby, 1978). What is needed is testing at high temperature but low confining pressure. Thus, under laboratory conditions that simulate the expectable natural environment of engineering concern, we are testing rock types that are likely candidates for drilling. Reported herein are the short-time ultimate strengths and ductilities determined at temperatures of 25° to 1050°C and a strain rate of $10^{-4}s^{-1}$ of (a) room-dry Mt. Hood Andesite, Cuerbio Basalt, and Charcoal (St. Cloud Gray) Granodiorite at confining pressures of 0, 50, and 100 MPa, (b) water-saturated specimens of the same three rocks at zero effective pressure (both pore and confining pressures of 50 MPa), and (c) room-dry Newberry Rhyolite Obsidian at 0 and 50 MPa. These strengths are then compared with the stresses developed at the wall of a borehole in an elastic medium at the appropriate temperatures and mean pressures to assess the problem of borehole stability.

## Conclusions

The major conclusions to be drawn from the experimental and petrofabric results now available are as follows:

1) The ultimate compressive strengths of the dry crystalline rocks decrease gradually with increasing temperature to about 900°C, and then more rapidly as partial melting is approached at between 1000° and 1100°C. The strengthening effect of increasing effective confining pressure diminishes with increasing temperature. The obsidian is even stronger than are the crystalline rocks up to 600°C, above which, however, the glass softens and its strength vanishes at 800°C.

2) There is pronounced water-weakening only of the Mt. Hood Andesite and that occurs between 850° and 880°C (zero effective presure). At 870°-880°C its ultimate strength is only 5 to 25 MPa compared to an average room-dry strength of 75 MPa at 1000°C. The Cuerbio Basalt may

be weakened slightly between 800° and 900°C, but the Charcoal Granodiorite is unaffected by the presence of water to 1000°C.

3) The crystalline rocks are essentially brittle throughout the pressure and temperature ranges explored until partial melting occurs. They deform primarily by fracture, with some ductile flow in the groundmass where it is present, particularly adjacent to faults, some gliding flow (kinking) in the biotite, and thermal alteration of biotite, hornblende and pyroxene contributing to the strength reduction by an unknown, but probably minor amount. Shortenings at failure are $\leq$ 3 percent in room-dry tests and $\leq$ 1 percent in wet ones. Virtually all the permanent shortening is ascribable to macroscopic faulting.

4) At confining pressures to 100 MPa the degradation of strength and continued brittle behavior with increasing temperature suggest that the crystalline rocks will be drillable by conventional methods up to temperatures of partial melting. In fact, rapid decreases in strength at the highest temperatures suggest that the penetration rate ought to increase as the roof rock-magma interface is approached.

5) Several facts strongly suggest that the temperature-weakening of the room-dry crystalline rocks is due to intrinsic effects of temperature on the processes leading to macroscopic shear fracturing (or faulting), and not merely to degradation of strength by thermal cracking, at least when the rocks are subjected to confining pressure. (a) Brittle fracture accounts for virtually all the permanent strain. (b) The degree of microfracturing associated with the mechanical loading, as distinguished from the thermoelastic stressing, is about the same at all temperatures from 25° to 1000°C. (c) Specimens heated to 900°C, cooled, and then deformed at 25°C are at least as strong as those that have not been preheated.

On the other hand, similar thermal cycling greatly degrades the strengths of the unconfined rocks, presumably because the effect of the thermal cracks on subsequent failure is not suppressed by confining pressure; that is, heating significantly modifies the mechanical

state of the material. Thus, data from unconfined tests alone cannot be used for valid predictions of rock properties under in situ conditions, particularly for geological or geophysical applications. However, such tests may be useful to estimate strengths during drilling where essentially unconfined conditions and rapid cooling may obtain.

Several workers have regarded fracturing as a thermally-activated process and by fitting their data to an equation they have derived an apparent activation energy (see Carter and Kirby, 1978). Owing of data on time effects, we cannot do so. However, even if brittle fracturing is indeed rate-controlled, how could we, or the previous workers for that matter, associate the purely empirical, apparent activation energy with a specific process? Is it the initiation and/or propagation of intragranular microfracturing? Is it grain-boundary sliding? Is it the condensation of microfracturing in preferred zones and/or the precursory coalescence that appears to cause the instability manifest in the macroscopic fracturing, stress drop, and work-softening that characterize the ultimate failure of these rocks? We claim that a lot more research on fracture must be done before a meaningful constitutive "law" can be written for inelastic deformations in the brittle state.

6) Water-weakening in the andesite, in light of its dominantly brittle behavior, probably is caused by hydrolytic weakening of silanol bonds in the silicate minerals which promotes stress-corrosion cracking and reduces melting temperatures. The andesite, rather than the basalt or granodiorite, is water-weakened probably because its greater porosity (10 to 12 percent) permits more pervasive contact between water and solid internal surfaces than in the other two rocks.

7) Because the deformations of the rocks are essentially cataclastic at all temperatures, we suppose that boreholes in these rocks will fail in shear when the differential stress reaches the ultimate compressive strength for a given mean stress. In general, the maximum depth for stable boreholes increases with decreasing temperature, and decreasing $\sigma_h \sigma_v$ and for dry rocks, filled boreholes are more stable than

open ones. Further, for similar conditions boreholes in granodiorite will be stable to greater depths than those in basalt or andesite, with the latter providing the least stable ones. Assessment of stability for a given rock type is, therefore, primarily a function of assumed or known borehole stress and temperature conditions. For example: for $\sigma_h/\sigma_v$ of 1.0, filled boreholes (medium with specific gravity of 1.0) in dry impermeable rock are apt to be stable to > 10 km even at temperatures of 900°C or higher. On the other hand, in open boreholes and the same stress ratio, boreholes in dry andesite are likely to fail at 2, 3, 4, or 5 km depth for temperatures of 900°, 700°, 400°, and 25°C respectively. For dry rocks, the $\sigma_h/\sigma_v$ ratio of 0.5 provides the greatest stability of the three ratios considered, but for water-saturated rocks and filled boreholes this same ratio provides a "worst-case" condition because the tangential borehole stress becomes tensile. Accordingly, stability of filled boreholes in saturated rocks would require smooth walls and temperatures no hotter than 600°C. On the other hand, even though the andesite is weakened by water at high temperature, it should sustain stable boreholes in open holes to depths 10 km and temperatures to 880°C if the effective pressure is zero and $\sigma_h/\sigma_v$ is 1.0.

Our predictions of borehole stability are optimistic because we have not accounted for stress concentrations due to irregularities in the borehole walls, the frictional sliding strength of pre-existing fractures intersecting the borehole and dangerously inclined to the borehole stresses, or the kinetics of water-weakening. Moreover, we have focused initially on the instantaneous strengths and ductilities of the rocks with borehole stability predictions pertinent only to relative short periods of time immediately after penetration by the drill. On the other hand, long term stability of the boreholes seems probable, at least in light of the few time-dependent strength data available in the literature. However, data under appropriate conditions are meager and pertinent testing has just begun. Also we have not considered the influence of thermoelastic stresses that would develop around cooled boreholes and that upon superposition would tend to stabilize the borehole. Predictions must remain qualitative until sophisticated

numerical methods can be applied to the problem.

## IV. Task 3 -- Magma Characterization

Definition of chemical and physical properties of magma is necessary to interpret results from geophysical sensing techniques, to estimate energy extraction mechanism and rates, and to evaluate materials compatibility. Since fugitive gases significantly affect properties, studies must be made on materials simulating in-depth compositions. Consequently, efforts of this program are (1) to predict in situ compositions using analyses of gases from volcanic eruptions and (2) to measure properties of simulated systems at in-situ conditions.

### Characterization of Volcanic-Magmatic Gases (T. M. Gerlach, 5541)

The characterization of high temperature volcanic-magmatic gases for basaltic and alkaline lavas has been completed. Approximately 150 restored analyses have been obtained and provide an adequate data base for materials compatibility investigations in C-O-H-S-Cl systems typical of mafic lavas.

The results of the gas studies for Mt. Etna (Gerlach, 1979), Kilauea (Gerlach, 1980A), and Erta Ale lava lake (Gerlach, 1980B) have recently been published. The results for Nyiragongo lava lake (Gerlach, 1980C), Surtsey volcano (Gerlach, 1980D), and Ardoukoba (Gerlach, 1981A) are in press. A brief summary of the results (Gerlach, 1981B) has been written as a chapter for a forthcoming volcanology book by H. Tazieff. A review of the results (Gerlach, 1980E) was also presented as an invited lecture at the First International Conference on Volcanic Gases, Paris, France (3-4 July 1980), hosted by PIRPSEV, a French volcanological group led by H. Tazieff.

Work is continuing on a model for predicting the gas compositions associated with upwards movement of mafic lava in the upper crust. This study will be useful for extrapolating the results of the volcanic gas investigations to moderate pressures ($\leq$ 2 kbar). The model also predicts

chemical relationships observed in the restored data, for example the $CO_2$ degassing trends and the effects of melt $O_2$ fugacity on sulfur content of volcanic gases.

A set of restored analyses has been obtained for gases collected in 1977, 1978, and 1979 from an active dacite dome at Merapi volcano, Indonesia. The data were obtained by F. LeGuern in a collaborative study. The data are noteworthy for being among the first high quality dacitic gas analyses, and for being the first results of the application of a new field gas chromatograph that gives analyses on site. The analyses are a considerable improvement over those obtained by previous analytical techniques; for instance, they provide the first set of reliable data for $H_2S$ concentrations in high temperature volcanic gases. The restored Merapi analyses are $H_2O$ rich (90-95%), contain 3% to 7% $CO_2$, 1% $SO_2$, and 1% $H_2S$. They have $O_2$ fugacities near the quartz-magnetite-fayalite buffer.

A computer code developed for the restoration of volcanic gas data has proven useful for the prediction of metal compound stability fields in systems of interest in chemical vapor deposition (CVD) technology. Two investigations have been completed employing the code to guide in the design and interpretation of CVD experiments (Randich and Gerlach, 1980A, 1980B).

Volatiles in Upper Crustal Magma Bodies (J. Eichelberger, H. Westrich, 5541)

Introduction -- Among the most important compositional parameters which bear on the feasibility of extracting energy from magma is volatile content. Volatiles greatly affect heat transfer characteristics of magmas both because they dissolve in and change the physical properties of the melt phase, and because under some circumstances they form a separate vapor phase. For example, viscosity of silicate melts decreases by roughly an order of magnitude for each weight percent of dissolved water (Shaw, 1963). Bubble growth may occur due to crystallization of anhydrous phases, and can significantly increase the effective viscosity of magma (Shimozuru, 1978). In addition, bubbles probably have a large effect on heat transfer characteristics and contribute to explosive volcanic eruptions.

Despite the importance of volatiles, as well illustrated by the recent eruptions at Mt. St. Helens, there exists an order of magnitude uncertainty (and perhaps an order of magnitude of actual variation) in the total volatile content of common continental magmas. Since all but the driest magmas vesiculate during eruption, there is no direct means of determining volatile content of magma from erupted samples. Gas samples contain important information about the composition of magmatic vapor and the concentrations of volatiles in magma (Gerlach, this report). However, few data are available from explosive volcanoes because of the hazards involved in sampling. Considerable work has focused on analyses of glass inclusions trapped within phenocrysts as representing samples of melt prior to degassing. This approach suffers from analytical difficulties and from uncertainty as to whether or not the inclusions are representative samples of melt. The work described here brings field, textural, phase assemblage, glass-compositional, and eventually experimental data to bear on the volatile problem. This includes analytical measurements of volatiles from fresh tephra of Mt. St. Helens by mass spectrometry and thermogravimetric (TGA) techniques, and field observations at certain key tephra deposits in western United States. The purpose of this investigation is to place constraints on the volatile content of common continental magmas, the distribution of volatiles within upper crustal magma chambers, and the mechanisms by which magmas gain and lose volatiles.

Progress in FY80 -- Following the explosive events at Mt. St. Helens, a suite of samples was collected (in cooperation with R. Hoblitt, USGS) representing much of the variation in clast size and vesicularity of tephra emplaced during the May 18 blast and May 18 and June 12 pyroclastic flows. Later, samples of the "June dome" and July 22 tephra were obtained from the USGS. Total volatile contents (by TGA) and bulk and grain densities have been determined for 10 samples of this suite, and modal analyses are in progress.

For comparison and broader application of the Mt. St. Helens results, field investigations were carried out in the Mono Craters and Medicine Lake volcanoes of California and Crater Lake in Oregon (in cooperation with C. Bacon, USGS). In each case, one or more sequences of tephra followed

by emplacement of a silicic dome were examined and sampled in detail. These sites are too old for volatile data from the silicic tephra to be meaningful, but will still yield useful information on textural features and phase assemblages in sequences characterized by greatly decreasing exposiveness.

Results -- Results from TGA analyses of Mt. St. Helens tephra are still preliminary, because the possibilities of contamination of samples before or during preparation has not been fully investigated. Nevertheless, an interesting pattern has emerged which cannot easily be ascribed to post eruption adsorption. Figure 24 shows that there exists a correlation between porosity (calculated from bulk and grain densities) and volatile content. Volumetrically, volatile-rich, frothy material is overwhelmingly dominant in all eruptions sampled except the May 18 blast. Degassing was found to occur over the range 200°C to 600°C and ranged from 0.0 wt. % total volatiles for the June dome to 0.65 wt. % for small (2 cm) clasts of June 12 pumice. The latter corresponds to about 1 wt. % in the glass, as calculated from modal analysis. Porosity ranges from 30 vol. % in the dome to 70 vol. % in the June 12 pumice. The positive correlation between vesicularity (porosity) and volatile content was unexpected, since it was anticipated that a more degassed magma would have a higher vesicle content, while the glass would be depleted in volatiles. Such a relationship should have been apparent in analyses of material from the interiors and exteriors of individual clasts (Fig. 24).

The large range of vesicularity within individual deposits was observed at the other sites as well. In these cases, erosion permitted thorough investigation of the stratigraphy. It was found that nonvesicular and highly vesicular clasts occur throughout each deposit, but that the proportion of nonvesicular clasts increases upward (i.e., with time). In some cases, this cycle was repeated several times before final dome emplacement.

Conclusions -- The positive correlation between bubble content and volatile content of the tephra samples indicates that bubble content does not reflect the amount of degassing of the magma. Rather, the growth

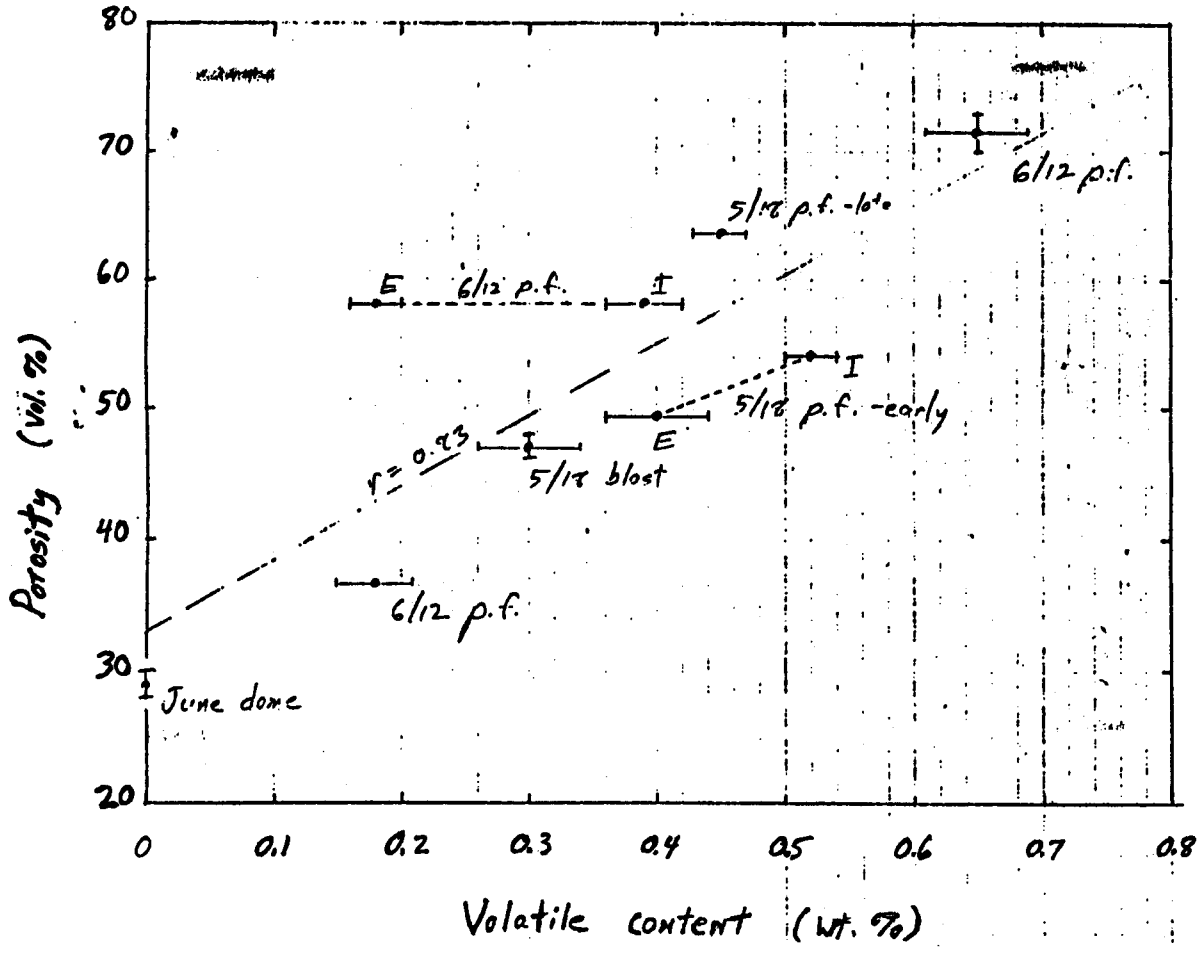


Figure 24. Porosity versus total volatile content of tephra and dome material from Mt. St. Helens. Porosity was determined by gravimetric methods by Holmes & Narver, Inc., except for June dome which is based on point counting on a polished surface. Volatile content is weight loss on heating. Abbreviations are: p.f., pyroclastic flow; E, exterior of clast; I, interior of clast.

rate of bubbles due to decompression apparently greatly exceeds the growth rate due to diffusion. Magma which flows rapidly from depth and is quickly disrupted into fragments both froths to a higher porosity foam and quenches more volatiles in the glass than magma, which resides longer at shallow depth. The limiting case for equilibration at shallow depth is dome material, which has the lowest porosity because it was confined during bubble growth (resulting in flow of gas through permeable magma rather than bubble expansion) and is completely degassed.

Equilibration at shallow depth is reflected in the phase assemblage of the samples as well. Hornblende typically has clean euhedral faces in the most volatile-rich pumice. Hornblende in the dome and more volatile-poor tephra has a reaction zone of plagioclase, oxides, and glass, representing dehydration or devolatilization of that phase.

The data also indicate that significant degassing of ash flows occurs after emplacement. The most volatile-rich samples are small pumice clasts associated with major ash flows. Devolatilization of these samples was found to occur at temperatures below temperatures measured in the interiors of these flows.

Characteristics of juvenile material in the May 18 blast deposit place constraints on the weight fraction of magmatic vapor which participated in the blast, if it is assumed that this vapor is dominantly water. Figure 25 shows the total water content of Mt. St. Helens-type magma as a function of pressure for vapor saturation and the observed bubble contents. The maximum-volatile case is represented by the curve for the blast fragments ($X_v = 0.5$), that is that the bubbles were fully formed before the blast. The growth of a large, localized bulge in the cone prior to the blast, with a volume comparable to the volume of juvenile material ejected in the blast, implies that magma had intruded the cone prior to May 18. This constrains pressure on the magma to less than 200 bars ($z \leq 1$ km, $\rho = 2.0$ g/cm), thereby constraining total water to a maximum of 2.6 wt.%. The amount of vapor present prior to unloading of the magma by the landslide was probably 1 wt.% or less. These conclusions are being tested by means of a hydrodynamic model (D. B. Hayes, 5510) which predicts velocity

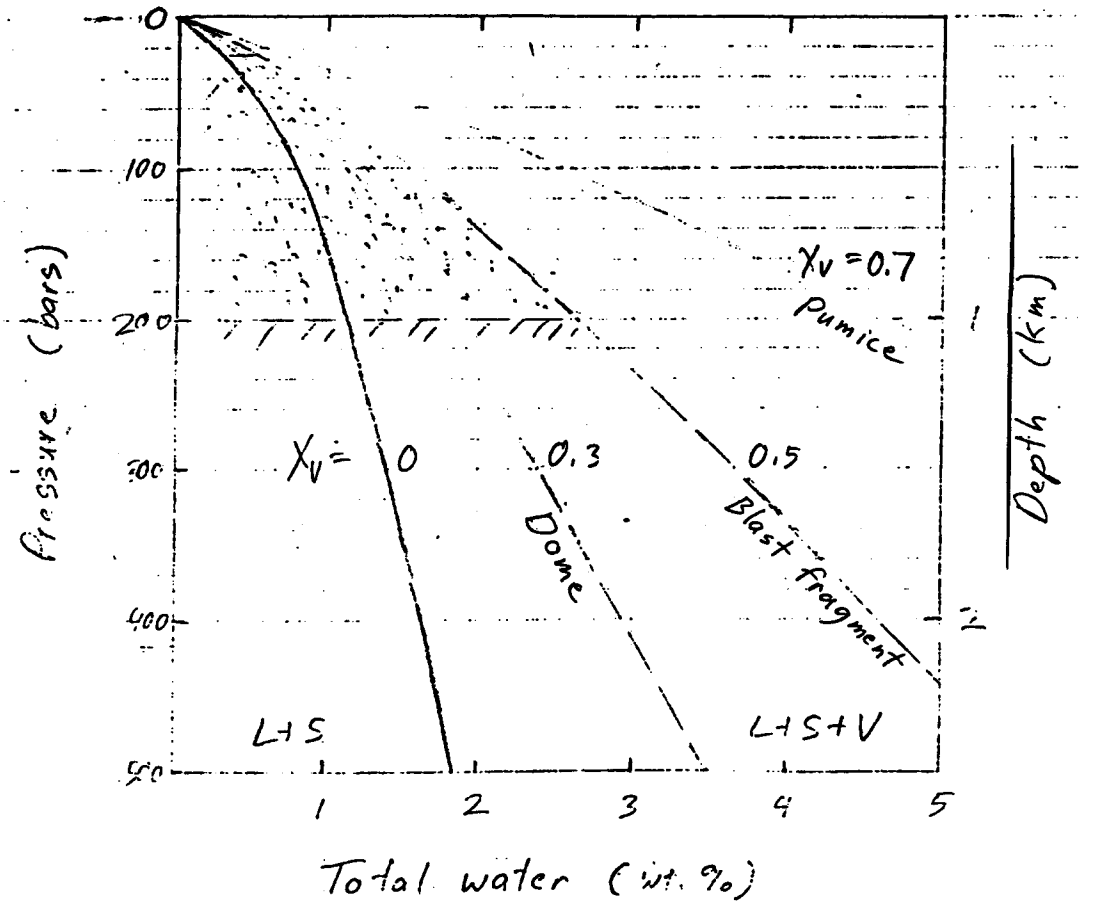


Figure 25. Water content of Mt. St. Helens magma (assuming water is only major volatile component) for bubble fractions by volume ($X_V$) of 0.03, 0.5, and 0.7 as a function of pressure, based on data of Shaw (1974) and modal analyses. Shaded area indicates possible conditions for magma involved in May 18 blast, as indicated by presence of bulge and characteristics of juvenile blast fragments.

of tephra and cooling due to gas expansion for specified water contents of magma and amount of overburden removed by the landslide. These observations do not constrain the initial volatile content of the magma if volatiles were lost during intrusion into the cone. However, if this were the case, a significant "magmatic"-type component would likely have been detected prior to May 18.

The repetition of explosive and dome-building cycles at Mt. St. Helens, and evidence of similar closely-spaced cycles at the other sites studied, is difficult to explain through the classical model of magma bodies zoned vertically in bulk volatile content. It is consistent, however, with a zonation in bubble content in the magma column due to variation in pressure with depth. If nucleation of bubbles is slow compared to the time span of eruptive events, then the tephra may represent the portion of the magma column which vesiculated prior to eruption and the dome the underlying vapor-undersaturated magma. The repose period between tephra-dome cycles would in part represent a period of bubble nucleation and growth. A further consequence for the other sites, where nonvesicular clasts are present in the tephra, is that these explosive eruptions were driven by only a few tenths of a weight percent vapor.

Magma Exploration (J. C. Eichelberger, 5541)

A model has been developed to explain petrologic features in intermediate composition igneous rocks, which may be useful in identifying shallow magma reservoirs from their surface volcanic expression. It was found that fine-grained mafic inclusions in lavas of mature andesitic volcanic fields are highly vesicular and consequently have a lower bulk density than the lavas in which they occur. These inclusions had been previously identified as representing basaltic magma chilled against cooler silicic magma, presumably within crustal magma reservoirs (Eichelberger, 1978; Heiken and Eichelberger, 1980). The density relationship suggests that the process by which these droplets become incorporated into large bodies of silicic magma is flotation. The inclusions appear to represent a buoyant foam, formed by vesiculation of basaltic magma during rapid transfer of heat to cooler reservoir magma. The conditions under which

flotation could occur can be calculated. For reasonable volatile contents of high alumina basaltic magma, the reservoirs in which this type of mixing occurs must be within 10 to 15 km of the surface. Thus, volcanoes which have recently-erupted lavas containing inclusions of mafic foam, should be fed from reservoirs at shallow depth. Evidence supporting this model has been found in the very large, exhumed plutons of the Sierra Nevada batholith (Reid & Eichelberger, 1981). A cooperative effort with J. B. Reid to obtain new information from the plutonic or frozen magma chamber environment is under way.

Magma Simulation Facility (4kbar/1600°C/800 cc. vol. (R. P. Wemple, 5836)

The pressure vessel/furnace system has been used for a limited number of viscosity experiments, basalt and andesite remelting for boule degassing, and quench rate experiments. Approximately 12 separate runs were made during the past year for these purposes. The system continues to function reliably and has been upgraded by the addition of several protective interlock systems.

Viscosity Measurement Activities

Electrogmagnetic Viscometer (EMV) Technique Development -- The high temperature, high pressure falling sphere viscometer has been developed to a higher level of reliability and the per unit cost has been reduced. However, detection problems were encountered when it was used in the Magma Simulation Facility system and the problems needed further resolution at 1 bar in a tube furnace. Another method of determining the real-time movement of the falling sphere in the molten rock was then developed by using a real-time x-ray scheme. Figure 26 illustrates the EMV in schematic form.

X-ray Technique Development (R. P. Wemple & M. P. Ryan)

The apparent viscosity of Hawaiian olivine tholeiite and Mt. Hood andesite has been measured using the Stokes flow approximation for the movement of a descending sphere. The approach uses a Norelco x-ray transmission

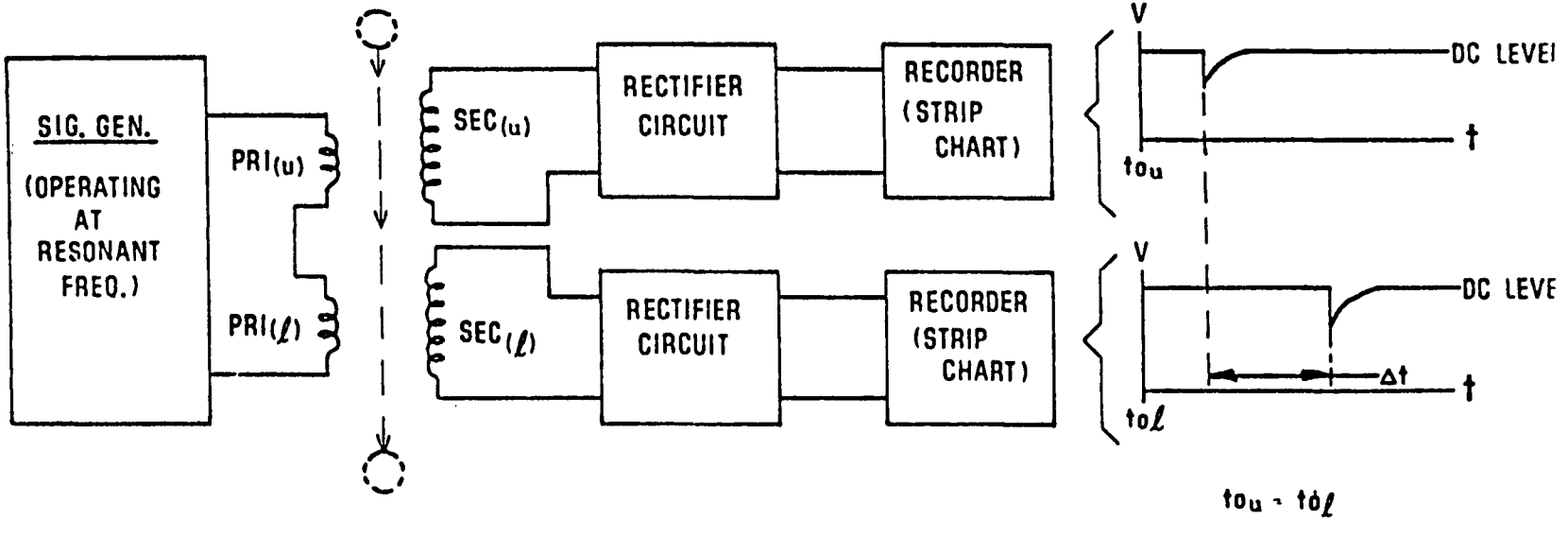


Figure 26. Electromagnetic Viscometer Schematic

system operated at 160 Kev, that is interfaced with a fluorescent screen-video recording system (Figure 27). The result is a continuous monitor, real time, direct observation viewing of the descent of the sphere, in which the acceleration, terminal velocity and deceleration phases of travel may be defined. Details of the experimental configuration are provided in Wemple et al (1980). Experiments have been conducted in argon, at 1 atm., to temperatures of 1300°C. Starting charges are large volume samples prepared by the boule approach discussed below. For Mt. Hood andesite, $Log_{10} \eta_a$ = 3.3 poises at 1300°C and $Log_{10} \eta_a$ = 3.9 poises at 1272°C. The reproducibility is Log $\eta_a$ = 3.296 p vs. Log $\eta_a$ = 3.296 poises for replicates run at 1300°C. For Hawaiian olivine tholeiite from Kilauea Iki, Log $\eta_a$ = 2.29 poises at 1245°C. Reproducibility is $\eta_a$ = 233.7 p vs. $\eta_a$ = 245.2 p for replicates at 1245°C.

Samples have been prepared for viscosity measurements with the kind help of Donn L. Stewart and the inorganic glass laboratory (Org. 1471). The procedure developed is:

1. Crush starting material to < 1 cm diameter chips. This step reduces the surface area to volume ratio.

2. Add material to a slowly deepening pool of melt in the crucible on a piece-by-piece basis. This step reduces the gas entrapment at the solid-liquid-gas interface.

3. Hold at 1550°-1600°C for 15-20 hrs, stirring continuously with a low rpm motor. This step reduces the viscosity of the liquid allowing bubbles to rise buoyantly and coalesce near the free surface of the liquid. Continuous stirring encourages bubbles of small diameter to rise to the free surface, due to the axial flow field of the impeller.

4. Pour in (split) cast iron molds held at 400°C (for basalt) or a low expansion coefficient graphite mold held at 1200°C (for andesites).

5. Remove thermal stresses in the samples by holding them approximately 50°C below the glass transition temperature for 2 to 3 hours (basalt)

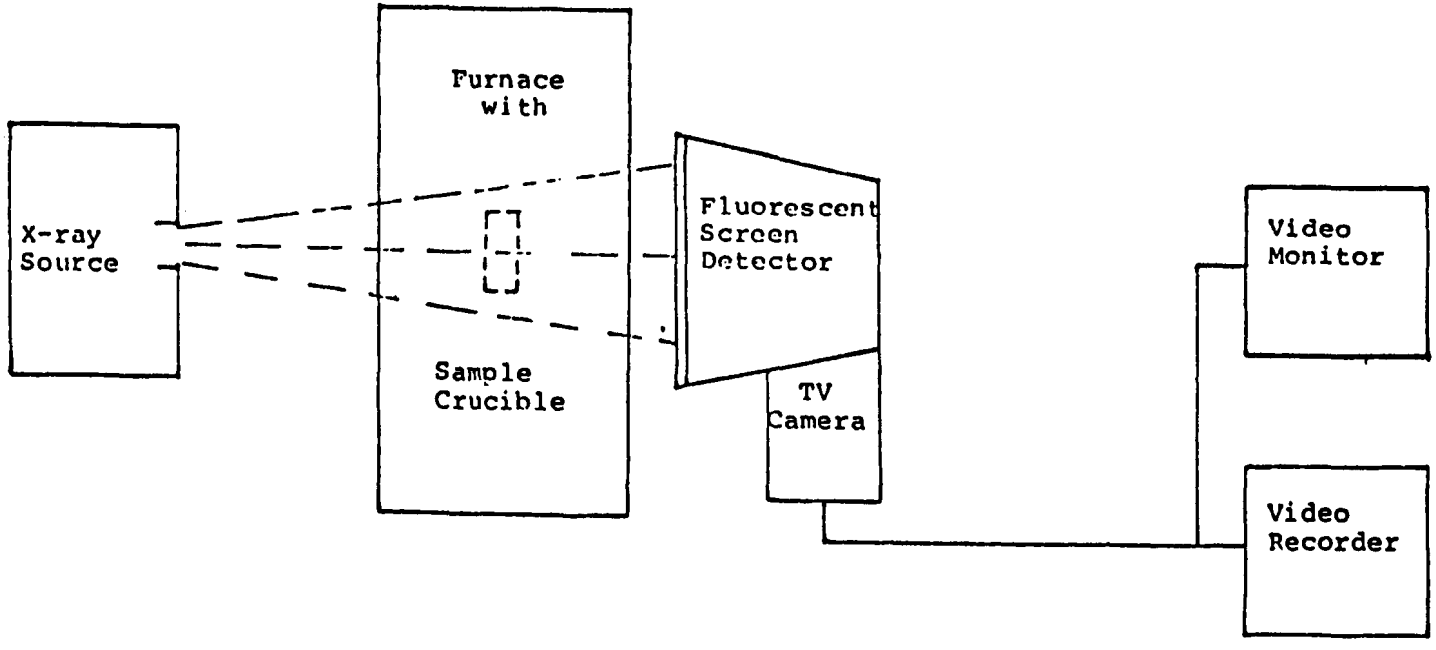


Figure 27. X-ray Viscometer Schematic

or 15 hours (andesite). Creep strains relax residual stresses to prevent sample fracture.

6. Remove from mold at temperature. Cool slowly in an annealing oven.

7. Lap the outer surface with a carborundum belt grinder, to machine off surface irregularities.

8. Cut to crucible length; lap the end to mate with the crucible bottom; this eliminates trapped air at the sample-crucible interface.

Data taken for the initial development of the EMV and x-ray viscometers was published in SAND80-0641, "Development of High Temperature Viscosity Measurement Techniques," Wemple, Hammetter, and Greenholt. A summary data plot from that report is shown in Figure 28. The report very explicitly states that these values can only be considered "apparent viscosities" due to the non-Newtonian nature of the sample materials.

Data taken during the summer months by Ryan and Wemple are shown in Figure 29 and again must be considered qualitative but are an improvement over the previous data in the referenced report due to the effort expended in reducing the formation of bubbles.

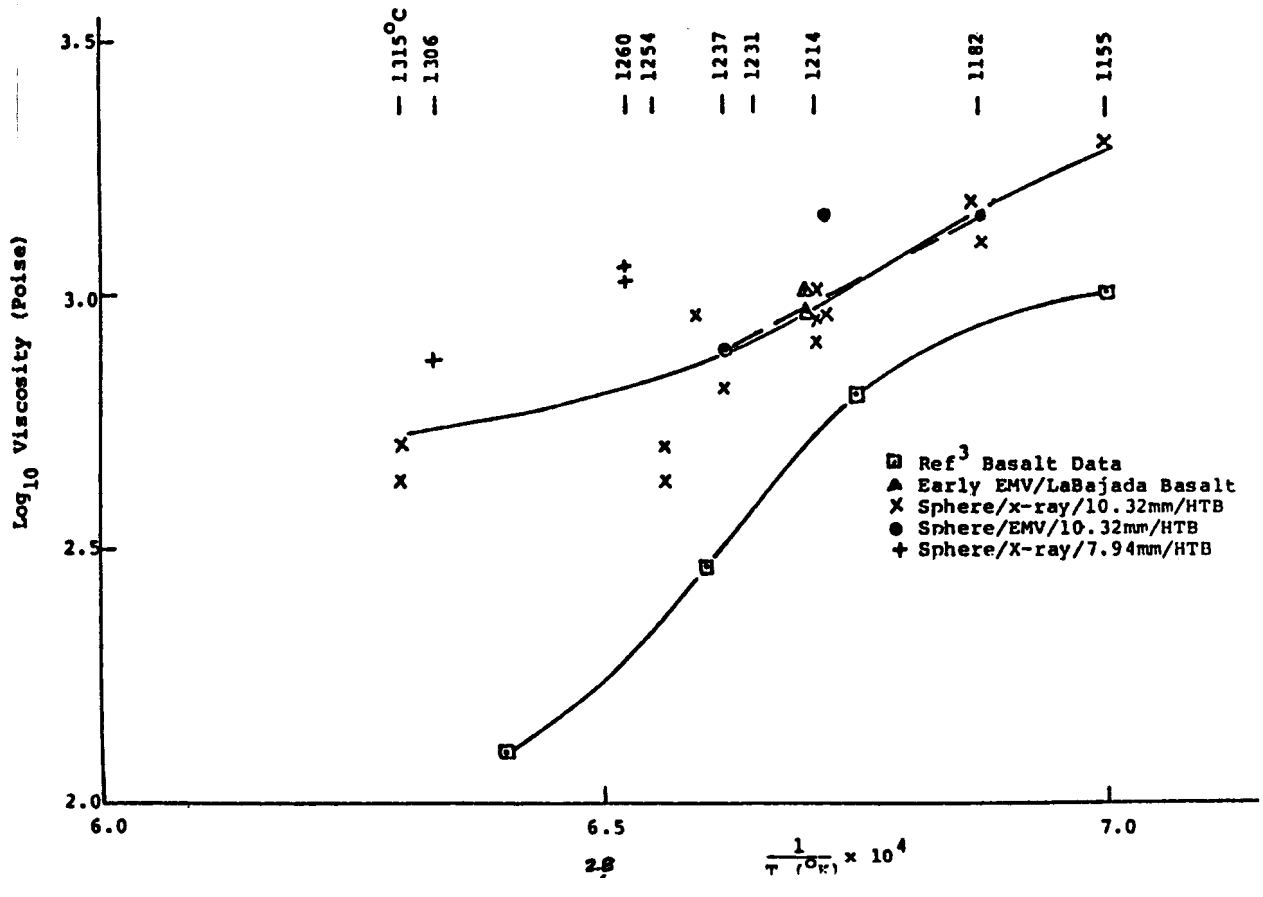


Figure 28. Viscosity Data Summary - Various Basalts (1 bar)

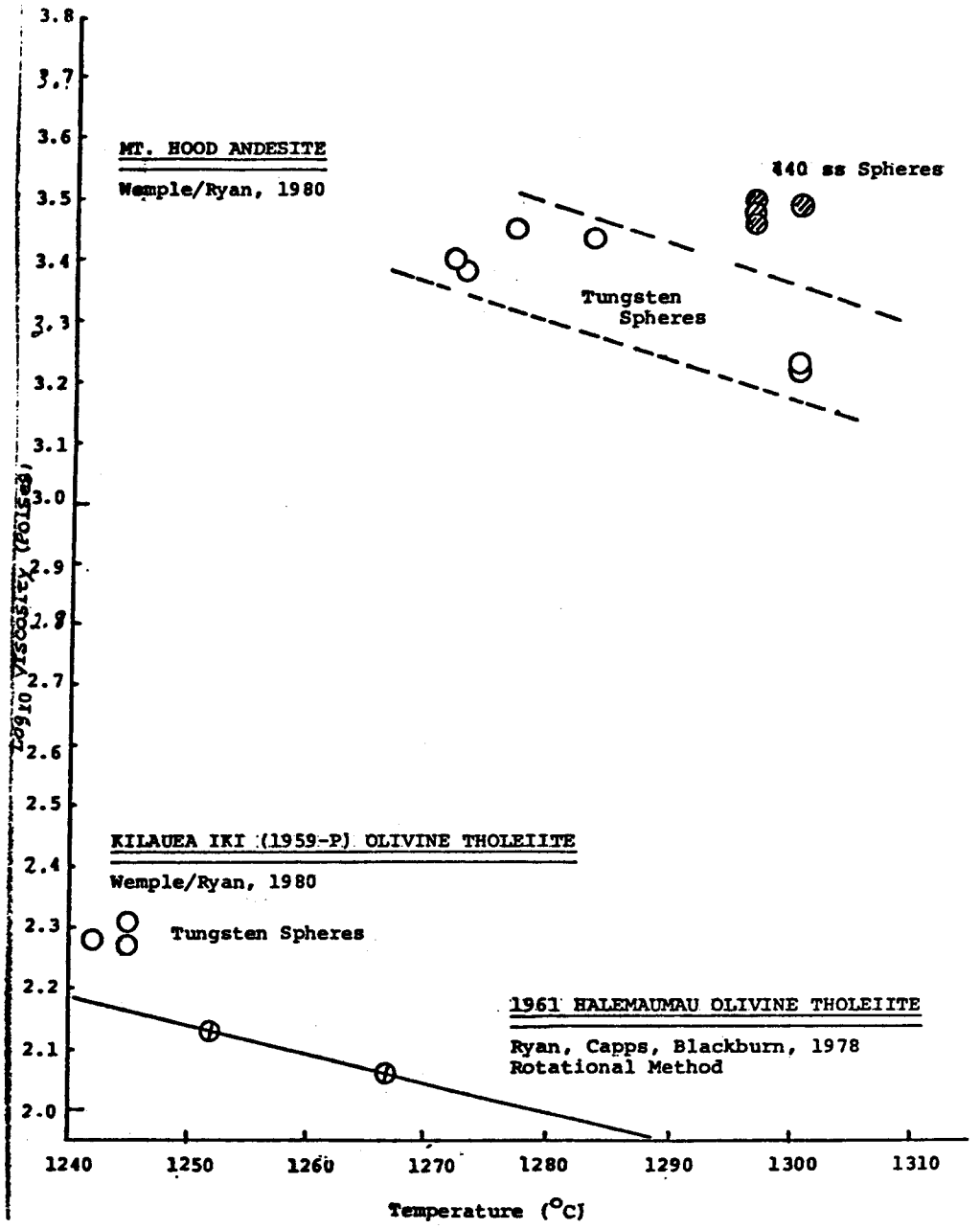


Figure 29. Viscosity Data Summary - with reduced Bubble Formation

## V. Task 4 - Magma/Material Compatibility (J. L. Colp)

The ability to build a heat-transfer device that can be inserted directly into a magma source is critical to the successful utilization of magma energy. The materials used for building a heat exchanger must retain their physical and structural properties sufficiently to allow the heat exchanger to perform for many years if the installation is to have an economic value.

Fifteen pure metals and 16 alloys have been evaluated in low-pressure, simulated-magma environments. Preliminary results suggest that iron, cobalt and molybdenum, each containing chromium, will show little degradation. The chromium content of both ferritic and austenitic stainless steels is the most important factor in providing corrosion resistance. Type 310 is by far the most corrosion-resistant alloy of any of the commercial stainless steels.

Compatibiltiy studies will continue in conjunction with Professor D. L. Douglass at the University of California at Los Angeles. The Magma Simulation Facility will be used for further studies at magmatic conditions.

## VI. Task 5 -- Energy Extraction

Molten magma bodies offer a source of high quality, pollution free thermal energy. Evaluation of the scientific feasibilty of energy extraction is the objective of this task of the Magma Energy Research Program.

A number of schemes for energy extraction have been considered; these include thermionics, thermoelectrics, steam generation for conversion to electricity, hydrogen production, and generation of synthesis gas ($H_2$, CO, $CH_4$). The last three extraction schemes (steam, hydrogen and synthesis gas) were chosen for these scientific feasibility studies, since thermodynamics and surface processing technologies are well defined. The basic questions of energy extraction are then questions of heat and mass transfer rates in and from magma bodies. Definition of the properties of molten

magmas (Task 3) is critical to understanding energy extraction limits. Efforts in the Energy Extraction Task have been aimed at limited studies on the dynamics of magma bodies, extraction rates from molten lavas, and preliminary studies on the internal dynamics of heat exchangers. Further information on past work can be found in Colp and Traeger (1979) and Colp (1979a).

Energy Extraction from Magma Body Margins (J. C. Dunn)

Potential methods of energy extraction from the margins of a magma body are being investigated. Maximum rates of energy transfer to a wellbore by pore fluid convection are of interest. Preliminary calculations have been carried out using a computer program based on the method of lines solution technique for one-dimensional, radial flow of a compressible, ideal gas through a porous medium. This analysis is being extended to include real gas effects which are important at depths in the earth corresponding to the location of magma bodies.

Heat Extraction Rate Studies (H. C. Hardee)

Heat extraction rates (energy transfer per unit area of heat exchanger surface) for conventional vertical cylindrical heat exchangers have been evaluated for a range of possible magma bodies. Convective heat transfer equations were used which considered the high Prandtl number ($Pr > 100$) of magma and the effect of cylindrical heat exchanger geometry. These calculations were compared with some limited laboratory test data. The effect of a solidified crust around the heat exchanger was included in the steady-state heat extraction estimates and the estimates were compared with a few selected transient numerical calculations.

When a heat exchanger is placed in a molten magma, a solid crust forms on the cooler heat exchanger surface. The crust grows in thickness until the conductive heat flux through the crust is equal to the convective heat flux in the magma at the edge of the crust as shown in Figure 30. At this stage, the convective heat coming from the molten magma is equal to the heat being conducted through the crust and in turn this heat is

equal to the heat being brought to the surface by the heat exchanger, which is termed the "heat extracted." If the temperature of the magma is well above the liquidus, the magma will tend to behave like a high Prandtl-number Newtonian fluid and the convective heat flux will be high. Magmas at liquidus or subliquidus temperatures will tend to behave like high Prandtl-number fluids but will likely exhibit non-Newtonian fluid behavior. In this latter case, the crust that forms may be quite thick and the convective heat flux, although small, may still be significant in terms of heat extraction rates because of the increased surface area of the thick crust.

A thick crust that forms around a cylindrical heat exchanger will have the geometry of a cylindrical annulus as shown in Figure 30. The heat transferred through the cylindrical crust by conduction is

$$q_o = \frac{K(T_o - T_e)}{r_o \ell n(r_o/r_e)}$$

The limiting heat extraction rate at the heat exchanger surface is similarly given by

$$q_o = \frac{K(T_o - T_e)}{r_e \ell n(r_o/r_e)}$$

By combining the two equations it can be seen that

$$q_e = q_o(r_o/r_e)$$

This heat extraction rate at the heat exchanger surface, $q_e$, may be several times larger than the convective heat flux, $q_o$, in the magma at the edge of the crust because of the difference in surface area between the heat exchanger surface and the outer surface of the solidified crust. The total heat extracted by the heat exchanger, $Q_T$, is simply $q_e$ times the surface

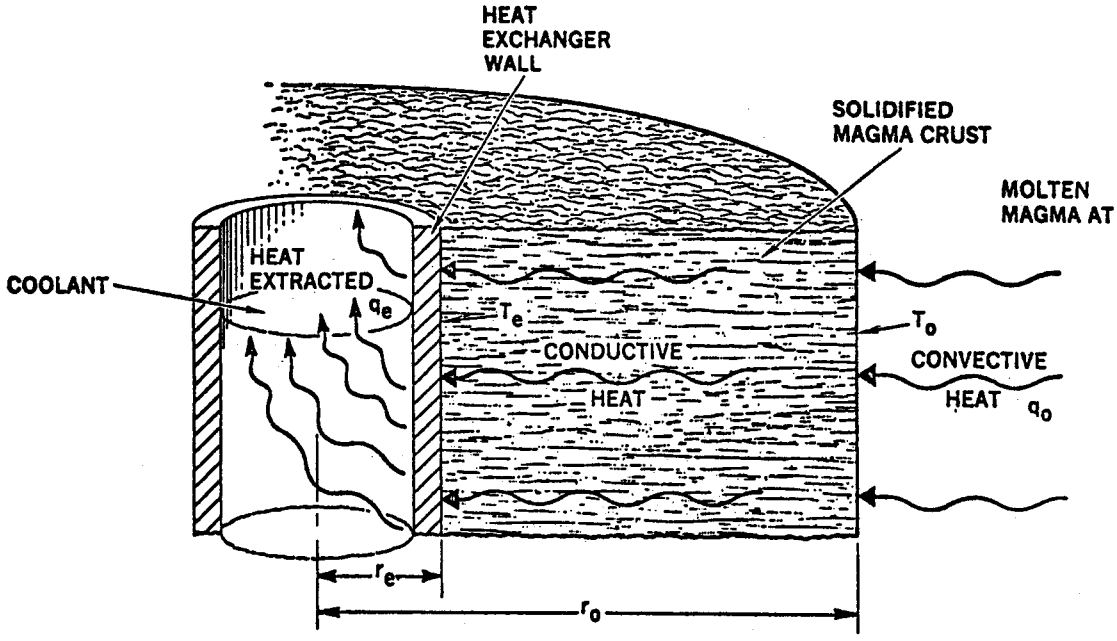


Figure 30. Flow of Heat from Molten Magma to the Heat Exchanger Working Fluid

area of the heat exchanger of

$$Q_T = Aq_e$$

The heat flux, $q_o$, entering the outer surface of the crust in Figure 30 is the heat flux reaching the crust by convection from the molten magma. This convective flow is caused by local density changes in the cooled magma in the vicinity of the heat exchanger surface. Convective heat flux correlations can be used to estimate the heat flux, $q_o$, on the assumption that Newtonian properties can be used to estimate convection in magma for magmas near the liquidus. Although the accuracy of these correlations near the liquidus is not known, they should be valid for magmas with appreciable superheat. For magmas and lava, the Prandtl number is at least 100 and generally much larger than this.

Convective heat transfer correlations are available for the infinite Prandtl number limit. This infinite Prandtl number is effectively reached when the Prandtl number exceeds 100. The infinite Prandtl number convection correlations are therefore applicable for all practical lava and magma situations. The principal difference between a convection correlation for unit Prandtl number and one for infinite Prandtl number is the relationship between the temperature and velocity boundary layers. The boundary layers are the regions where significant changes in temperature and velocity occur as shown in Figure 31. In a fluid with Prandtl number near unity, the temperature and velocity boundary layers will be of approximately equal thickness as shown in Figure 31a. If the Prandtl number is very large, however, the velocity boundary layer will be thicker than the thermal boundary layer and the peak velocity will occur at a distance roughly equal to the thickness of the thermal boundary as shown in Figure 31b. The high Prandtl number heat transfer correlations predict convective heat transfer correlations for Prandtl number fluids near unity.

The most favorable magma bodies for heat extraction are basaltic bodies and andesitic or wet ( > 5% $H_2O$) rhyolitic bodies because of their potential for convection. Heat extraction calculation were performed for

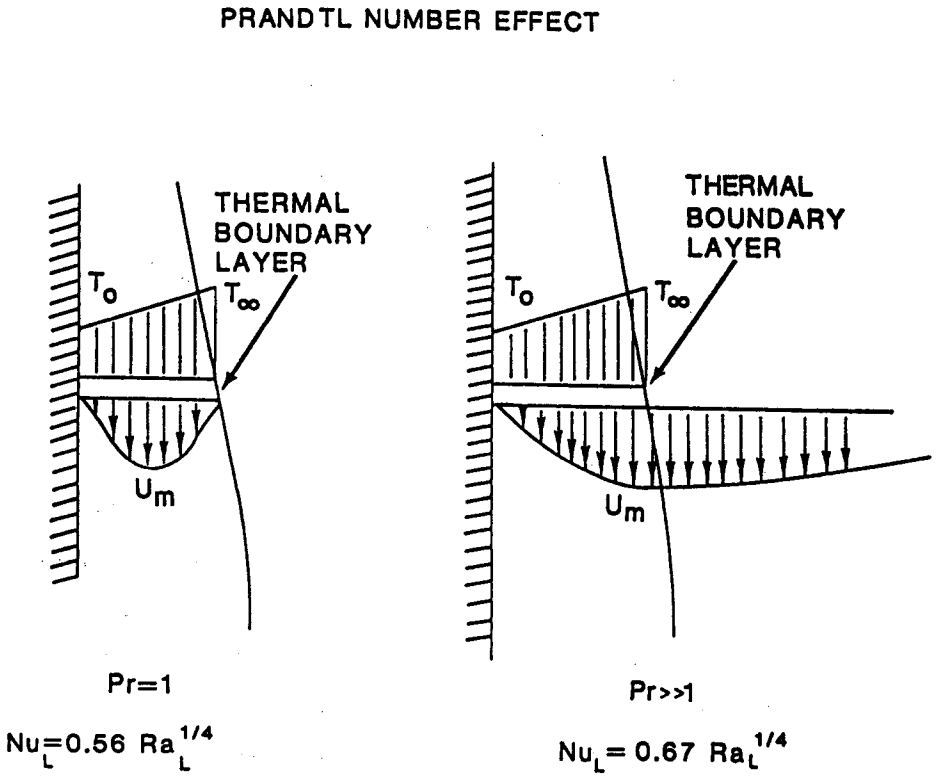


Figure 31. Temperature and Velocity Distribution in the Convection Boundary Layer for an Ordinary Fluid (a) and for a High Prandtl - number Fluid (b).

1000 m vertical cylindrical heat exchanger in contact with hypothetical magmas at or slightly above the liquidus temperature at an equilibrium pressure in the 5 to 10 km depth range. This places the temperature of a basaltic or andesitic magma body at about 1250°C. The result of these calculations is shown in Table 7.

These calculations are valid only after steady conditions have been reached and they neglect effects such as phase change in the solidifying crust. A more detailed finite-difference analysis of this problem was performed numerically and the results are shown in Figure 32 and Table 7. This numerical solution includes transient effects and phase change in the crust. Several convective heat flux rates in the magma were considered, ranging from $q_o$ = 50 kW/m$^2$ down to $q_o$ = 0, or conduction only. The effective increase of the heat exchanger heat flux $q_e$ over the convective flux $q_o$ in the magma is clearly evident, especially at the lower values of $q_o$. Results of the finite-difference calculations are in agreement with the steady state analysis for the assumed 30-year plant lifetimes shown in Figure 32. Note that the final heat extraction rate is closely approached after about the first week of operation.

The convective heat extraction rate for dry granite is low, and is only about twice as much as the straight conduction rate of 1 kW/m$^2$. The heat extraction rates range from 5 to 25 kW/m$^2$ for andesitic and wet rhyolitic magmas and from 15 to 50 kW/m$^2$ for basaltic magmas. The range in heat extraction values results from the difference between the laminar and turbulent calculation. In the basaltic magma case the critical Rayleigh number condition is exceeded. In this case the convection would definitely be turbulent and the higher heat extraction rate $q_e$ = 51 kW/m$^2$ would apply. In the andesite case the possibility of turbulent convection is marginal.

Heat extraction from molten magma in the upper 10 km of the continental crust represents a significant potential energy resource. Basaltic magmas offer heat extraction rates in the range of 15-50 kW/m$^2$ (20-80 MW per well) and andesitic and wet rhyolitic magmas offer heat extraction rates in the range of 5-25 kW/m$^2$ (8-40 MW per well).

Table 7.

Heat extraction rates $q_e$ and total heat extraction $Q_T$ for a 25 cm radius, 1000 m vertical cylindrical heat exchanger in magma

| $q_o$, kW/m | $r_o$, cm | $q_e$, kW/m$^2$ (Numerical Solution) | $q_e$, kW/m$^2$ (Eqn. 4) | $Q_T$, MW (Eqn. 5) | |
|---|---|---|---|---|---|
| 0.1 | 562 | -- | 2.3 | 3.6 | Dry Rhyolite |
| 0.5 | 220 | 4.6 | 4.4 | 6.9 | -- |
| 1.0 | 138 | 5.9 | 5.1 | 8.0 | -- |
| 1.06 | 122 | -- | 5.17 | 8.1 | Dry Andesite or Wet Rhyolite (Laminar) |
| 2.0 | 91 | 7.8 | 7.3 | 11.5 | -- |
| 3.24 | 66 | -- | 8.52 | 13.3 | Wet Andesite (Laminar) |
| 5.0 | 54 | 12.2 | 10.8 | 17.0 | -- |
| 6.19 | 49 | -- | 12.1 | 19.0 | Dry Andesite or Wet Rhyolite (Turbulent) |
| 7.55 | 45 | -- | 13.7 | 21.5 | Basalt (Laminar) |
| 10. | 43 | 19.4 | 17.2 | 27.0 | -- |
| 19.4 | 34 | -- | 26.5 | 41.6 | Wet Andesite (Turbulent) |
| 20 | 34 | 30.0 | 27.0 | 42.4 | -- |
| 43.3 | 30 | -- | 51.1 | 80.3 | Basalt (Turbulent) |
| 50.0 | 29 | 59.6 | 57.5 | 90.3 | -- |

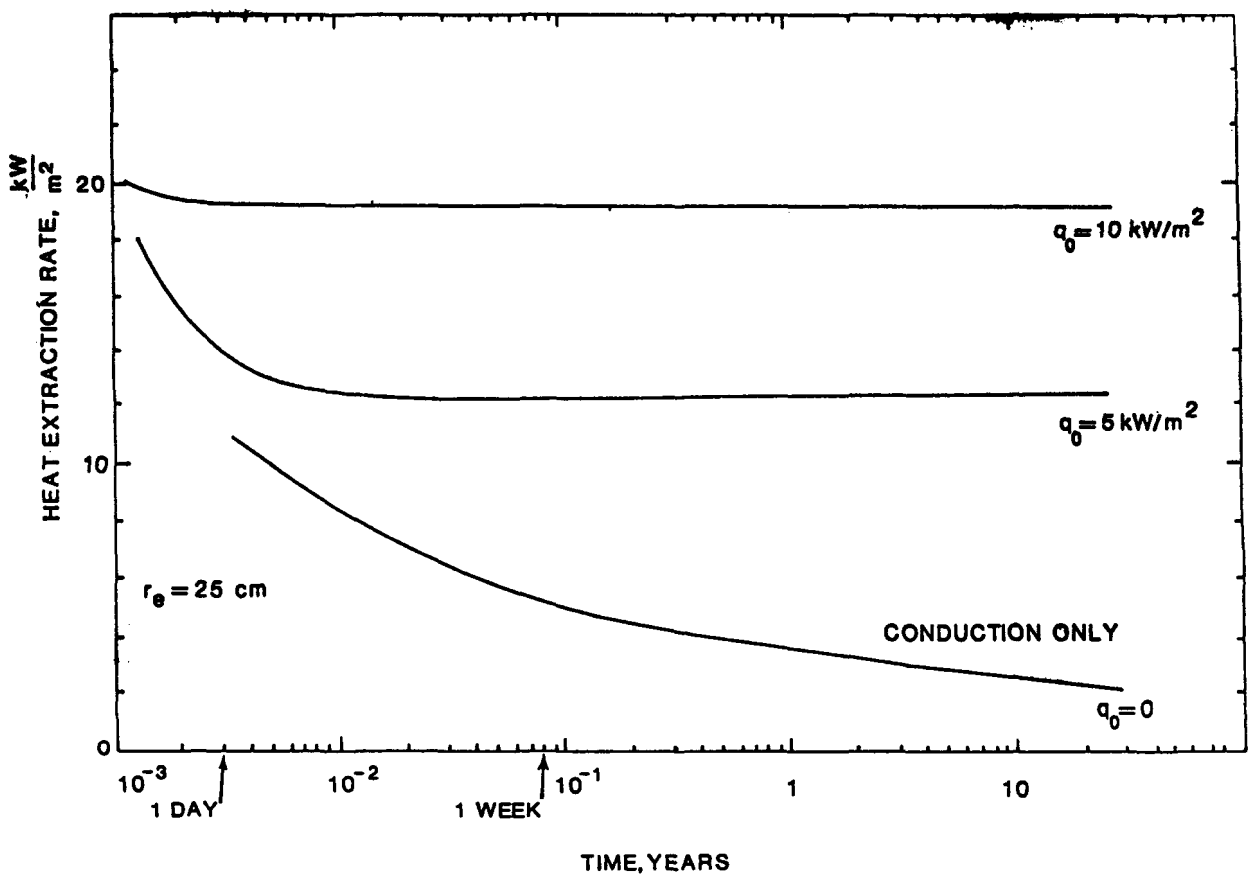


Figure 32. Heat Exchanger Rates for a Vertical Cylindrical Heat Exchanger Exposed to Different Magma Convective Heat Flux Levels.

Although evidence for shallow basaltic magma bodies in a continental crust environment is limited, the existence of andesitic or wet rhyolitic magma beneath a number of continental geothermal areas is likely.

The estimates for a magma heat exchanger (8-80 MW thermal/well) are comparable to those for conventional geothermal applications. For instance, Kruger (1976) estimates extraction rates of 17 MW thermal/well for typical liquid-dominated geothermal plants. The Cerro Prieto Geothermal field averages about 15 MW thermal/well (Guiza, 1975). In the vapor-dominated Geysers field, one new well is required per year for each 100 $MW_e$ (Crow, 1979). Assuming a 30 year plant life and a 16 percent thermal efficiency (Collie, 1978) gives an average extraction rate of 21 MW thermal/well for this field.

Thermal Aspects of the Emplacement and Evolution of Magma Bodies (C. R. Carrigan, 5512)

A study has recently been initiated to investigate the thermal requirements for the formation and evolution of basaltic magma intrusions in the earth's crust. While seismic techniques can be used to locate an intrusion or chamber, they lack sufficient resolution to allow the determination of the state of the chamber. The melt may only be partial; it may be contained in a dendritic system of cracks; it may be above the liquidus and convecting or some combination of these possible states. The efficiency of heat extraction depends vitally on the state of the chamber.

Realistic models for the emplacement and evolution of intrusions have been suggested by several researchers, notably Smith and Fedotov. However, the development of these models has been largely qualitative and more extensive calculations are needed. It will be necessary to ascertain the relationship between the physical state of the chamber and the volume, chemical composition and frequency of flows which provide the only direct information about the underlying source. Using thermal models, the analysis of flows will be useful in determining a chamber's previous thermal history and its current potential as a source of thermal energy. A better understanding of magma chamber evolution will also provide clues to the mantle

and crustal environments which are most likely to support igneous intrusives of the required kind.

Bounds have been obtained for the cooling rates of chambers as a function of volume, aspect ratio, and the degree to which the reservoir is dendritic (see Figure 33). Minimum injection rates which maintain the magma body at a temperature above the solidus have been deduced from such calculations. These in turn are being used to obtain a bound on the eruption frequency and volume relationship required to maintain a chamber of given size.

The possible resupply mechanisms are critical to any model and are also being considered. Which mode or combination of modes that is relevant will probably be a function of the crustal and mantle structure in the vicinity of the intrusive. Several possible mechanisms are currently being studied for their effectiveness in supplying emplaced chambers with thermal energy and new magma. The diapiric rise of the liquid fraction of a partial melt in a thermal chimney in the lithosphere is one possibility. Free convection within a conduit is another, although there is some question that the flow can be driven to sufficient amplitude to supply the needed heat. The empirical eruption frequency versus flow volume relation of Smith will be used as a basis for comparing these resupply mechanisms.

Natural Convection in Magma Chambers (R. H. Nilson, 5512)

The fluid mechanics of magma convection has been studied analytically and numerically (and supportive laboratory experiments have been designed) in order to determine whether or not a low-viscosity stratified melt might be present at the top of a magma chamber as a result of thermsolutal natural convection. If so, direct-contact heat extraction rates could be greatly enhanced, since magma viscosity varies by orders of magnitude, depending upon water content and crystal content. Solutions of the transport equations indicate that a double-diffusive counterflow is likely to occur, with either water-rich (during wall-rock melting) or crystal-depleted (during crystallization) magma rising along the walls of the chamber where the upward positive buoyancy due to compositional gradients overpowers the downward negative buoyancy due to temperature gradients. But, analytical

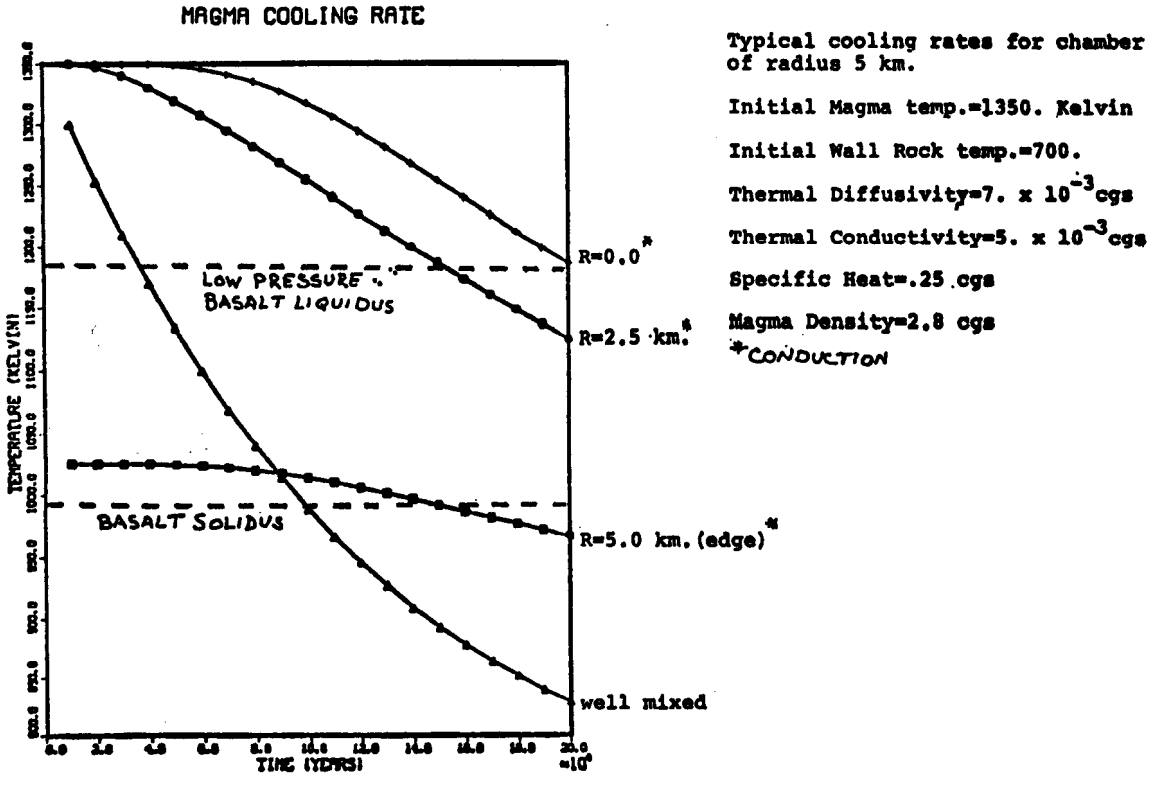


Figure 33. Magma Cooling Rates

arguments suggest that such counterflows could produce a stably stratified cap only if the boundary layers are sufficiently thin, and that this condition might or might not be met, depending upon the chamber configuration. In support of these modeling efforts, two computational tools are being developed: Navier-Stokes equations within a spherical cavity; and Prandtl boundary-layer equations which include surface-normal as well as surface-parallel components of buoyancy. Also, laboratory experiments are currently under construction to aid in formulation and verification of analyses.

Theoretical considerations and field data together suggest that natural convection is the dominant mechanism of energy and mass transport within even the most viscous of magma chambers. Analytical modeling of the convective transport process is necessary in order to: estimate cooling rates of magma chambers, determine the available heat flow in magma/hydrothermal systems, assess the potential energy extraction rates of direct-contact heat exchangers immersed in magma, quantify the internal mass transfer processes which have radical influence on the thermophysical properties (notably viscosity) which control heat transfer rates, and better understand the layering and stratification phenomena which are suggested by field data and are implicated in eruptive behavior.

The natural convection in magma chambers is driven not only by temperature gradients, but also by the gradients in chemical composition which result from phase-change and/or species-diffusive processes at the boundary between molten magma and solid country-rock.

1. At a melting boundary (Shaw, 1974), the country-rock melt has a higher $H_2O$ content than the magmatic core causing an upward buoyancy in the boundary layer (because $H_2O$ is lighter than rock). This has been suggested as a possible mechanism for the water-capping phenomenon which is inferred from the expulsion history of active volcanos in which boundary melting is presumably taking place.

2. At a solidifying boundary (Chen & Turner, 1980; McBirney, in press; Turner, 1980) the unsolidified fluid phase adjacent to the boundary may become lighter than the magmatic core, because the heavier species

are the first to crystallize at the boundary. This has been suggested as a possible mechanism for the observed layering in frozen magma bodies which were later exhumed.

In opposition to these upward buoyancy forces due to species concentration, there is a downward buoyancy force due to the thermal contraction near the relatively cold wall of the magma chamber. The upward-acting concentration-induced force is much stronger than the downward-acting temperature-induced force, but the upward force acts only within a thin species-diffusion boundary layer which is much narrower than the thermal-diffusion boundary layer (since $\alpha_{mass} << \alpha_{thermal}$). In such circumstances, neither of the opposing buoyancy forces is clearly dominant.

Three possible dispositions of the magmatic boundary-layer are as follows:

a. upward unidirectional flow in which the solutal buoyancy overpowers the thermal buoyancy,

b. downward unidirectional flow in which the thermal buoyancy overpowers the solutal buoyancy, and

c. counterflow configuration with a rising wall-region and a falling far field.

As a result of recent analytical/numerical work (Nilson, 1980) it has been determined which of these configurations is likely to occur, depending upon the relative strength, $\Gamma$ (in which $\beta$'s are volumetric expansion coefficients),

$$\Gamma \equiv |\beta_t \Delta T / \beta_c \Delta C|$$

and the relative diffusivity, Le,

$$Le \equiv \alpha_t / \alpha_c$$

of the opposing buoyancy mechanisms. (Subscripts: t for thermal, c for concentration.)

Aside from the counterflow question, there is also a question concerning the extent of the viscous boundary layers relative to the size of the magma chamber. Two limiting situations might occur within the parameter range appropriate to magma chambers:

i. thin boundary layers with high velocity near the wall and a very slow return-flow in the core -- a condition which is conducive to stratification;

ii. thick boundary layers with comparable velocities near the wall and in the core -- a condition less favorable to stratification, but well within reason for high-viscosity fluids.

Thus, to predict stratification behavior it is necessary to answer two key questions: Does upflow occur in the wall region, despite the opposing thermal buoyancy (i.e. can counterflow occur), and can a stratified layer persist at the top of the chamber?

A map of the unidirectional and counterflow regimes, constructed in (6) by the methods of (Gebhart & Pera, 1971), is presented in Figure 34 for the case of asymptotically high Prandtl number, as is certainly appropriate for the magmatic flows in which Pr is believed to lie in the range $10^6 < Pr < 10^{12}$.

a. For sufficiently small $\Gamma$ (below the lower line) the flow is strictly upwards.

b. For sufficiently large $\Gamma$ (above the upper line) the flow is strictly downward.

c. Between these unidirectional regimes there lies a broad, and almost entirely unexplored, region in which counterflows may occur.

Superimposed upon the flow map of Fig. 34 there are shaded regions which represent the expected parameter ranges for the thermosolutal phenomena which might occur in magma chambers.

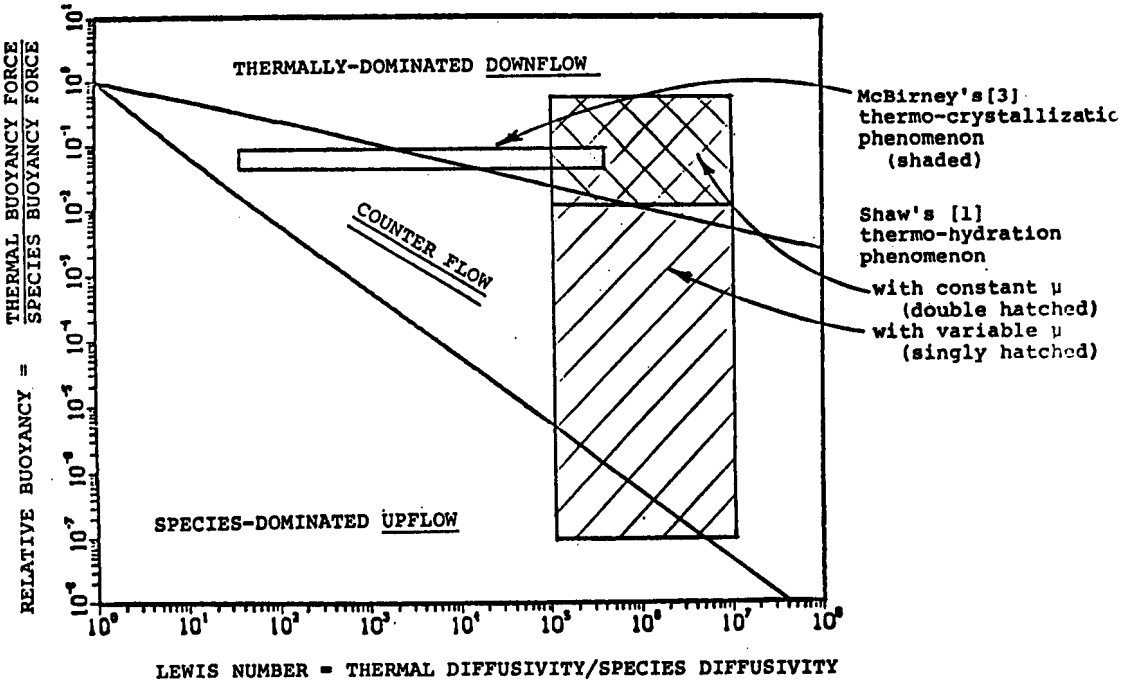


Figure 34. Flow Regime Map Showing the Parameter Ranges for Double-Diffusive Magma Flows.

1. At a melting boundary, Shaw's (1974) estimates of the parameter range suggest that the flow would probably be a thermally-dominated downflow (doubly crosshatched rectangle), were it not for the fact that the water-rich melt layer is 1 to 5 orders of magnitude less viscous than the magmatic interior. The effect of variable viscosity can be accounted for, in a preliminary sense at least, by redefining the relative buoyancy, $\Gamma$, in the following way

$$\Gamma \equiv \frac{|\beta_t \Delta T|}{|\beta_c \Delta C|} \frac{\mu_{wet}}{\mu_{dry}}$$

which extends the expected parameter range downward into the heart of the counterflow regime (singly crosshatched rectangle in Fig. 34). This treatment of the variable viscosity is a tentative result (now being further verified) based on the analysis in (Nilson, 1980).

2. At a solidification boundary, McBirney's (in press) estimates of the parameter range (shaded rectangle) suggest that the flow is likely to be a counterflow, even though there is a possibility of thermally-dominated upflow.

Thus, counterflow with rising fluid along the wall is likely to occur either during melting or during freezing conditions at the chamber wall.

Continuing Research

Little is known about the formation of stratified layers in highly viscous fluids, since the previous work (Chen & Turner, 1980; Turner, 1980) addresses the thin boundary-layer regime which is observed at moderate Prandtl numbers. It may be that a thin boundary layer is a necessary condition for the formation of a stratified cap-layer of low-density and low-viscosity magma at the top of the chamber. Based upon Kuiken's (1968) boundary-layer analysis for high Prandtl numbers, it can be argued that

$$\delta/R \sim Pr^{1/2}/Ra^{1/4}$$

in which Pr is the Prandtl number and Ra the Rayleigh number. Thus if $Ra < Pr^2$ the boundary layers will fill the chamber, perhaps precluding stratification. To further investigate this consideration, an experiment is being designed and constructed by P. C. Montoya (5513). The Thymol Blue technique will be used to visualize the transient natural convection in a wall-cooled sphere for the distinctly different cases of water (where $Ra >> Pr^2$) and glycerol (where $Ra << Pr^2$).

Computational capabilities are being developed in support of the predictive modeling outlined above. Two complementary approaches are being pursued in parallel. The first is an analysis based on Prandtl's boundary-layer equations, including not only the surface-parallel component of buoyancy, but also the surface-normal component which is known to have a radical influence on the velocity distribution in those regions where the surface-normal component carries the fluid away from the wall. The second is an analysis based on the Navier-Stokes equations for a spherical enclosure. The first provides estimates of the boundary-layer structures which may be present on the walls of the chamber. The latter is necesssary to account for the strong coupling between boundary layer and core, which is characteristic of very viscous flows. Both tools are operational.

## VII. REFERENCES


Aki, K., B. Chouet, M. Fehler, G. Zandt, R. Koyanagi, J. Colp, and R. Hay "Seismic Properties of Shallow Magma Reservoir in Kilauea Iki by Active and Passive Experiments" Jour. Geop. Res., v. 83, n. 85, May 10, 1978.

Carter, N. L., Steady state flow of rocks: Rev. Geophys. and Space Phys., 14, 301-357, 1976.

Carter, N. L. and Kirby, S. H., Transient creep and seimbrittle behavior of crystalline rocks: Pure and Applied Geophys., 116, 806-839, 1978.

Chen, C. F. and J. S. Turner, "Crystallization in a Double-Diffusive System," J. Geoph. Res. 85, (B5), 2573-2593, 1980.

Collie, M. J., Geothermal Energy - Recent Developments. Noyes Data Corporation, Park Ridge, N.J., pp. 146-147, 1968.

Colp, J. L., R. W. Decker, J. F. Hermance, D. L. Peck, and P. L. Ward. Magma Workshop Assessments and Recommendations. SAND75-0306, Sandia Laboratories, Albuquerque, NM, July 1975.

Colp, J. L., FY 79 Lava Lake Drilling Program - Geoscience Studies, Plans and Results. SAND79-1361, Sandia Laboratories, Albuquerque, NM, Oct. 1979.

Colp, J. L., Magma Energy Research Project FY79 Annual Progress Report, SAND79-2205, Sandia Laboratories, Albuquerque, NM, 1979a.

Colp, J. L., and R. K. Traeger. Magma Energy Research Project - Status Report as of October 1, 1978. SAND78-2288, Sandia Laboratories, Albuquerque, NM, December 1979.

Crow, N. B., 1979. An environmental overview of geothermal development: The Geysers--Calistoga KGRA, 4. Environmental Geology. Lawrence Livermore Lab. Rep. UCRL-52496, October 9, 1979.

Eaton, G. P. Christiansen, R. L., Iyer, H. M., Pitt, A. M., Mabey, D. R. Blank, H. R. Zietz, I., and Gettings, M. E. Magma beneath Yellowstone National Park, Science, 188:787-796, 1975.

Eichelberger, J. C., Andesitic volcanism and crustal evolution. Nature 275:21-27, 1978.

Flanigan, V. J., and C. J. Zablocki, Mapping the lateral boundaries of a cooling basaltic lava lake, Kilauea Iki, Hawaii, USGS Open-File Report 77-94, 21 pp., 1977.

Friedman, M., J. Handin, N. G. Higgs, and J. R. Lantz. "Strength and Ductility of Four Dry Igneous Rocks at Low Pressures and Temperatures to Partial Melting." 20th U. S. Symposium on Rock Mechanics, Austin, TX, June 1979.

Friedman, M., J. Handin, N. G. Higgs, J. R. Lantz, and S. J. Bauer, "Strength and Ductility of Room-Dry and Water-Saturated Igneous Rocks at Low Pressures and Temperatures to Partial Melting," SAND80-7159, Sandia National Laboratories, Albuquerque, NM, Nov. 1980.

Gebhart, B. and L. Pera, "The Nature of Vertical Natural Convection Flows Resulting from the Combined Buoyancy Effects of Thermal and Mass Diffusion," Int. J. Heat and Mass Transfer, 14, 2025-2049, 1971.

Gerlach, T. M., Evaluation and restoration of the 1970 volcanic gas analyses from Mount Etna, Sicily. Jr. Volc. and Geoth. Res., 6, 165-178, 1979.

Gerlach, T. M., Evaluation of volcanic gas analyses from Kilauea Volcano. Jr. Volc. and Geoth. Res., 7, 295-317, 1980A.

Gerlach, T. M., Investigation of volcanic gas analyses and magma outgassing from Erta Ale lava lake, Afar, Ethiopia. Jr. Volc. and Geoth. Res., 7, 415-441, 1980B.

Gerlach, T. M., Chemical characteristics of the volcanic gases from Nyiragongo lava lake, and the generation of $CH_4$-rich fluid inclusions in alkaline rocks. Jr. Volc. and Geoth. Res., in press, 1980C.

Gerlach, T. M., Evaluation of volcanic gas analyses from Surtesy Volcano. Jr. Volc. and Geoth. Res., in press, 1980D.

Gerlach, T. M., Interpretation of volcanic gas data from tholeiitic and alkaline mafic lavas, Proc. of the Int'l Workshop on the Analysis and Interpretation of Volcanic Gases, Gif-sur-Yvette, France, 1980E.

Gerlach, T. M., Restoration of new volcanic gas analyses from basalts of the Afar region: Further evidence of $CO_2$-degassing trends. Jr. Volc. Geoth. Res., in press, 1981A.

Gerlach, T. M., Intrinsic chemical variations in high-temperature volcanic gases from basic lavas. Chapter in Eruptive Volcanology (H. Tazieff, ed.), Elsevier, 1981B.

Guiza, J. L., Power Generation at Cerro Prieto Geothermal Field. Proc. Symp. on Development and Use of Geothermal Resources, San Francisco, Calif., May 20-29, 1975, pp. 1976-1978, 1975.

Handin, J., Strength and ductility: Section 11 In: Handbook of Physical Constants, Rev. Ed., Geol. Soc. American Mem. 97, 223-289, 1966.

Hardee, H. C., Solidification in Kilauea Iki Lava Lake, Jour. Volcan. Geotherm. Res. Vol. 7, p. 211-223, 1980.

Heiken, G. and Eichelberger, J. C., Eruptions at Chaos Crags, Lassen Volcanic National Park, California. J. Volcanol. Geotherm. Res., 7:443-481, 1980.

Hermance, J. F., D. W. Forsyth, and J. L. Colp. Geophysical Sensing Experiments on Kilauea Iki Lava Lake. SAND78-0828, Sandia Laboratories, Albuquerque, NM, November 1979.

Kruger, P., Geothermal Energy Annu. Rev. Energy, 1:159-183, 1976.

Kuiken, H. K., "An Asymptotic Solution for Large Prandtl Number Free Convection," J. Eng. Math II (4), 3-5-371, 1968.

McBirney, A. R., "Mixing and Unmixing of Magmas," J. Volcanol. and Geothermal Res., in press.

Murata, K. J. and D. H. Richter. "Chemistry of the Lavas of the 1959-60 Eruption of Kilauea Volcano, Hawaii." USGS Prof. Pap. 537-A, 26 p., 1966.

Murrell, S. A. F. and Chakravarty, S., Some new rheological experiments on igneous rocks at temperatures up to 1120° C: Geophys. J. R. Astr. Soc., 34, 211-250, 1973.

National Academy of Science. Continental Scientific Drilling Program. National Acad. Sci., Washington, DC, 1979.

Neel, R. R., R. P. Striker, and R. M. Curlee. FY79 Lava Lake Drilling Program - Results of Drilling Experiments. SAND79-1360, Sandia Laboratories, Albuquerque, NM, November 1979.

Nilson, R. H., "Thermosolutal Natural Convection in Magma Chambers: Does Counterflow Occur?", private communication to H. C. Hardee, October, 1980.

Randich, E. and T. M. Gerlach, A Simple Method for the Calculation and Use of CVD Diagrams with Applications to the Ti-B-C2-H System, 1200K - 800K, SAND80-0308, Sandia National Laboratories, Albuquerque, NM, March 1980A.

Randich, E. and T. M. Gerlach, The Calculation and Use of Chemical Vapor Deposition Phase Diagrams with Applications to the Ti-B-C2-H System Between 1200K and 800K, Thin Solid Films, v. 75, p. 271-291, 1980B.

Reid, J. B., Jr., 1980, Mixing of rhyolitic and high alumina basaltic magmas in plutons in the central Sierra Nevada: EOS, in press.

Reid, J. B. and J. C. Eichelberger, Basaltic Droplets in Silicic Host Magmas: A Comparison of Mixed Magmas in Volcanic and Plutonic Settings, EOS, v. 62, p. 433, 1981.

Shaw, H. R., Obsidian-$H_2O$ Viscosities at 1000 and 2000 Bars in the Temperature Range 700° - 900°C., Jour. Geop. Res., v. 68, p. 6337-43, 1963.

Shaw, H. R, "Diffusion of $H_2O$ in Granitic Liquids: Part I. Experimental Data; Part II. Mass Transfer in Magma Chambers," Geochemical Transport and Kinetics, Carnegie Institution of Washington, 1974.

Shimozurv, D., Dynamics of Magmas in a Volcanic Conduit - Special Emphasis on Viscosity of Magma with Bubbles, Bull. Volcan., v. 41, p. 333-40, 1978.

Smith, B. D., C. J. Zablocki, F. C. Frischknect and V. J. Flanigan, Summary of results from electromagnetic and galvanic soundings on Kilauea Iki lava lake, USGS Open File Report 77-59, 27 pp., 1977.

Smith, B. D., C. J. Zablocki, F. C. Frischknect and D. B. Jackson, "Results from Electrical Studies of Kilauea Iki Lava Lake, Abs., Hilo Geothermal Conference, 1978.

Smith, B. D. and F. C. Frischknect, Progress Report on 1980 Electromagnetic Experiments on Kilauea Iki Lava Lake, Submitted to Sandia Laboratories, June 2, 1980.

Stauber, D. A., Progress Report on the Kilauea Iki Seismic Experiments of March 1980, Submitted to Sandia Laboratories, June, 1980.

Turner, J. S., "A Fluid-Dynamical Model of Differentiation and Layering in Magma Chambers," Nature, 285, (22), 213-215, 1980.

Varnado, S. G. and J. L. Colp. Report of the Workshop on Magma/Hydrothermal Drilling and Instrumentation. SAND78-1365C, Sandia Laboratories, Albuquerque, NM, July 1978.

Wemple, R. P., W. F. Hammetter, and C. J. Greenholt, Development of High Temperature Viscosity Measuring Techniques, SAND80-0641, Sandia National Laboratories, Albuquerque, NM, 1980.

Zablocki, C., Some electrical and magnetic studies on Kilauea Iki lava lake, Hawaii, USGS Open-File Report 76-304, 19 pp., 1976.

## VIII. Recent Publications

Banister, J. R., "Calculation of the Mount St. Helens Pressure Wave," Transactions of the American Geophysical Union, Vol. 61, No. 46, p. 1136, 1980.

Bass, R. C., Banister, J. R., "Dusty Gas Flow Calculations," Transactions of the American Geophysical Union, Vol. 61, No. 46, p. 1136, 1980.

Carrigan, C. R., "Multiple Scale Convection in the Earth's Mantle: A Three-Dimensional Study," submitted to Science, 1981.

Colp, J. L., R. R. Neel, Sandia National Laboratories, MAGMA ENERGY RESEARCH, 79-1, SEMIANNUAL REPORT, October 1, 1978-March 31, 1979, SAND79-1344, July 1979.

Colp, John L., Sandia National Laboratories, FY-79 LAVA LAKE DRILLING PROGRAM -- GEOSCIENCE STUDIES: PLANS AND RESULTS, SAND79-1361, October 1979.

Colp, J. L., and R. K. Traeger, Sandia National Laboratories, MAGMA ENERGY RESEARCH PROJECT -- STATUS REPORT AS OF OCTOBER 1, 1978, SAND78-2288, December 1979.

Colp, J. L., Sandia National Laboratories, MAGMA ENERGY -- A FEASIBLE ALTERNATIVE, SAND80-0309, Proceedings of United Nations Institute for Training and Research Conference on Long Term Energy Resources, Montreal, Canada, November 26 - December 7, 1979.

Colp, John L., Sandia National Laboratories, MAGMA ENERGY RESEARCH PROJECT -- FY 1979 ANNUAL PROGRESS REPORT, SAND79-2205, December 1979.

Colp, John L., Sandia National Laboratories, MAGMA ENERGY RESEARCH PROJECT -- FY 1980 SEMI-ANNUAL PROGRESS REPORT, SAND80-2377, July 1980.

Davis, M. J., Graeber, E. J. "Temperature Estimates of May 18 Eruption of Mount St. Helens Made from Observations of Material Response," Transactions of American Geophysical Union, Vol. 61, No. 46, p. 1136, 1980.

Douglass, D. L. and J. T. Healey, "The Corrosion of Some Pure Metals in Basaltic Lava and Simulated Magmatic Gas at 1150°C," SAND79-1981, Sandia Laboratories, Albuquerque, NM 1979.

Douglass, D. L., P. J. Modreski, and J. T. Healey "The Corrosion of Some Pure Metals in Basaltic Lava at 1150°C," ABS Proceedings, Hawaii Symposium on Intraplate Volcanism and Submarine Volcanism, Hilo, Hawaii, July 1979.

Dunn, J. C. and H. C. Hardee "Measurement of In Situ Permeability in Kilauea Iki Lava Lake, Hawaii," ABS, Proceedings, Hawaii Symposium on Intraplate Volcanism and Submarine Volcanism, Hilo, Hawaii,

Dunn, J. C. and P. C. Montoya "Water Jet Drilling into Liquid Lava," ABS Proceedings, Hawaii Symposium on Intraplate Volcanism and Submarine Volcanism, Hilo, Hawaii, July 1979.

Dunn, J. C. and H. C. Hardee "Superconvecting Geothermal Zones," SAND80-1106J, Sandia National Laboratories, Albuquerque, NM. Journal of Volcanology and Geothermal Research (in press).

Dunn, J. C., and R. G. Hills, KILAUEA IKI LAVA LAKE EXPERIMENT PLANS, SAND80-1653, Sandia National Laboratories, Albuquerque, NM, in press.

Eichelberger, J. C., "Vesiculation of Mafic Magma During Replenishment of Crustal Magma Reservoirs," Nature, in press.

Friedman, M., J. Handin, N. C. Higgs, and J. R. Lantz. "Strength and Ductility of Four Dry Igneous Rocks at Low Pressures and Temperatures to Partial Melting," 20th U. S. Symposium on Rock Mechanics, Austin, TX, June 1979.

Friedman, M., J. Handin, N. G. Higgs, and J. R. Lantz, Texas A&M University, BOREHOLE STABILITY IN IGNEOUS ROCKS AT LOW PRESSURES AND TEMPERATURES TO PARTIAL MELTING, Proceedings of Symposium on Intraplate Volcanism and Submarine Volcanism, Hilo, Hawaii, July 16-22, 1979.

Friedman, M., J. Handin, N. G. Higgs, J. R. Lantz, S. J. Bauer, "Strength and Ductility of Room-Dry and Water-Saturated Igneous Rocks at Low Pressures and Temperatures to Partial Melting--Final Report," Sandia Laboratories Report, SAND80-7159, Nov., 1980.

Gerlach, T. M. "Volcanic Gases and Compatibility with Pure Metal" ABS, Proceedings, Hawaii Symposium on Intraplate Volcanism and Submarine Volcanism, Hilo, Hawaii, July 1979.

Gerlach, T. M. "Evaluation of Volcanic Gas Analysis from Tholeiitic and Alkaline Mafic Lavas. Presented at the Workshop on Remote Sensing of Volcanic Gases. Conference Report available from Lunar and Planetary Institute, Houston, TX 77058.

Gerlach, T. M. "Volcanic Gases and Compatibility with Pure Metals," ABS, Proceedings, Hawaii Symposium on Intraplate Volcanism and Submarine Volcanism, Hilo, Hawaii, July 1979.

Gerlach, T. M. "The Gas Phase of Tholeiitic and Alkaline Magmas," ABS, Abstracts with Programs, 1979 Annual Meeting, Geol. Soc. Am., San Diego, CA, November 1979.

Gerlach, T. M. "Evaluation and Restoration of the 1970 Volcanic Gas Analyses from Mount Etna, Sicily," Jr. Volc. and Geoth. Res., 6, 165-178, 1979.

Gerlach, T. M. "Chemical Characteristics of the Volcanic Gases from Myiragongo Lava Lake, and the Generation of $CH_4$-rich Fluid Inclusions in Alkaline Rocks," Jr. Volc. and Geoth. Res., 1980.

Gerlach, T. M. "Investigation of Volcanic Gas Analysis and Magma Outgassing from Erta Ale Lava Lake, Afar, Ethiopia," J. Volc. and Geoth. Res., v. 7, 415-441, 1980.

Gerlach, T. M. "Evaluation of Volcanic Gas Analyses from Surtsey Volcano, Iceland, 1964-1967," J. Volc. and Geoth. Res., 1980.

Gerlach, T. M. "Evaluation of Volcanic Gas Analyses from Kilauea Volcano," J. Volc. and Geoth. Res., v. 7, 295-317, 1980.

Gerlach, T. M., Interpretation of Volcanic Gas Data from Tholeiitic and Alkaline Mafic Lavas, Workshop on Volcanic Gases C.N.R.S., Bull. Volcan., v. 43, p. 69-92, 1980.

Gerlach, T. M. and W. C. Luth, "Mass Balance Differentiation Models for the 1959 Kilauea Iki Lava Lake," Transactions of the American Geophysical Union, Vol. 61, No. 46, p 1434, 1980.

Gerlach, T. M., "Intrinsic Chemical Variations in High-Temperature Volcanic Gases from Basic Lavas," Chapter in Eruptive Volcanology, H. Tazieff, ed., Elsevier, in press.

Gerlach, T. M., "Restoration of New Volcanic Gas Analyses from Basalts of the Afar Region: Further Evidence of $CO_2$-Degassing Trends," Jr. Volc. Geoth. Res., Vol. 10, 1981.

Hardee, H. C. "Heat Transfer Measurements in the 1977 Kilauea Lava Flow," Transactions American Geophysical Union, Vol. 59, p. 311, 1979.

Hardee, H. C. "Temperature Measurement in the Crust of Kilauea Iki Lava Lake," ABS, Proceedings, Hawaii Symposium on Intraplate Volcanism and Submarine Volcanism, Hilo, Hawaii, July 1979.

Hardee, H. C. "Heat Extraction from Magma Bodies," ABS Proceedings Hawaii Symposium on Intraplate Volcanism, Hilo, Hawaii, July 1979.

Hardee, H. C. "Heat Transfer Measurements in the 1977 Kilauea Lava Flow, Hawaii," Jour. Geoph. Res., v. 184, No. B13, pp 7485-7493, 1979.

Hardee, H. C. "Temperature Measurements in the Crust of Kilauea Iki Lava Lake," Proc. Hawaii Symposium on Intraplate Volcanism and Submarine Volcanism, Hilo, Hawaii, July 1979.

Hardee, H. C. "Heat Extraction from Magma Bodies" Proc. Hawaii Symposium on Intraplate Volcanism and Submarine Volcanism, Hilo, Hawaii, July 1979.

Hardee, H. C. "Solidification in Kilauea Iki Lava Lake," J. Volc. and Geoth. Res., v. 7, 211-223, 1980.

Hardee, H. C. "Convective Heat Extraction from Molten Magma," Journal of Volcanology and Geothermal Research, Vol. 10, 1981.

Hardee, H. C. "Permeable Convection Above Magma Bodies," SAND81-0619J, 1981.

Hardee, H. C. "Thermal Property Measurements in a Fresh Pumice Flow at Mount St. Helens," Geophysical Research Letters (in press).

Hardee, H. C. and D. W. Larson "Thermal Techniques for Locating and Characterizing Buried Magma Bodies," ABS, Proceedings Hawaii Symposium on Intraplate Volcanism and Submarine Volcanism, Hilo, Hawaii, July 1979.

Hardee, H. C. and D. W. Larson, "Thermal Techniques for Characterizing Magma Body Geometries," Geothermics: International Journal of Geothermal Research and Its Application, Vol. 9, No. 3 and 4, 237-249, 1980.

Hardee, H. C. and J. C. Dunn "Convective Heat Transfer in Magmas Near the Liquidus," J. of Volcanology and Geothermal Research, Vol. 10, 1981.

Hardee, H. C. and R. G. Hills "The Resonant Acoustic Pulser--A Continuous Frequency Marine Seismic Source," Submitted to Geophysics.

Hermance, J. F., D. W. Forsythe, and J. L. Colp "Summary of Geophysical Sensing Experiments on Kilauea Iki Lava Lake" ABS, Proceedings, Hawaii Symposium on Intraplate Volcanism and Submarine Volcanism, Hilo, Hawaii, July 1979.

Hermance, J. F., D. W. Forsythe, and J. L. Colp, Geophysical Sensing Experiments on Kilauea Iki Lava Lake. SAND77-0828, Sandia Laboratories, Albuquerque, NM, 1979.

Luth, W. C. and T. M. Gerlach, "Compositions and Proportions of Major Phases in the 1959 Kilauea Iki Lava Lake in December 1976," Transactions of the American Geophysical Union, Vol. 61, No. 46, p. 1142, 1980.

Modreski, P. J. Experiment Plan for Characterization of the Properties of Molten Rock at Atmospheric and Elevated Pressures: Magma Energy Research Project. SAND78-2227, Sandia Laboratories, Albuquerque, NM, February 1979.

Neel, R. R., Striker, R. P., and Curlee, R. M., FY79 Lava Lake Drilling Program - Results of Drilling Experiments SAND79-1360, Sandia Laboratories, Albuquerque, NM, 1979.

Randich, E. and Gerlach, T. M., "A Simple Method for the Calculation and Use of CVD Phase Diagrams with Applications to the Ti-B-CL-H System, 1220K-800K," SAND80-0308, 1980.

Randich, E. and Gerlach, T. M., "The Calculation and use of CVD phase diagrams with applications to the Ti-B-Cl-H System 1200K-800K," Journal of Thin Solid Films, v. 75, p. 271-291, 1980.

Reed, J. W., "Air Pressure Waves from Mt. St. Helens," Transactions of the American Geophysical Union, Vol. 61, No. 46, p. 1136, 1980.

Reid, J. B. and J. C. Eichelberger, Basaltic Droplets in Silicic Host Magmas: A Comparison of Mixed Magmas in Volcanic and Plutonic Settings, EOS, v. 62, p. 433, 1981.

Traeger, R. K., J. L. Colp, and R. R. Neel Magma Energy Research 79-1, SAND79-1344, Sandia Laboratories, Albuquerque, NM, July 1979.

Vortman, L. J., "Deduced Physical Characteristics of the May 18, 1980 Eruption," Transactions of the American Geophysical Union, Vol. 61, No. 46, pp 1135-1136, 1980.

Wemple, R. P., W. P. Hammeter, and C. J. Greenholt, "Development of High Temperature Viscosity Measurement Technique," SAND80-0641, Sandia National Laboratories, Albuquerque, NM, April 1980.

## IX. Recent Presentations

Dunn, J. C., Thermal Analysis and Models, DOE/BES Program Review, July 1980.

Eichelberger, J. C., "Replenishment and Mixing in Crystal Magma Reservoirs," invited lecture:

| | |
|---|---|
| University of Arizona | 5/80 |
| University of Western Ontario | 9/80 |
| University of Waterloo | 9/80 |
| Pennsylvania State University | 9/80 |
| 5 College Group: | 9/80 |
| University of Massachusetts | |
| Hampshire College | |
| Amherst College | |
| Mt. Holyoke College | |
| Smith College | |

Hardee, H. C., "Status of Magma Energy Research Program," National Energy Authority of Iceland, Reykjavik, Iceland, May 30, 1980.

Hills, R. G., Geophysical Models, DOE/BES Program Review, July 1980.

Do Not Microfilm Distr

DISTRIBUTION:

DOE/TIC-4500-R67 UC-66 (235)

Massachusetts Institute of Technology
Dept of Earth Science
Cambridge, MA 02139
Attn: Keiiti Aki, 54-526

Lawrence Berkeley Laboratory (3)
University of California
Berkeley, CA 94720
Attn: J. A. Apps
I. S. Carmichael
P. A. Witherspoon

Shigeo Aramaki
Earthquake Research Inst
University of Tokyo
Bunkyo-ku
Tokyo 113, Japan

US Department of Energy (4)
Div of Geothermal Energy
Washington, DC 20545
Attn: L. Ball
C. Carwile, Chief
Adv Tech Br
J. W. Salisbury
Hydrothermal Support Br
J. Walker, Chief
Technology Div.
MS 3122C

United National Inst for Trn & Res
(UNITAR)
801 United Nations Plaza
New York, NY 10017
Attn: J. Barnea, Special Fellow

Sveinbjorn Bjornsson
Science Institute
University of Iceland
Bunhaga 3
107 Reykjavik, Iceland

Argonne National Laboratory
9700 South Cass Avenue
Argonne, IL 60439
Attn: M. Blander, Bldg 205

Office of Nucl and Energy Tech Affairs
Department of State
Washington, DC 20520
Attn: J. L. Bloom

Oregon State University
Corvallis, OR 97331
Attn: G. Bodvarsson

University of Texas
Engineering - Sci Bldg 623
Austin, TX 78712
Attn: F. X. Bostick

Stanford University
Petroleum Eng Dept
Stanford, CA 94306
Attn: W. E. Brigham

Los Alamos National Lab (6)
P. O. Box 1663
Los Alamos, NM 87545
Attn: R. Brownlee, G-DO, MS 570
C. E. Holley, CNC-2, MS 738
A. W. Laughlin, G-6, MS 978
R. E. Reicker, G-DOT, MS 26
M. C. Smith, G-DOT, MS 26
C. Herrick, CMB-8

State Univ of NY at Albany
E215
1400 Washington Ave.
Albany, NY 12222
Attn: K. Burke

US Geological Survey (5)
345 Middlefield Road
Menlo Park, CA 94025
Attn: R. Christiansen
W. A. Duffield, MS 18
J. G. Moore
H. Shaw, MS 18
P. Ward

US Geological Survey (2)
Hawaiian Volcano Observatory
Hawaii Volcanoes National Park
Hawaii 96718
Attn: R. W. Decker
Library

University of Texas
Center for Energy Studies
Austin, TX 78712
Attn: M. Dorfman

US Geological Survey (2)
Mt. St. Helens Field Office
301 E. McLoughlin
Vancouver, WA 98660
Attn: Don Peterson
R. Holcomb

US Geological Survey (5)
956 National Center
Reston, VA 22092
Attn: G. Eaton, MS 911
R. T. Helz, MS 959
D. Peck, Chief
Geologist, MS 911
R. Tilling, MS 906
C. Zablocki, MS 906

Ingvar B. Fridleifsson
National Energy Authority
Laugavegur 116
Reykjavik, Iceland

Texas A&M University
Center for Tectonophysics
College Station, TX 77843
Attn: M. Friedman

US Geological Survey
Box 25046
Denver Federal Center
Denver, CO 80225
Attn: F. Frischknecht, MS 964

University of Hawaii at Manoa
Hawaiian Inst of Geophysics
Honolulu, HI 96822
Attn: A. S. Furumoto

University of Hawaii (2)
Hawaii Inst of Geophysics
Honolulu, HI 96822
Attn: C. Helsley, Head
M. Ryan

Brown University
Dept of Geological Sciences
Providence, RI 02912
Attn: J. F. Hermance

Technical Consultant
Subcommittee on Adv Energy
and Technologies
House Committee on Science
and Technology
Rayburn Office Bldg B374
Washington, DC 20515

University of Alaska
Geophysical Institute
Fairbanks, AK 99701
Attn: J. Kielne

US Dept of Energy (10)
Office of Basic Energy Science
Washington, DC 20545
Attn: G. A. Kolstad, MS J-309

Oak Ridge National Lab
P. O. Box X
Oak Ridge, TN 37830
Attn: W. L. Marshall

Kazuaki Nakamura
Earthquake Research Inst.
University of Tokyo
Hongo
Tokyo 113, Japan

Hans-Ulrich Schmincke
Rohr-Universitat Bochum
Institut fur Mineralogie
D-463 Bochum Postfach 102148
West Germany

Daisuke Shimozuru
Earthquake Research Institute
University of Tokyo
Bunkyo-ku
Tokyo 113, Japan

University of Hawaii at Manoa
College of Engineering
Honolulu, HI 96822
Attn: Dean John Shupe

University of Minnesota
Inst of Technology
107 Lind Hall
207 Church St, SE
Minneapolis, MN 55455
Attn: Dean Roger Staehle

Dartmouth College
Hanover, NJ 03755
Attn: R. E. Stoiber

Superintendent
Hawaii Volcanoes National Park
Hawaii 96718

Captain William J. Barattino, P.E.,
USAF
Chief, At Energy Liaison Office
Department of Energy
Albuquerque Operations Office
P. O. Box 5400
Albuquerque, NM 87185

Thomas A. Ladd
Geothermal Program Manager
Department of Energy
200 Stovall Street
Alexandria, VA 22332

University of Hawaii
Hawaii Geothermal Project
240 Holmes Hall
2540 Dole St
Honolulu, HI 96822
Attn: P. C. Yuen

Dr. Richard Taschek
2035 47th St.
Los Alamos, NM 87544

1000 J. K. Galt*
1510 D. B. Hayes*
1512 D. McVey
1541 W. C. Luth
1541 T. M. Gerlach
1800 J. K. Galt (Act'g)
1820 R. E. Whan*
1822 E. J. Graeber
1830 M. J. Davis
1832 J. L. Ledman
7000 W. Herrmann
9000 G. A. Fowler
9700 E. H. Beckner
9740 R. K. Traeger
9743 H. C. Hardee
9743 J. L. Colp (30)
9743 J. C. Dunn
9743 R. K. Striker
9750 V. L. Dugan*
9770 G. E. Brandvold*
8214 M. A. Pound
3141 L. J. Erickson (5)
3151 W. L. Garner (3)
For DOE/TIC
(Unlimited Release)

*To receive abstract only



☆U.S. GOVERNMENT PRINTING OFFICE: 1982-0-576-021/611